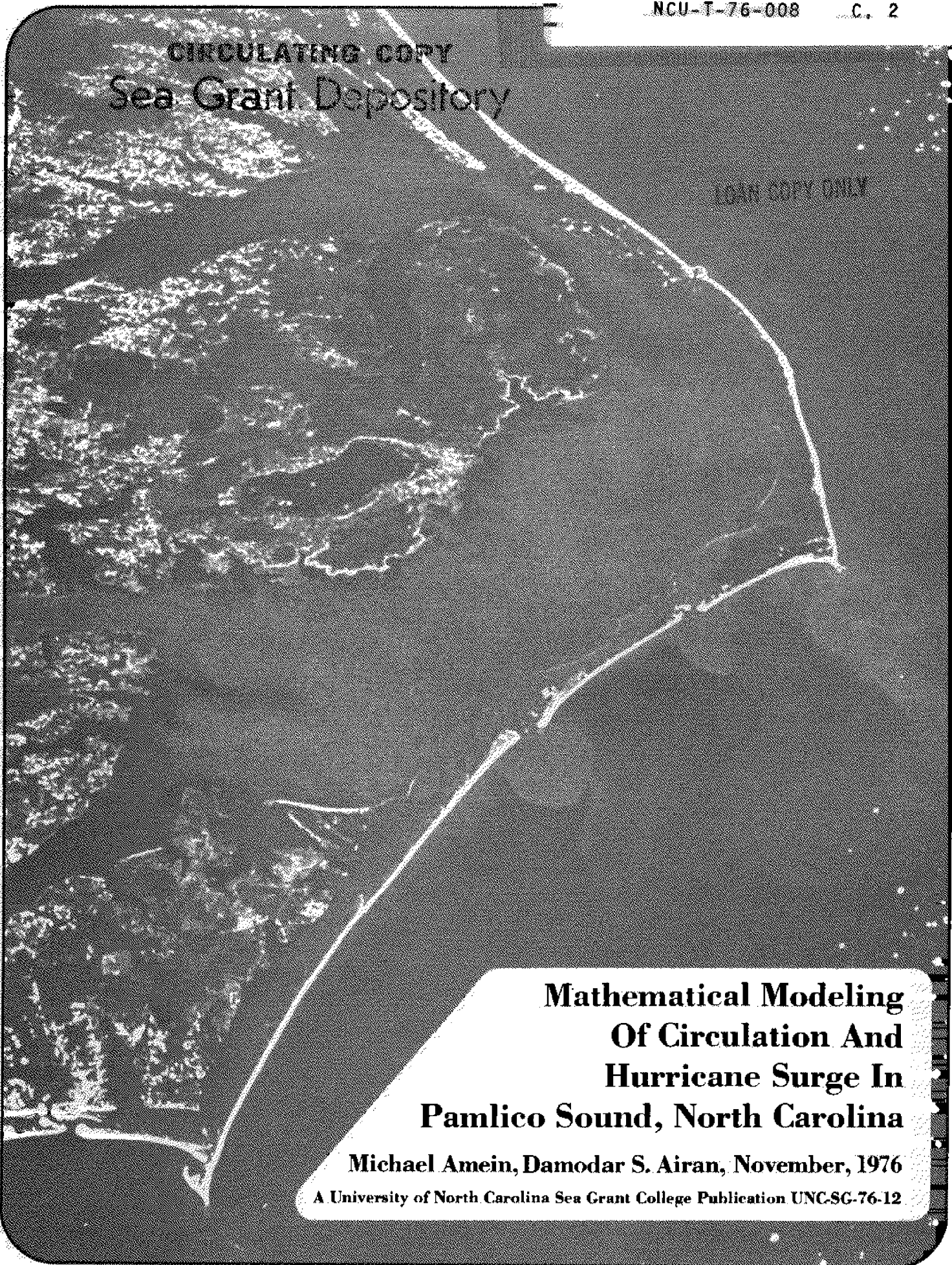


CIRCULATING COPY
Sea Grant Depository

LOAN COPY ONLY



**Mathematical Modeling
Of Circulation And
Hurricane Surge In
Pamlico Sound, North Carolina**

Michael Amein, Damodar S. Airan, November, 1976

A University of North Carolina Sea Grant College Publication UNC-SG-76-12

Price: \$3.00

Copies are available from: UNC Sea Grant
1235 Burlington Labs
NCSU Campus
Raleigh, N.C. 27607

Residents of North Carolina may obtain a single copy free of charge.

LOAN COPY ONLY

MATHEMATICAL MODELING OF CIRCULATION AND HURRICANE SURGE

IN PAMLICO SOUND, N. C.

by

Michael Amein

and

Damodar S. Airan

Department of Civil Engineering
North Carolina State University
Raleigh, N. C.

This work was partially supported by the Office of Sea Grant, NOAA, U. S. Department of Commerce, under Grant Number 04-6-158-44054 and the State of North Carolina, Department of Administration. The U. S. Government is authorized to produce and distribute reprints for governmental purposes notwithstanding any copyright that may appear hereon.

SEA GRANT PUBLICATION UNC-SG-76-12 November, 1976

University of North Carolina Sea Grant Program, 1235 Burlington Laboratories,
North Carolina State University, Raleigh, North Carolina 27607

ABSTRACT

Pamlico Sound is a large semi-enclosed body of partially saline water on the coast of North Carolina separated by a narrow strip of barrier islands from the Atlantic Ocean. Freshwater inflow is from two major rivers and from Albemarle Sound. There is tidal flow across the inlets. Wind is a major factor in circulation, and there is considerable surge action during the hurricanes.

A numerical model based on the two-dimensional shallow water hydrodynamic equations is used to compute water surface elevations and currents. The model uses an explicit finite difference representation, and includes convective acceleration, and nonlinear surface and bottom stress. The time dependent water movements are computed for an observed hurricane with good success. The model can be used to predict surge heights for coastal protection, and it will provide data for water resource management and for pollution control. A user's manual consisting of the listing of the computer program and instructions is given in the appendix to the report.

CONTENTS

	Page
ABSTRACT	i
LIST OF FIGURES	ii
LIST OF TABLES	iv
NOMENCLATURE	v
I. INTRODUCTION	1
II. BASIC EQUATIONS	2
III. REVIEW OF LITERATURE	7
IV. NUMERICAL MODELING	8
A. Overview of Available Numerical Techniques	8
B. The Explicit Method	10
C. Initial and Boundary Conditions	15
D. Stability Considerations	16
E. Computations	17
F. Interior Grid Points	18
V. HYDROGRAPHY OF PAMLICO SOUND	19
A. Factors Affecting Circulation	21
VI. APPLICATION OF NUMERICAL MODELING TO PAMLICO SOUND	26
A. Numerical Simulation	28
B. Boundary Conditions	29
C. Tidal Exchange Computations	30
D. Selection of Time Step	32
E. Calibration of the Mathematical Model	32
VII. CIRCULATION DUE TO FRESHWATER INFLOW AND WIND	33
A. Circulation Due to Freshwater Inflow	33
B. Circulation Due to Uniform Wind	33
C. Pamlico Sound Subject to Variable Wind Stress	37
D. Effect of Size of Time Step	41
VIII. MODELING OF HURRICANE SURGE	41
IX. SUMMARY AND DISCUSSION	59
X. REFERENCES	63
XI. COMPUTER PROGRAMS	
A. Description of Input Data	70
B. Description of Output Data	70
C. Use of Basic Programs for Various Flow Conditions	71
D. DEFINITIONS	73
APPENDIX. COMPUTER PROGRAM LISTINGS	76

LIST OF FIGURES

	Page
1. Fixed Rectangular Network for Explicit Method	12
2. Computational Module at Interior Grid Points	20
3. Location Map of Pamlico Sound and its Tributary Waters	23
4. Floods at Kinston and Tarboro to Estimate the Flows from the Neuse and Pamlico River	27
5. The Boundary and Grid System Used for the Pamlico Sound	34
6. Variation in Velocity and Depth of Water at Time = 360 Minutes with Freshwater Inflow, No Outflow and No Wind	35
7. Variation in Velocity and Depth of Water at Time = 1440 Minutes with Freshwater Inflow, No Outflow and No Wind	36
8. Variation in Velocity and Depth of Water at Time = 29 minutes, with a Northerly Wind at 70 MPH. No Inflow or Outflow $C_d = 2.5 \times 10^{-3}$	38
9. Water Surface Profiles along Longitudinal Section at J = 20 at Time = 2880 Minutes for 70 MPH Winds from Different Directions.	39
10. Variation in Velocity and Depth of Water at Time = 240 minutes with a Westerly Wind at 70 MPH, No Inflow or Outflow of Water. $C_d = 2.5 \times 10^{-3}$	40
11. The Track of Hurricane Donna During August 30, 1960 To September 13, 1960	45
12. The Forward Movement of Hurricane Donna in the Vicinity of Pamlico Sound, September 11-12, 1960	46
13. Division of Pamlico Sound into Six Zones for Variable Winds	47
14. Calculated Water Elevations in Pamlico Sound due to Hurricane Donna at Time = 10.0 Hours, Inflow and Outflow Permitted, $C_d = 2.5 \times 10^{-3}$	51
15. "Observed" Water Elevations in Pamlico Sound Due to Hurricane Donna at Time = 10.0 Hours	52
16. Calculated water elevation in Pamlico Sound due to Hurricane Donna at Time = 11 Hours, Inflow and Outflow Permitted, $C_d = 2.5 \times 10^{-3}$	53
17. "Observed" Water Elevations in Pamlico Sound due to Hurricane Donna at Time = 11.0 Hours.	54
18. Calculated Water Elevations in Pamlico Sound due to Hurricane Donna at Time = 14 Hours, Inflow and Outflow Permitted, $C_d = 2.5 \times 10^{-6}$	55
19. "Observed" Water Elevations in Pamlico Sound due to Hurricane Donna at Time = 14.0 Hours.	56

20. Calculated Water Elevations in Pamlico Sound due to Hurricane Donna at Time = 16.0 Hours. 57
21. "Observed" Water Elevations in Pamlico Sound due to Hurricane Donna at Time = 16.0 Hours. 58

LIST OF TABLES

	Page
1. Drag Coefficient, C_d , and Other Parameters for Light and Strong Winds.	6
2. Mean Annual Discharge from the Drainage Basins Contributing to Pamlico Sound.	24
3. Mean Annual Discharge and the Percentage of Discharge from the Entries to Pamlico Sound.	24
4. Estimated 5, 10 and 20 Year Flood Flow from the Entries to Pamlico Sound.	25
5. Values of Discharge Coefficients for Tidal Inlets.	31
6. Effect of Time Step on the Computed Values of Parameters	41
7. Effect of Time Step on Computation Cost	42
8. Velocity (in miles per hour) and Direction of Wind at Four Stations During Hurricane Donna of 1960	47
9. Velocity and Direction of Wind in Wind Zones	48

NOMENCLATURE

The following symbols are used in this report:

c	= wave propagation velocity in shallow water
C_d	= coefficient of drag for wind stress
d	= water depth at the initially undisturbed level, usually at mean sea level.
f	= Coriolis coefficient
g	= acceleration due to gravity
H_1	= water surface in the basin
H_2	= water surface in the sea
i	= an index identifying the x-position
j	= an index identifying the y-position of a point on the grid
k	= an index identifying the time step
K	= coefficient of discharge
m	= an exponent
MLW	= mean low water
n	= Manning's coefficient of friction
Q	= volume rate of flow
R	= hydraulic radius
S_f	= friction slope
S_{fx}	= friction slope in the x-direction
S_{fy}	= friction slope in the y-direction
t	= time
u	= average velocity in the x-direction
v	= average velocity in the y-direction
V	= absolute velocity
V_w	= wind speed
W_x, W_y	= wind stress term in the equation of motion in the x-and y-directions.
x	= horizontal coordinate axis (abscissa)

y = horizontal coordinate axis (ordinate)

α = a variable

β = angle between the current direction and the x-axis.

Δt = time step

Δx = distance step

δ = angle between the wind direction and the x-axis.

θ = tidal time

ρ = density of water

ρ_a = density of air

τ_{bx} = bottom shear stress in the x-direction

τ_{by} = bottom shear stress in the y direction

τ_s = wind stress

τ_{sx} = surface shear stress in the x-direction

τ_{sy} = surface shear stress in the y-direction

ψ = geographical latitude

ω = angular speed of earth's rotation

I. INTRODUCTION

This report is concerned with the development of a numerical model for computing the flow dynamics in the Pamlico Sound, N. C. The model predicts the changes in the water velocity and water surface elevation under the action of freshwater inflows, tidal exchange and the winds.

Pamlico Sound is a large shallow body of partially saline water on the North Carolina coast separating the mainland from the offshore sandy beaches known as the Outer Banks. Freshwater flows into the Sound from the mainland rivers while the inlets cut in the Outer Banks provide for the exchange of seawater between the Sound and the Atlantic Ocean. The astronomical tide is significantly dampened as the tide moves through the inlets. However, strong wind tides can develop in the Sound.

The numerical model determines the magnitude and direction of currents in the Sound, the changes in the flow across the inlets and the fluctuation in water levels at all locations in the Sound. The information would be useful in water resource management. In particular, determination of surge heights under hurricane conditions is of critical importance in protection of life and property and in the planning of protective measures.

The numerical model is based on the two-dimensional long-wave equations of hydrodynamics. The equations are used to determine circulation, tidal flows and wind tides. However, they do not generally apply to short-crested waves. Therefore, short-crested waves are excluded from this study. For the purpose of this report, the fluid is assumed to be homogeneous and density stratification, if any, is neglected. The use of long-wave equation implies the existence of a hydrostatic pressure distribution and shallow water. Limited available data indicates that the assumptions involved in the theory are valid for the Sound. The average depth is only 16 feet and the measurements of salinity have indicated almost uniform vertical distribution representing well-mixed waters.

Measurements of velocities, even in the deeper parts of the inlets, show that water flows in the same direction at different depths, there being negligible vertical circulations.

A significant aspect of the study reported here is that it treats a spatial two-dimensional flow in a basin with very irregular bottom topography and very irregular shape. The Sound contains shoals as well as deeper areas. The boundaries do not follow a regular contour and contain cuts of various sizes at the inlet.

The numerical model has been made possible by the advent of the digital computer. It is feasible to handle irregular configuration and bottom topography, and also the nonlinear effects of advection, bottom stress and wind stress. Although much work has been done on modeling of one-dimensional flows in rivers and estuaries, however, two-dimensional modeling is not used widely. The two-dimensional problems generally involve unique boundary conditions. The basic principles apply in general, but each case requires considerable effort limited to the particular application.

The objective of this study is to compute the dynamics of flow in Pamlico Sound focusing on currents and water levels fluctuation due to a) river flows, b) tidal exchange across inlets, c) winds, and d) hurricanes.

II. BASIC EQUATIONS

The basic hydrodynamic equations consist of the equations for the conservation of mass and momentum. Under the restriction of hydrostatic pressure distribution or shallow water, the equations are known as the shallow water equations, the tidal equations and the long-wave equations. The shallow water assumption implies that the water depth is much smaller than the wave-length. The derivation of the shallow water equations is given in well-known reference works (Lamb 1932, Stoker 1957, Ippen 1966, Phillips 1969, and Dronkers 1964). The equations have been rederived in a report by Leendertse (1967) and in a

thesis by Chu (1970). For the sake of brevity, their derivation will be omitted from this report. The shallow water equations in two-dimensional flow are,

$$\frac{\partial u}{\partial t} + u \frac{\partial u}{\partial x} + v \frac{\partial u}{\partial y} + g \frac{\partial h}{\partial x} - fv = \frac{1}{\rho(h+d)} (\tau_{sx} - \tau_{bx}) = 0 \quad (2.1)$$

$$\frac{\partial v}{\partial t} + u \frac{\partial v}{\partial x} + v \frac{\partial v}{\partial y} + g \frac{\partial h}{\partial y} + fu = \frac{1}{\rho(h+d)} (\tau_{sy} - \tau_{by}) = 0 \quad (2.2)$$

$$\frac{\partial}{\partial x} \{u(h+d)\} + \frac{\partial}{\partial y} \{v(h+d)\} + \frac{\partial h}{\partial t} = 0 \quad (2.3)$$

In these equations, u = the average velocity in the x direction, v = average velocity in the y direction, h = the depth above the initially undisturbed water surface (usually taken at mean sea level), d = the initially undisturbed water depth above the bottom, f = coriolis coefficient, τ_{sx} = surface shear stress in the x direction, τ_{sy} = surface shear stress in the y direction, τ_{by} = bottom shear stress in the y direction, ρ = density of fluid (water), x = abscissa, y = ordinate and t = time. Equation (2.1) expresses the conservation of momentum in the x direction, equation (2.2) expresses the conservation of momentum in the y direction and equation (2.3) expresses the conservation of mass. Equation (2.3) is commonly known as the equation of continuity. The equations are also known as the long-wave equations, as the tidal equations and as the vertically integrated hydrodynamic equations. In one-dimensional form, the equations are known as the unsteady flow equations in open channels or as the St. Venant equations. The shallow water equations can be derived from the generalized Euler-Navier-Stokes equations under the assumption of long waves by integrating each term over the depth and dividing the result by the depth. Thus the average velocity implies a velocity averaged over the depth. The expressions

for the bottom shear stress are also related to the average velocity.

The value of f , the Coriolis coefficient, is $2 w \sin \psi$, where w is the angular speed of earth's rotation and ψ is the geographical latitude. The Coriolis force becomes important when the flow occurs in a relatively large body of water. In this study, only the horizontal components of the Coriolis force are considered important because the vertical component is negligible compared to the gravitational force.

The relationship between the shear stress and the average velocity is nonlinear when the flow is turbulent. The values of τ_{bx} and τ_{by} can be related to the energy gradient (friction slope) where the latter is given by some semi-empirical formula dependent on the boundary roughness. Thus,

$$\tau_{bx} = \rho g(h+d) S_{fx} \quad (2.4)$$

$$\tau_{by} = \rho g(h+d) S_{fy} \quad (2.5)$$

where $S_{fx} = S_f \cos \beta$, $S_{fy} = S_f \sin \beta$, S_f = friction slope, β = angle between the flow direction and the x-axis. In engineering applications, Chezy and Manning's formulas are commonly used. Then, using Manning's formula

$$S_f = \frac{n^2 V |V|}{2.22 R^{4/3}} \quad (2.6)$$

where n = Manning's friction coefficient, V = resultant velocity and R = hydraulic radius. In two-dimensional flows, the velocity components u and v are related to the resultant velocity by

$$u = V \cos \beta \quad (2.7)$$

$$v = V \sin \beta \quad (2.8)$$

and $R =$ water depth $(h+d)$. An approximate value for n for sand bottom is $n = 0.020$.

The surface stress due to the wind is usually given by the formulas

$$\tau_s = C_d \rho_a (V_w)^m \quad (2.9)$$

where $\tau_s =$ wind stress, $\rho_a =$ density of air, $V_w =$ surface wind velocity, $m =$ an exponent and $C_d =$ a dimensionless parameter.

It is to be noted that bottom stress and surface stress are basically the same type of physical process and both are expressed by similar formulas. The magnitude of the stress is related to some power of the fluid velocity at the interface, in one case between two different fluids (air and water) and in the other case between the fluid (water) and a solid (bottom boundary).

Wilson (1960) conducted an extensive review of literature to find suitable values for the wind stress over water. The tabulated values of C_d for light and strong winds (velocity measured at 10 meter height) are abstracted in Table 1. If the average value of C_d for strong winds is taken equal to 2.4×10^{-3} , and ρ_a , the air density is approximately 2.42×10^{-3} slugs/ft.³, then the value of the wind stress τ_s becomes

$$\tau_s = 5.8 \times 10^{-6} V_w^2 \frac{\text{slugs}}{\text{ft}^3} \quad (2.10)$$

The shear stress acquires the dimension of lb/ft^2 when the wind velocity V_w is given in ft/sec. The wind stress in the equation of motion becomes

$$\frac{\tau_s}{\rho(d+h)} = \frac{3.0 \times 10^{-6}}{\rho(d+h)} V_w^2 \quad (2.11)$$

with the dimension of acceleration. It will be expressed in ft/sec. when V_w is given in ft/sec, d and h are in feet, and ρ the water density is given in slugs/ft.³.

TABLE 1.

DRAG COEFFICIENT, C_d AND OTHER PARAMETERS FOR LIGHT AND STRONG WINDS,
AFTER WILSON (1960)

<u>Parameter</u>	<u>Light Wind</u>	<u>Strong Wind</u>
Range	0.4×10^{-3} to 6.2×10^{-3}	1.5×10^{-3} to 4.0×10^{-3}
Overall Average	$1.5 \times 10^{-3**}$	2.4×10^{-3}
Standard Deviation	0.83×10^{-3}	0.56×10^{-3}
ρ_a in slugs/ft ³	2.42×10^{-3}	2.42×10^{-3}
$\tau_s = C_d \rho_a \cdot V_w^2$ using the average	$3.63 \times 10^{-6} \cdot V_w^2$ lb/ft ² with V_w in ft/sec.	$5.8 \times 10^{-6} \cdot V_w^2$ lb/ft ² with V_w in ft/sec.
$\tau_s^* = \tau_s / \rho$ (in ft ² /sec. when V_w is given in ft/sec.)	$1.875 \times 10^{-6} \cdot V_w^2$ ft ² /sec ² with V_w in ft/sec.	$3.0 \times 10^{-6} \cdot V_w^2$ ft ² /sec ² with V_w in ft/sec.

**One value of $C_d = 6.2 \times 10^{-3}$ derived for a wind velocity of 10 MPH over Gulf of Mexico was disregarded in the averaging.

III. REVIEW OF LITERATURE

Two-dimensional long-wave propagation has received considerable attention from numerical modelers because the system of equations describes a physical situation of great practical interest in the management of coastal waters. Hansen (1956) was the first to perform the computation of long waves in the sea by using a computer. He used the explicit finite difference scheme, with a forward difference in time and a central difference in space. Harris et al (1964) indicated the difficulties encountered in the treatment of two-dimensional long wave problems by the explicit method. Jelesnianski (1966) applied a linearized form of the two-dimensional equations to compute the storm surge on the open coast. Reid and Bodine (1968) modeled the hydrodynamic behavior of Galveston Bay, Texas, for storm surge conditions. The vertically integrated forms of the equations of motion and continuity were solved by the explicit finite difference method. The effect of rainfall, wind stress and quadratic bottom friction were taken into consideration but the terms dealing with convective acceleration and the coriolis force were ignored. Heaps (1969) has formulated an explicit finite difference sea model involving forward and backward differences in time, and central differences in space. Comparisons have been made between the computed and observed surge profiles at a number of ports distributed around the shores of the North Sea. Some of the discrepancies between the computed and observed values appear to have been due to incomplete representations in the models of the actual conditions in coastal waters along with the neglect of nonlinear effects.

Leendertse (1967) developed the semi-implicit scheme using implicit alternating-direction method. The accuracy of the computation scheme has been extensively tested on tidal-flow models of the estuary of the Rhine River and of the North Sea by comparing measured data with the computed results.

Sobey (1970) compared several difference schemes for two-dimensional long wave propagation by means of the propagation factor described by Leendertse (1967). He demonstrated the usefulness of the propagation factor as a measure of the stability of the finite difference schemes. Chu (1970) used the Lax-Wendroff method for the numerical solution of two-dimensional equations. Recently Hess and White (1974) developed the numerical model of Narragansett Bay using the basic approach of Leendertse (1967), but with several modifications. Airan (1975) applied the explicit two-dimensional model to idealized basins and to Pamlico Sound for determination of circulation, hurricane surge and water quality. Considerable material in this report is shared with the thesis by Airan.

IV. NUMERICAL MODELING

Overview of Available Numerical Techniques

The techniques for solving partial differential equations can be classified as analytical and numerical. Analytical solutions of the hyperbolic partial differential equations are practically impossible especially if the shape of the waterbody is not regular. The following observations are based mostly on experience with one-dimensional flows but are basically applicable to two-dimensional cases as well.

The numerical techniques can be subdivided into finite element and finite differences. The finite element technique has been successfully applied to problems in structures and other engineering disciplines. However, its use in river and estuarine modeling is new and will not be discussed here.

The finite difference techniques are based on the general assumption that partial derivatives can be approximated by using the values of functions at points which are separated by finite increments of distance or time. Thus, the differential equations are transformed to algebraic equations by replacing each derivative with corresponding finite difference term. These equations are solved

subject to the considerations for stability, convergence, accuracy, and efficiency of numerical procedures.

Before the availability of high-speed computers, the equations were mostly solved by approximate methods based upon simplified assumptions. However, it is now possible to attempt numerical solution of the complete (unsimplified) equations. The complete methods can be of characteristic or direct type.

In the characteristic approach, the equations are first transformed into the so-called characteristic form and then solved by implicit or explicit finite difference representation. In both cases, either a characteristic network or a fixed mesh of points is used on the time-distance plane to identify the points at which solutions are obtained. The direct methods are those in which the finite difference representation is based directly on the primary equations. They include implicit, explicit, and Lax-Wendroff methods all of which use the fixed rectangular grid.

Each method presented above could have many variations depending on what type of mesh is selected and what procedure is used for the solution of finite difference equations. However, the following finite difference methods have been found most useful in the analysis of hydrodynamic problems:

- 1) The characteristic implicit method using characteristic network
- 2) Direct implicit method using fixed mesh
- 3) Direct explicit method using fixed mesh, and
- 4) Direct Lax-Wendroff method using fixed mesh

These four methods are generally known as method of characteristics, implicit method, explicit method, and Lax-Wendroff method respectively (Amein and Fang, 1969; Chu, 1970).

The method of characteristics involves numerical integration along selected curves on the time-distance plane (Amein, 1966b; Fletcher and Hamilton, 1967; Ellis, 1970). The main disadvantage of this method is that considerable interpolation becomes necessary when presenting the results. It is very awkward for

natural water-basins of irregular shape (Amein, 1967).

In the implicit method, an unknown in a given time step depends upon the variables in the previous time step as well as on the other unknowns in the given time-step (Amein, 1968; Amein and Fang, 1969 and 1970). In this method, it becomes necessary to solve by iteration a great number of simultaneous non-linear algebraic equations. Wylie (1970) compared the different numerical methods and concluded that in the implicit method an incorrect result is possible if the reach lengths and corresponding time increments are increased to extreme values. It has been observed that under certain conditions, the implicit difference equations exhibit oscillations (Liggett and Woolhiser, 1967; Baltzer and Lai, 1972; Fread, 1973).

In the Lax-Wendroff method, the computations are tedious, the programming is complex, and changes in the program are difficult to make. However, the technique offers the benefits of stability, relatively longer time steps and accuracy (Amein, 1971). The method was used to analyze circulation patterns in Pamlico Sound by Chu (1970).

In the explicit method, the numerical procedure for the solution of equations is essentially based on finding the values at a future time step by extrapolating from the previous time step, subject to the laws of mechanics as well as the initial and boundary conditions. In this study, the direct explicit method is used because it is simple to formulate, provides greater flexibility in making changes or improvements in the programs, facilitates the introduction of input data or physical parameters, and the step-size is relatively independent of the size of the system (Amein, 1971; WRE, 1966).

The Explicit Method

This method is based on the basic differential equations without going through some intermediate transformations. The method is called explicit because the unknowns can be computed explicitly from the algebraic finite difference

equations.

Stoker, Isaacson, and their colleagues (1953, 1954, 1956, 1957) have done pioneering work in applying the explicit method to flood routing in Ohio and Mississippi rivers. Schaaque (1965), Amein (1966a), Liggett and Woolhiser (1967), and Garrison et al. (1969) have also applied different forms of the explicit method to other types of flow problems. The grid size and time steps in the explicit method are governed by considerations for the stability of its numerical scheme for computations. The surge computations of Reid and Bodine (1968) and of Jelesnianski (1966) are based on the explicit method.

Figure 1 shows a rectangular network for the explicit method. The x and y coordinates are represented by i and j whereas the time step is given by k.

The finite difference approximations which are used to represent the partial derivatives can be derived by truncating a Taylor series expansion of a function at a point (Hildebrand, 1968; Ames, 1969; Mitchell, 1969; Stark, 1970):

$$\alpha(x+\Delta x, y) = \alpha(x, y) + \Delta x \frac{\partial \alpha}{\partial x}(x, y) + \frac{(\Delta x)^2}{2!} \frac{\partial^2 \alpha}{\partial x^2}(x, y) + \frac{(\Delta x)^3}{3!} \frac{\partial^3 \alpha}{\partial x^3}(x, y) + \dots \quad (4.1)$$

where α represents the variable of interest. Dividing by Δx and rearranging

$$\frac{\partial \alpha}{\partial x}(x, y) = \frac{\alpha(x+\Delta x, y) - \alpha(x, y)}{\Delta x} + 0(\Delta x) \quad (4.2)$$

where $0(\Delta x)$ represents the order of magnitude of the truncation error. In the subscripted notation, equation (4.2) could be written as:

$$\frac{\partial \alpha_{i,j}^k}{\partial x} = \frac{\alpha_{i+1,j}^k - \alpha_{i,j}^k}{\Delta x} + 0(\Delta x) \quad (4.3)$$

where i, j, and k represent x, y, and t axes as given before. Equation (4.3) is generally described as the "forward difference" form of the finite difference representation. Similarly, other forms of such relationships can be derived or, more simply, written by visualizing the relationship between slopes and values of

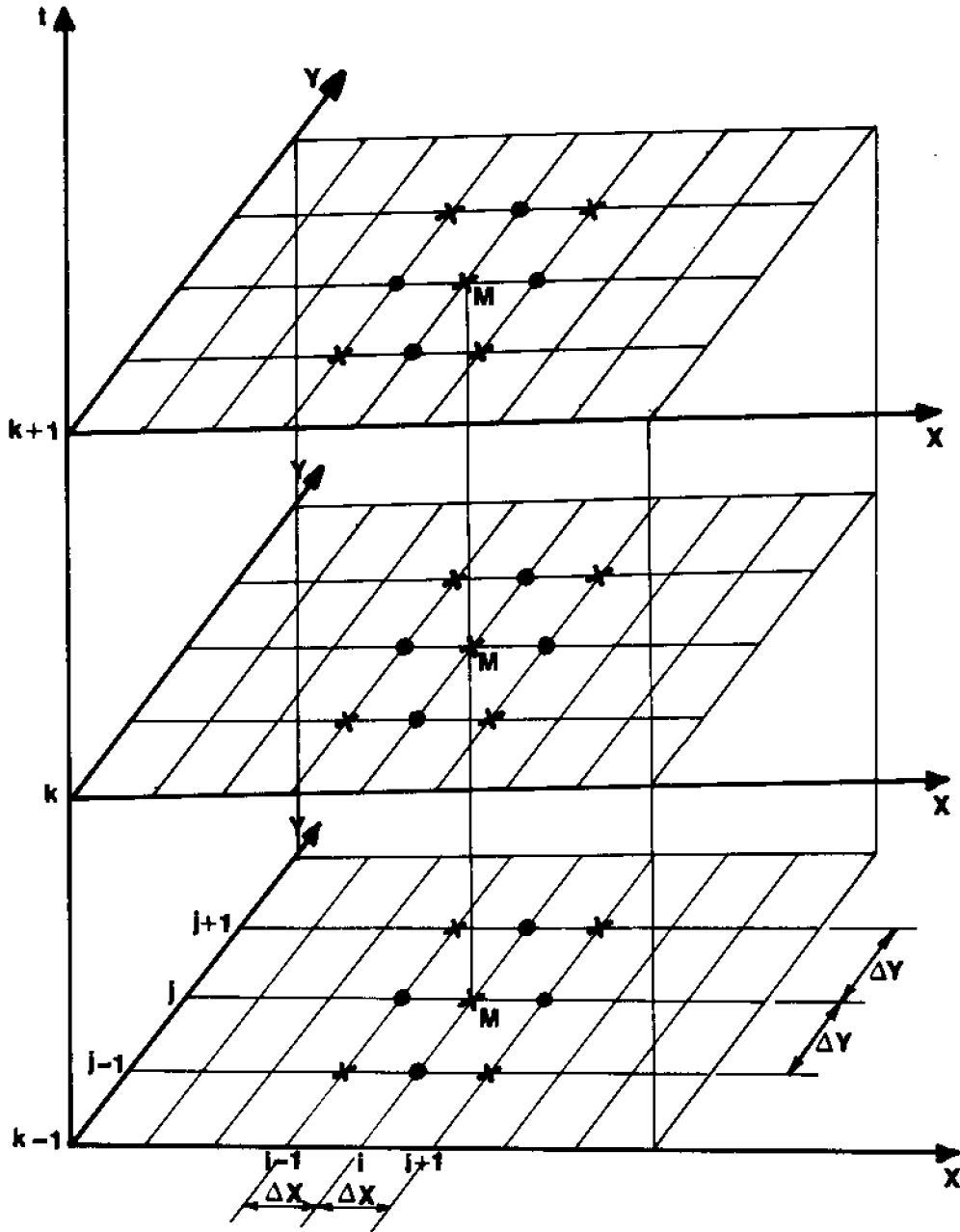


FIGURE 1. Fixed Rectangular Network For Explicit Method

a function at separated points. For example,

$$\frac{\partial \alpha_{i,j}^k}{\partial x} = \frac{\alpha_{i,j}^k - \alpha_{i-1,j}^k}{\Delta x} + O(\Delta x) \quad (4.4)$$

$$\frac{\partial \alpha_{i,j}^k}{\partial x} = \frac{\alpha_{i+1,j}^k - \alpha_{i-1,j}^k}{2\Delta x} + O[(\Delta x)^2] \quad (4.5)$$

Similar expressions can be written for partial derivations with respect to y. Equation (4.4) shows the "backward difference" and equation (4.5) shows the "central difference" forms of the given partial derivatives. By using more neighboring points, an unlimited number of other finite difference approximations can be obtained. However, the three forms as given above are compact and have been found to be the most useful in finite difference modeling of river and estuarine systems.

In this study, the central difference form is used to get the finite difference expressions for all partial derivatives with respect to x and y. Similarly, the partial derivatives with respect to t are approximated by using the forward difference scheme as given below:

$$\frac{\partial \alpha_{i,j}^k}{\partial t} = \frac{\alpha_{i,j}^{k+1} - \bar{\alpha}_{i,j}^k}{\Delta t} \quad (4.6)$$

where

$$\bar{\alpha}_{i,j}^k = \frac{1}{4} \{ \alpha_{i+1,j+1}^k + \alpha_{i-1,j+1}^k + \alpha_{i+1,j-1}^k + \alpha_{i-1,j-1}^k \} \quad (4.7)$$

it should be noted that in equation (4.6) $\bar{\alpha}_{i,j}^k$ as defined by equation (4.7) is used instead of what would generally be expected, $\alpha_{i,j}^k$. This is essential in order to satisfy the stability considerations.

When all the partial derivative terms in the basic equations (2.1, 2.2, and 2.3) are replaced by their corresponding finite difference forms as given in equations (4.3) through (4.7), the following algebraic equations are obtained:

$$h_{i,j}^{k+1} = \frac{-\Delta t}{2\Delta x} \left[u_{i+1,j}^k (h_{i+1,j}^k + d_{i+1,j}) - u_{i-1,j}^k (h_{i-1,j}^k + d_{i-1,j}) \right] - \frac{\Delta t}{2\Delta y} \left[v_{i,j+1}^k (h_{i,j+1}^k + d_{i,j+1}) - v_{i,j-1}^k (h_{i,j-1}^k + d_{i,j-1}) \right] + \bar{h}_{i,j}^k \quad (4.8)$$

$$u_{i,j}^{k+1} = -\frac{u_{i,j}^k}{h_{i,j}^k} \left[u_{i+1,j}^k - u_{i-1,j}^k \right] \frac{\Delta t}{2\Delta x} - v_{i,j}^k \left[u_{i,j+1}^k - u_{i,j-1}^k \right] \frac{\Delta t}{2\Delta y} - g \left[h_{i+1,j}^k - h_{i-1,j}^k \right] \frac{\Delta t}{2\Delta x} + f \cdot v_{i,j}^k \cdot \Delta t - g \cdot s_f \cdot \bar{u}_{i,j}^k \cdot \Delta t + \frac{w_x \cdot \Delta t}{h_{i,j}^k + d_{i,j}} + \bar{u}_{i,j}^k \quad (4.9)$$

$$v_{i,j}^{k+1} = -\frac{v_{i,j}^k}{h_{i,j}^k} \left[v_{i+1,j}^k - v_{i-1,j}^k \right] \frac{\Delta t}{2\Delta x} - \frac{v_{i,j}^k}{h_{i,j}^k} \left[v_{i,j+1}^k - v_{i,j-1}^k \right] \frac{\Delta t}{2\Delta y} - g \left[h_{i,j+1}^k - h_{i,j-1}^k \right] \frac{\Delta t}{2\Delta y} - f \cdot \bar{u}_{i,j}^k \cdot \Delta t - g \cdot s_f \cdot \bar{v}_{i,j}^k \cdot \Delta t + \frac{w_y \cdot \Delta t}{h_{i,j}^k + d_{i,j}} + \bar{v}_{i,j}^k \quad (4.10)$$

where

$$s_f = \frac{n^2 \left[(\bar{u}_{i,j}^k)^2 + (\bar{v}_{i,j}^k)^2 \right]^{4/3}}{2.22 (h_{i,j}^k + d_{i,j})} \quad (4.11)$$

$$w_x = \frac{\tau_{sx}}{\rho} = \frac{C_d \rho_a V_w^2}{\rho} \cos \delta \quad (4.12)$$

and

$$w_y = \frac{\tau_{sy}}{\rho} = \frac{C_d \rho_a V_w^2}{\rho} \sin \delta \quad (4.13)$$

where δ is the angle between the wind direction and the x-axis.

If values of all the variables are known at all locations at a given time, say k , then the three algebraic equations can be solved explicitly at time $(k+1)$ and point (i,j) . The values for other grid points at $(k+1)$ are also obtained in the same way. The computations can then be extended to succeeding time steps $(k+2), (k+3)$, until all the desired values become known.

Initial and Boundary Conditions

The solution of finite difference equations, as described above, requires that the initial and boundary conditions be satisfied. The initial conditions would be given by the known values of water velocity, direction and depth at all locations in the waterbody at a given time.

The boundary conditions would be prescribed by the values of water discharge with respect to time at all inflow and outflow locations. If necessary, the discharge can be replaced by water surface elevations at the points where rivers make a junction with the waterbody and at tidal inlets. At all other boundary points, it is assumed that there is no flow across the boundary, i.e., at the points on solid boundary, $u=0$ and $v=0$. In the case of wind-driven circulation and resulting water quality, the wind speed and direction with respect to time would also be required at all points.

It should be noted that in applying the model, specific numerical values of some parameters are needed. These parameters are: the coriolis coefficient, the bottom friction coefficient and wind stress coefficients in longitudinal and lateral directions. Many of these coefficients are difficult to evaluate

and are governed by the natural processes of complex nature specific to the waterbody. If the relationships are not known precisely, empirical or semi-empirical values based upon the available data and good judgement have to be adopted. Sometimes, these values can be verified by conducting appropriate field investigations.

Stability Considerations

A converging solution for the set of finite difference equations is possible only when the rounding off errors in the numerical procedure are not amplified in an unlimited manner. A complete stability criterion for the numerical solution of nonlinear equations of free-surface flow is not available. Generally, the equations are reduced to linearized forms and then the stability conditions are established. The familiar criterion of stability known as Courant condition (Isaacson et al., 1958; Liggett and Woolhiser, 1967; and Strelkoff, 1970) is given as:

$$\Delta t \leq \frac{\Delta x}{\sqrt{g(d+h)}} \quad (4.14)$$

in which c , the wave propagation velocity = $\sqrt{g(d+h)}$

Richtmyer and Morton (1967) investigated the stability condition for linear explicit finite difference schemes and found that the system is locally stable provided:

$$\frac{\Delta t}{\Delta x} \leq \frac{1}{2} \frac{1}{\sqrt{g(d+h)_{\max}}} \quad (4.15)$$

If the equations include the effects of friction, lateral flow, or the terms to describe the non-prismatic character of the channel, the limits for stability are not clearly presented in the literature, even when the equations are linearized (Wylie, 1970).

An approximate criterion for the stability of non-linear difference equations can be obtained by Fourier analysis of the error propagation properties

of the corresponding linearized forms. This stability analysis, by O'Brien et al. (1951), has been used by Abbott and Ionescu (1967), Leendertse (1967) and others. For the hydrodynamic equations, this approach results in the following limit on allowable time step in rectangular grid explicit formulation:

$$\frac{\Delta t}{\Delta x} \leq \frac{1}{c} \sqrt{1 - f_1 \frac{\Delta t}{2}} \quad (4.16)$$

in which $f_1 = gn^2 \frac{2}{\bar{V}} \frac{2}{2.22 \bar{R}} \frac{4}{3}$, the barred quantities representing average flow conditions.

In this study, the basic Courant condition as given by equation (4.14) was used as the stability criterion. While calculating the size of time step, the minimum value of numerators and maximum value of denominators were used. This approach leads to a conservative estimate of Δt , since the maximum and minimum values of the relevant parameters would rarely occur at the same point.

Computations

The water body to be studied is simulated on a rectangular grid system and a boundary is drawn through the grid points so as to fit a map of the natural boundary closely. A suitable scale determining the grid size and grid density is selected. The coordinates of a point in the water body are identified by the subscripts (i,j), where i represents the abscissa, and j represents the ordinate. Time is represented by the superscript k.

To begin with, the values of local depths at mean low water (MLW) are known at some grid points. The depths at other points are determined by interpolation. The minimum value of depth was assumed to be five (5) feet, which implies that the boundary chosen in the model lies well inside the natural boundary. With initial conditions being known, the circulation parameters are computed at each future time step by the following schedule:

1. Compute u, v and h at the interior points marked by "squares" on alternate rows with even numbered values of x. Use basic equations and get necessary

data from previous time step.

2. Compute u , v and h , at the interior points marked by "squares" on alternate rows with odd numbered value of x . Use basic equations and get necessary data from previous time step.
3. Compute u , v , and h , at interior points marked by "circles" on one grid inside the boundary. Use basic equations and get necessary data from previous time step.
4. Compute u , v , and h at the remaining interior points marked by "circles" on alternate rows with odd numbered values of x . Use mid-side averages of the values already computed in current time step.
5. Compute u , v and h at the remaining interior points marked by "circles" on alternate rows with even numbered values of x . Use mid-side averaging of the values already computed in current time step.
6. Compute h at all boundary points using the condition of geometric compatibility.
7. Compute u and v at inflow junctions using the current values at the corresponding nearest interior points and at outflow locations from the computed values of discharges and depths in the current time step. The values of u and v at all other boundary points are equal to zero.

Interior Grid Points

The interior grid points are marked by "squares" and "circles" alternately in both directions as explained above. Knowing all the initial boundary conditions at a time, $t=k$, the values of u , v , and h are computed at interior "square" points by using the finite difference equations (4.8 to 4.10). Figure 2a gives the computational module for an interior "square" point, (i,j) . It is noted that the previous time step values at eight neighboring points are used in the computations.

The values of parameters at interior "circle" points are found by mid-side averaging of the current type step values already computed at the four neighboring "square" points (Figure 2b).

V. HYDROGRAPHY OF PAMLICO SOUND

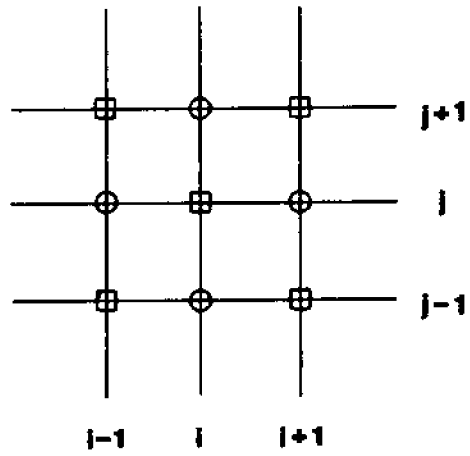
Hydrological Information

The Pamlico Sound, located in eastern North Carolina, is the largest of the embayments formed behind a narrow strip of barrier beaches along the Atlantic Coast of the United States. As compared to other embayments along the U. S. Coast, it is relatively shallow and has an estimated total drainage area of 20,000 square miles (Roelofs and Bumpus, 1953).

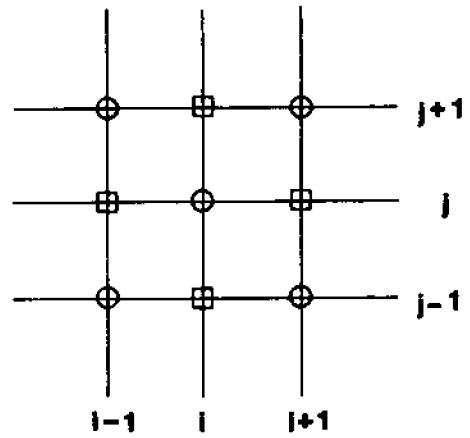
The Pamlico Sound (Figure 3) is bordered by the mainland with its tributary rivers on the western side, and by the Outer Banks on the eastern side. At its northern end, it connects with the Albemarle Sound through the Croatan and Roanoke Sounds. In the southern direction, it is continuous with the Core Sound. The main tidal inlets that connect Pamlico Sound to the Atlantic Ocean are Oregon, Hatteras, and Ocracoke Inlets.

Pamlico Sound covers an area of approximately 1700 square miles. It is nearly 70 miles long in the southwest-northeast direction and 10 to 30 miles wide in the southeast-northwest direction, being narrowest at the northern end and widest opposite Hatteras Island. The average depth in the sound is approximately 16 feet. A deeper water area is found on the west side of the main body with a maximum depth of 22 feet. Shoaling regions are located near the entrances for Neuse and Pamlico rivers and near the tidal inlets.

Two large river systems, the Neuse-Trent and the Tar-Pamlico, discharge directly into the sound. Two other rivers, Chowan and Roanoke, empty into the Albemarle Sound which in turn discharges to Pamlico Sound through Croatan and Roanoke Sounds. In addition to the four river systems, there are many short,



a. Computational Module For Interior "Square" Points



b. Computational Module For Interior "Circle" Points

FIGURE 2. COMPUTATIONAL MODULE AT INTERIOR GRID POINTS

wide streams which contribute to the water supply of Pamlico Sound complex by draining the surrounding swampy areas. However, the quantitative nature of such contributions has not been fully evaluated.

The average annual rainfall on the contributing basins exclusive of the coastal region itself is in excess of 45 inches. Runoff, however, is only 30% of this amount or about 14 inches per year. Maximum runoff takes place in the spring months and minimum runoffs occur in June and again in October and November. Evaporation data are sparse but from preliminary studies it appears that during the summer months, evaporation and rainfall are about equal (Smallwood and Amein, 1967).

Factors Affecting the Circulation

There are many natural factors which significantly influence the hydrodynamics of Pamlico Sound. These include the evaporation and rainfall, surface wind stress, freshwater inflows, tidal exchange, coriolis force due to rotation of the earth, and bottom topography.

The influence of evaporation and rainfall can be neglected because they are evenly distributed over the sound. The coriolis force is significant only for water bodies much larger than Pamlico Sound and therefore in this study, the coriolis stress coefficient is assumed to be zero. The frictional forces due to the irregular bottom topography have been calculated using a Manning coefficient of 0.02.

The mouths of Oregon, Hatteras and Ocracoke Inlets are small as compared to the width and size of the Sound. Therefore, there are no perceptible lunar tides away from the inlets (Posner, 1959). The dominating factor in determining the flow pattern in the sound is the wind force. According to Roelofs and Bumpus (1953), the currents in Pamlico Sound, which are relatively weak, depend mainly upon the direction and velocity of the wind and, not upon tidal oscillations. Hurricane driven tides may be in excess of five feet in some parts of the sound

(Smallwood and Amein, 1967). Minimum wind influence occurs in the months of June and July.

The effect of mean annual freshwater inflow to the sound is also small. Therefore, except during the flooding season, the runoff current would easily be overpowered by the currents due to the wind friction.

Freshwater is discharged to the sound from the Neuse and Pamlico rivers and from Roanoke and Croatan Sounds. Gage records at Tarboro and Kinston can be used to estimate the flow from the Pamlico River and the Neuse River. A statistical analysis of the flood flow for these two rivers is given in Figure 4 (Chu, 1970). It is estimated that 52% of the flow from the Neuse River and 49% of that for the Pamlico River is contributed by ungaged parts of their drainage basins. Therefore, in determining the total flow from these two basins into the sound, it is assumed that the discharge from ungaged areas is proportional to that for the gaged areas.

The average inflow from Roanoke and Croatan Sounds is assumed to be equal to the discharge from the Chowan River, the Roanoke River, and 4000 square miles of marshes into the Albemarle Sound. The average annual flow from the Chowan and Roanoke rivers is estimated to be 1.10 cfs per square mile (USGS, 1963; Hammack, 1969). The discharge from marsh areas is estimated by Hammack (1969) to be 1.00 cfs per square mile. The distribution of Albemarle Sound discharge between the Roanoke and Croatan sounds is assumed to be directly proportional to their cross sectional areas. Based upon this assumption, Jarrett (1966) estimated that 85% of the flow passes through Croatan Sound and only 15% is carried by the Roanoke Sound.

Tables 2 and 3 give the mean annual values and percentages of all freshwater inflows to the Pamlico Sound and Table 4 shows the estimated values of 5, 10, and 20-year flood flows as given by Chu (1970).

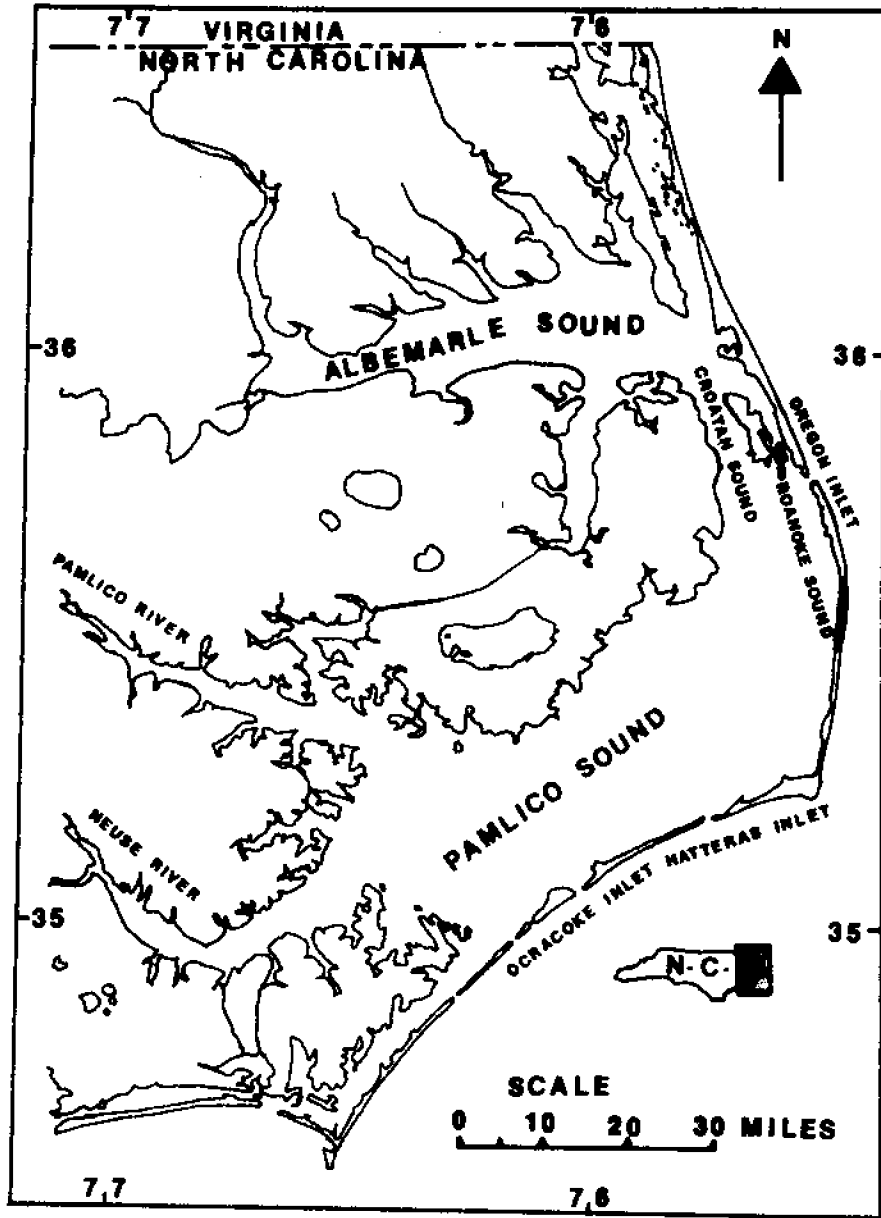


FIGURE 3 Location Map Of Pamlico Sound And Its Tributary Waters

TABLE 2. MEAN ANNUAL DISCHARGE FROM THE DRAINAGE BASINS CONTRIBUTING TO PAMLICO SOUND

Basin	Gaged Area (mi ²)	Discharge (cfs)	Ungaged Area (mi ²)	Estimated discharge (cfs)	Total discharge (cfs)
Neuse River	3601	3938	2039	1242	5180
Pamlico River	2233	2420	1967	2150	4570
Roanoke River	8410	8155	1220	1185	9340
Chowan River	255	315	4555	5020	5335
Marshes	0	0	4000	4000	4000

TABLE 3. MEAN ANNUAL DISCHARGE AND THE PERCENTAGE OF DISCHARGE FROM THE ENTRIES TO PAMLICO SOUND

Entry	Mean annual discharge (cfs)	Percentage of discharge (%)
Neuse River	6180	21
Pamlico River	4570	15.5
Croatan Sound	15,830	53.7
Roanoke Sound	2845	9.8
Total Amount	29,425	100

TABLE 4. ESTIMATED 5, 10, AND 20 YEARS FLOOD FLOW
FROM THE ENTRIES TO PAMLICO SOUND

Entry	5 years flood (cfs)	10 years flood (cfs)	20 years flood (cfs)
Neuse River	36,000	46,000	70,000
Pamlico River	42,000	54,000	80,000
Croatan Sound	92,000	117,400	178,800
Roanoke Sound	16,800	21,400	32,600

VI. APPLICATION OF NUMERICAL MODELING TO PAMLICO SOUND

The limited field data on Pamlico Sound indicate that there is little vertical circulation in Pamlico Sound and the shallow water conditions prevail (Roelofs and Bumpus, 1953; Amein, 1971). The vertical salinity gradients are uncommon in the sound and it can be assumed to be well mixed in the vertical direction (Roelofs and Bumpus, 1953; Posner, 1959; Woods, 1967; and Amein, 1971). Therefore, in this study, the shallow water equations derived in Section 3 were used for analyzing the circulation in the sound. The Pamlico Sound was represented by the zig-zag boundary on a two dimensional 61x35 grid as shown in Figure 5. Each cell represents a distance of 7422 ft. in either direction. The grid points have been marked by "squares" and "circles" alternately in both directions as explained previously. There are three openings representing the mouths of the Neuse River, the Pamlico River and the Croatan and Roanoke Sounds. Three more openings simulate the locations of Oregon, Hatteras and Ocracoke Inlets.

The local water depths, d , have been noted from the hydrographical maps of U. S. Coast and Geodetic Survey and other sources. A minimum value of 2 feet depth has been assumed implying that the boundary is drawn slightly inside of the actual shoreline. It has been assumed that at time $t = 0$, the sound is still at the mean low water level (MLW), that is, at all interior points, the velocity in longitudinal direction - u , the velocity in lateral direction - v , and the variation of depth with respect to MLW - h are all equal to zero. Unless specified otherwise, it is assumed that the sound receives a constant freshwater inflow equal to the estimated 20-year flood flows as given in Table 4, that is:

Neuse River, Q_1	70,000 cfs
Pamlico River, Q_2	80,000 cfs
Croatan and Roanoke Sounds, Q_3	211,400 cfs

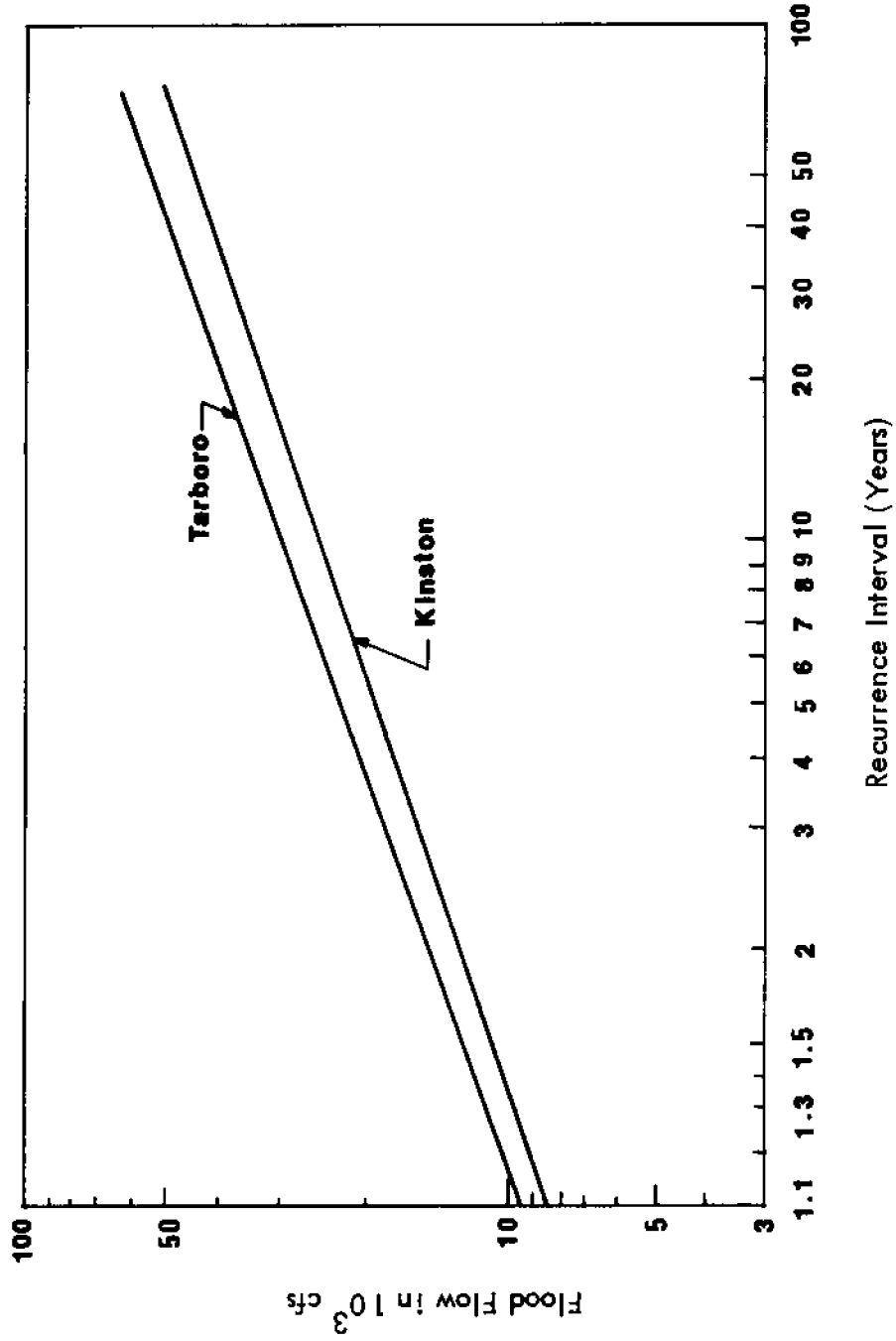


FIGURE 4. Floods at Kinston and Tarboro to estimate the Flows From the Neuse and Pamlico Rivers.

When the tidal inlets are assumed to be open, their flow is calculated from the difference in water elevations in the sound and those in the sea.

Numerical Simulation

The Pamlico Sound is represented on a two-dimensional 61x35 grid as shown in Figure 5. The origin for the grid system is taken at the intersection of 35°N latitude with 76°W longitude. Each cell represents a square 7422 ft. x 7422 ft. The x-axis makes an angle of 45° clockwise with the 76°W longitude. Each point on the grid is identified by the double subscript (i,j) where i measures the number of Δx steps from the origin along the x-axis and j represents the number of Δy steps along the y-axis. Each point is further designated as a square if the sum of i and j at that point is even, and each point is designated as a circle if the sum of i and j at that point is odd.

The grid points identifying the boundaries are numbered consecutively clockwise from 1 to 192 starting at (5,24). Thus the Neuse River confluence with the Sound is identified as grid points (5,23), (5,24), (5,26), and (5,27), and also as boundary points Nos. 192, 1, 2, 3 and 4.

The procedure for numerical modeling consists of applying the equations of motion in finite difference form between the lowest and highest values of i on a given row. The computations are started at the bottom row (lowest j value) and the solutions are marched row by row until the highest value of j is reached. Assuming that the values of all variables are known at time t^k , then a complete sweep of the grid system inside the boundary points furnishes the values of the variables at time step $t^{k+1} = t^k + \Delta t$. To avoid possible instability conditions, a staggered computational scheme is used in that the variables are computed at staggered points on the network by finite difference equations based on the hydrodynamic equation and the values at the remaining points are calculated by averaging the values from the adjacent neighborhood. The two sets of points are recognized by the sum of i and j. Thus the value of

of u, v, and h may be computed by the finite differences at points marked by squares, and the values at points marked by circles may be determined by averaging. For example, the values of u, v and h are computed by the use of equations 4.9, 4.10 and 4.11 at points (15,21), (17,21), (16,22), (15,23) and (17,23) and the value of u, v and h at (16,21) is calculated as:

$$\begin{aligned} u(16,21) &= \frac{1}{4} \left\{ u(17,21) + u(15,21) + u(16,22) + u(16,20) \right\} \\ v(16,21) &= \frac{1}{4} \left\{ v(17,21) + v(15,21) + v(16,22) + v(16,20) \right\} \\ h(16,21) &= \frac{1}{4} \left\{ h(17,21) + h(15,21) + h(16,22) + h(16,20) \right\} \end{aligned}$$

For the sake of consistency, the values at points marked by squares are computed by equations 4.9, 4.10 and 4.11, and the values at points marked by circles are computed by averaging the values at adjacent points. It is also expedient to compute the values at all points one grid inside the boundary by the use of equations 4.9 through 4.11 regardless of whether the sum (i+j) is odd or even.

Boundary Conditions

A major problem in the computation of flow in two dimensions is the specification of boundary conditions. If the values of the discharge or water surface elevations are known, then these values could be prescribed as the boundary conditions. However, with the possible exception of using the sea-level as the boundary, the water surface elevation or the discharge at the boundaries of a water basin may not be known. Furthermore, the determination of these values at the entrances to the basins may be the primary purpose of the modeling effort.

The boundary conditions used in this model at the confluence of the rivers with the Sound are given as "geometric compatibility" conditions. The "geometric compatibility" condition assumes a linear variation of water surface elevation and water velocity with distance extending outward from the Sound into the rivers.

This condition permits the reversal of flow from the Sound into the rivers under the action of strong winds. However, from the hydrodynamic point of view, it is a weak condition and is not as satisfactory as the use of values of stage or discharge.

The "geometric compatibility" condition is also used for the computation of water depth at the land boundaries. The water surface is assumed to have the same slope at the land boundary as at points one grid inside the boundary. The velocity, however, is taken to be zero at the land boundary.

The boundary points are classified into eight (8) types depending upon the location of the point. Each type requires a special boundary equation. For example, the equation for determining the stage at (50,10) is different from that at (30,22). The boundary points under each type of classification and the boundary equations pertaining to a given type are given in the computer programs and are printed in Section 11.

Tidal Exchange Computations

The flow through a tidal inlet is derived from the hydraulic gradient between water surfaces in the basin and the sea. The discharge is influenced by many factors including the turbulent frictional resistance of the connecting passage, channel and basin geometry, and the relative values of water elevations in the basin and the sea. A number of methods have been developed for the flow computations in a tidal inlet (Brown, 1928; Baines, 1957; Dronkers and Schonfeld, 1955; Baines and Knapp, 1965). However, these methods are applicable to relatively small basins of regular shape. Keulegan and Hall (1950) and Keulegan (1967) formulated the rheological system of a relatively long inlet connecting a basin with uniformly changing water surface to a sea:

$$\frac{dH_1}{d\theta} = K \sqrt{H_2 - H_1} \quad \text{When } H_2 > H_1 \quad (6.1)$$

or

$$\frac{dH_1}{d\theta} = -K \sqrt{H_1 - H_2} \quad \text{When } H_1 > H_2 \quad (6.2)$$

where H_1 is the water stage in the basin with respect to mean sea level, H_2 is the water stage in the sea with respect to mean sea level, θ is the specific tidal time and K is a coefficient of discharge.

Keulegan's method is applicable for systems in which the propagation of the tidal wave may be neglected (Broome, 1968). Therefore, it was applied to find the flow through Oregon, Hatteras, and Ocracoke inlets between Pamlico Sound and Atlantic Ocean. Equations (6.1) and (6.2) were rewritten for Pamlico Sound as:

$$Q = K \cdot \sqrt{H_2 - H_1} \quad \text{when} \quad H_2 > H_1 \quad (6.3)$$

or

$$Q = -K \cdot \sqrt{H_1 - H_2} \quad \text{when} \quad H_1 > H_2 \quad (6.4)$$

In applying this formula to the tidal inlets at Pamlico Sound, it was assumed that the sea water surface remains at mean sea level. H_1 was found by averaging the values of water stage at the inlets. The coefficients of discharge for Oregon, Hatteras and Ocracoke inlets were taken as 98800, 108500, and 165400 respectively as calculated in Table 5. The sign convention followed for Q was that it was positive for inflow and negative for outflow.

TABLE 5. VALUES OF DISCHARGE COEFFICIENTS FOR TIDAL INLETS

Inlet	Observed transport during flood conditions* m ³	Mean tidal range* ft.	Mean half tidal range (Δh) ft.	Estimated proportionate discharge (Q) cfs	K=Q/ Δh
Oregon	56 x 10 ⁶	1.8	0.9	93,500	98800
Hatteras	65 x 10 ⁶	2.0	1.0	108,500	108500
Ocracoke	96 x 10 ⁶	1.9	0.95	159,400	165400
TOTALS	217 x 10 ⁶			361,400	

*SOURCE: Roelofs and Bumpus (1953)

Selection of Time-Step

The size of the computational time-step, Δt , is governed by stability considerations and desired accuracy of the results. If Δt is reduced below a certain value, the benefits of accuracy may be far less than additional expenses in terms of computing time. On the other hand, if Δt is increased beyond a certain value, the savings in computing time may be at the expense of stability of the numerical scheme thereby introducing significant errors into the results.

The condition of stability used in this study is the famous Courant condition as given earlier, that is:

$$\Delta t \leq \frac{\Delta x}{V + \sqrt{gh}} \quad (6.5)$$

In the present model for Pamlico Sound, $\Delta x = 7422$ ft., maximum assumed value of $V = 5$ ft/sec., maximum value of $h+d = 22$ ft., and g is the gravitational constant. Using these values in equation (6.5) shows that Δt should be less than or equal to 4 minutes. It should be noted that the parameters in the denominator are estimated at their maximum values. Under actual conditions, it is improbable that the values of velocity and depth will be maximum at the same time at a point. Therefore, values of Δt as high as 5 minutes can be used.

Calibration of the Mathematical Model

It needs to be emphasized that mathematical models, such as the one presented in this report, must be calibrated before they can be used with confidence. The procedure calls for a sensitivity analysis of the model on a known set of field data. The different factors in the model are thus adjusted so that the computed values of the parameters under consideration would closely match the values actually observed in the field. After such fine tuning of the model, it would be called "reliable", that is, the results predicted by it would be accurate and reproducible.

VII. CIRCULATION DUE TO FRESHWATER INFLOW AND WIND

The general computer program prepared for Pamlico Sound can be used to determine the circulation patterns due to freshwater inflow, tidal exchange and the wind. This section is concerned with the presentation of computational results using freshwater inflow and wind.

Circulation Due to Freshwater Inflow

The finite difference equations representing the hydrodynamic equations subject to the boundary conditions are solved at appropriate grid points in the Sound. The values of freshwater inflows for 20 year floods as given in Table 4 were used. It was assumed that there is no flow through the inlets, therefore the coefficients of discharge were assigned zero values. Figures 6 and 7 give the velocity vectors and contours for water levels at Time 360 and 1440 minutes respectively. The time-step used for calculations was 1 minute. The arrows represent the magnitude and direction of water velocity. The water level contours show that the incoming water slowly gets distributed in the interior space. It is noted that all values of h are positive because there is no outflow and the water keeps piling up. However, because of the large size of the sound, the absolute values of increments in depth are relatively small.

Circulation Due to Uniform Wind

When a wind of constant speed is assumed to blow uniformly over the sound, and no inflows or outflows are permitted, the circulation patterns reflect the true effects of uniform wind stress. The input data, in this case, is prepared such that the speed and direction of wind is the same at all points and remains constant with respect to time. The inflow and outflow terms Q_1, Q_2, Q_3, Q_4, Q_5 and Q_6 are all set equal to zero. The wind stress coefficient C_d of 2.50×10^{-3} is used in all cases. The minimum value of total depth under the influence of wind force is assumed to be 2.0 ft. to avoid singularity condition as explained earlier.

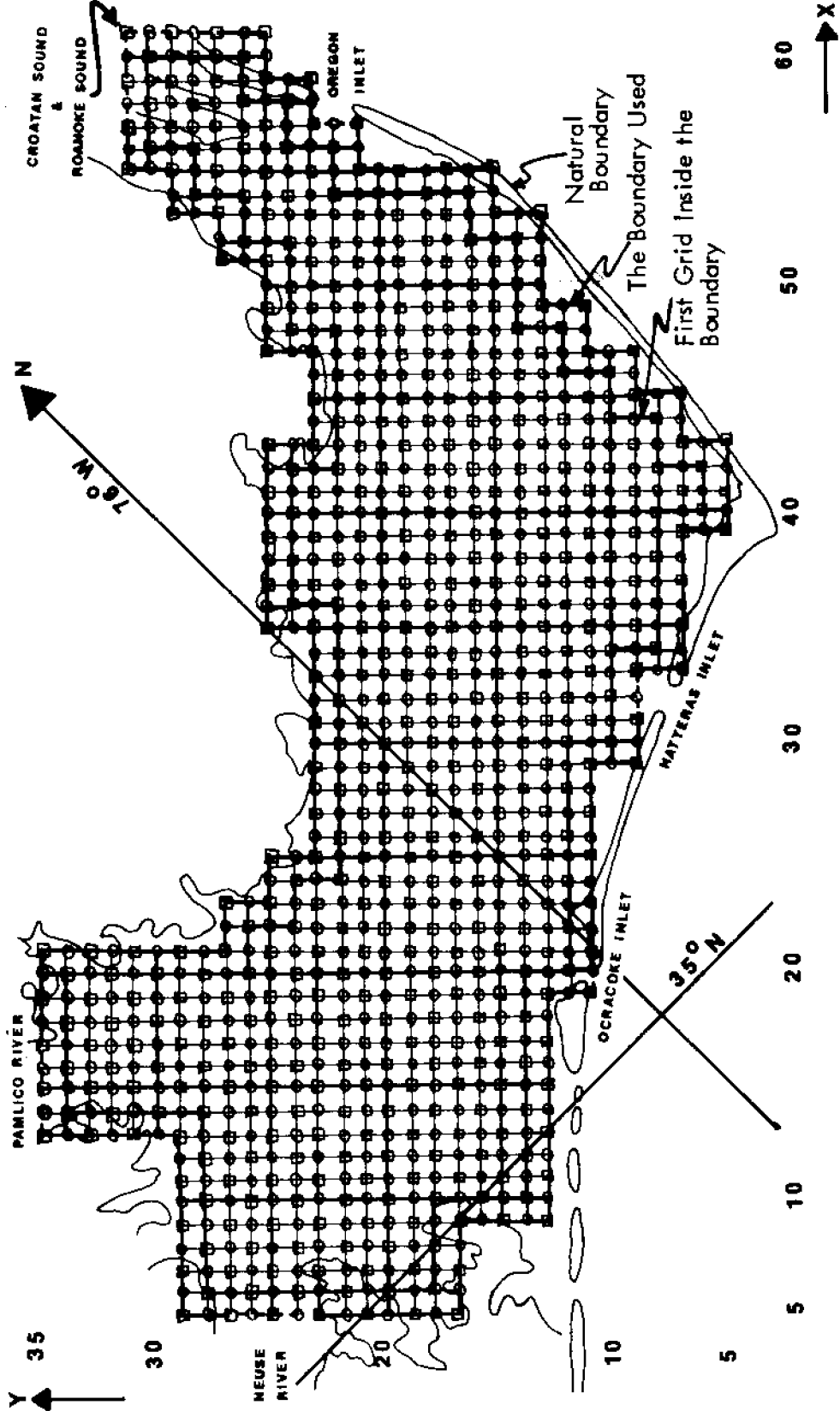


FIGURE 5 The Boundary And Grid System Used For The Pamlico Sound

Scale: One Grid = 7422 Feet

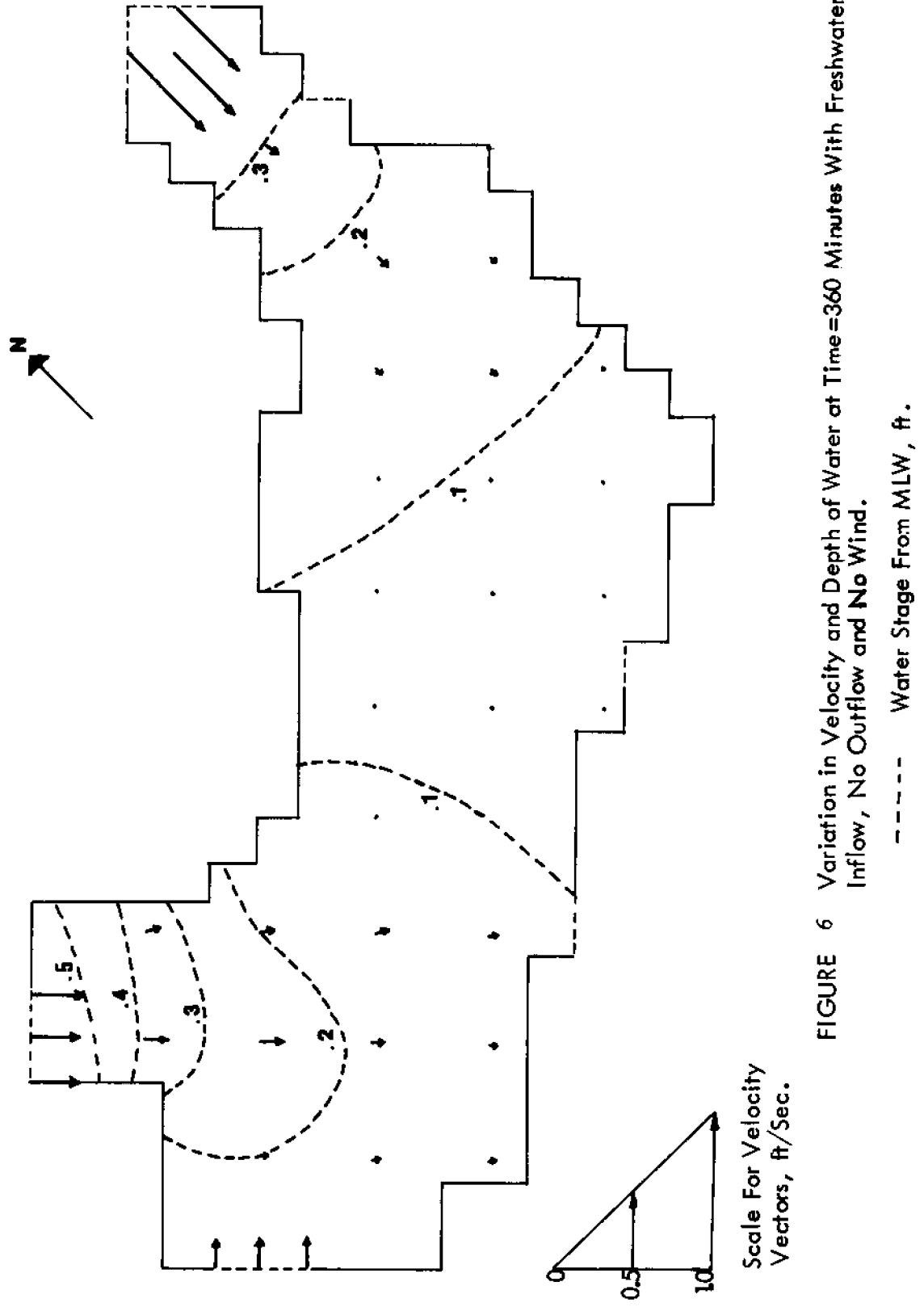


FIGURE 6 Variation in Velocity and Depth of Water at Time=360 Minutes With Freshwater Inflow, No Outflow and No Wind.

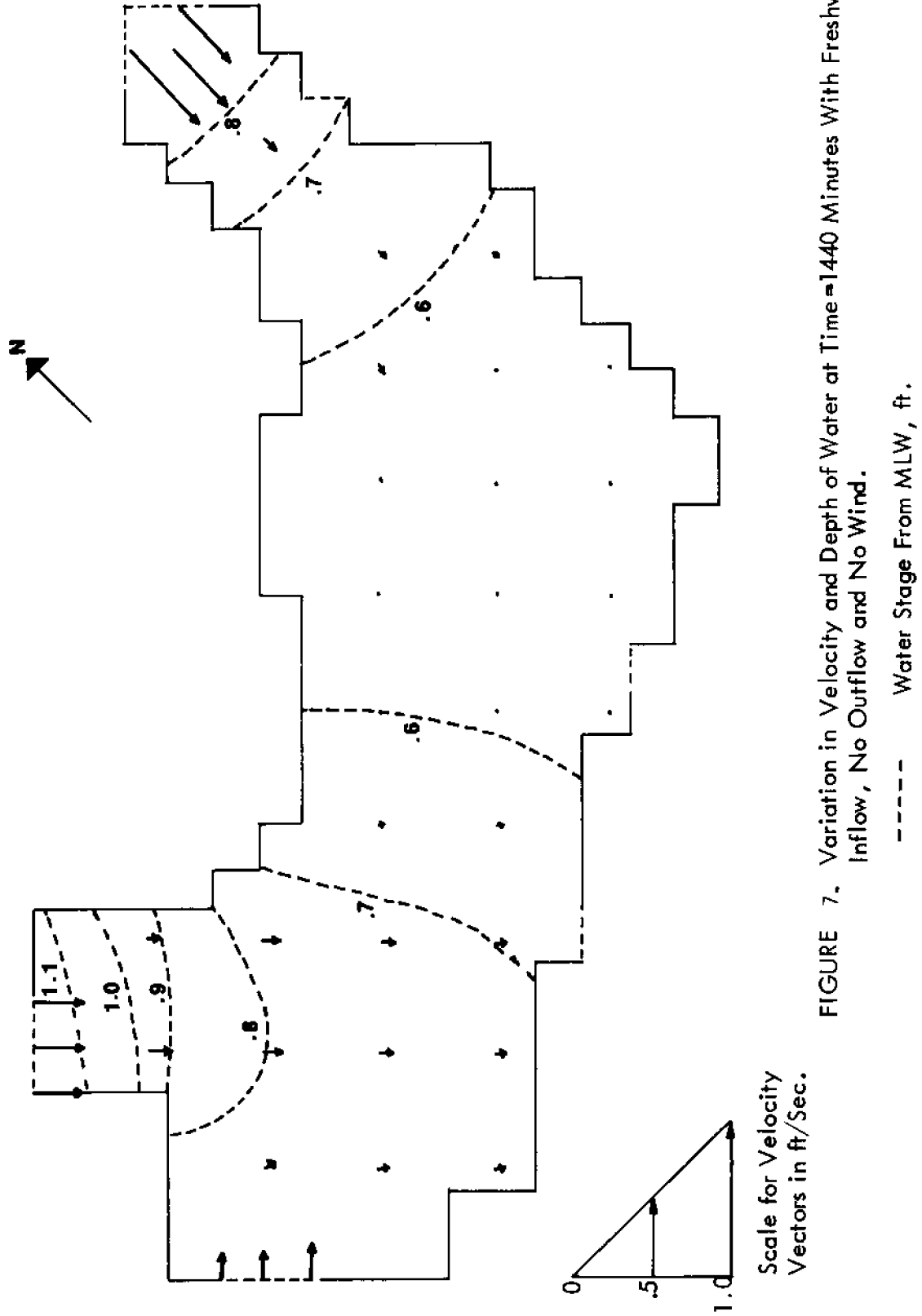


FIGURE 7. Variation in Velocity and Depth of Water at Time = 1440 Minutes With Freshwater Inflow, No Outflow and No Wind.

(a) Northerly Wind at 70 Miles Per Hour:

In this case, the direction of wind makes an angle of 225° with the positive x-axis. Performing the computations for a time-step of 1 minute, the resulting circulation patterns at 29 minutes are shown in Figure 8. It is noted that the wind induced water velocities are much larger than those given previously for freshwater inflows only. The water surface is depressed below the MLW on windward side and is elevated on the leeward side. The water surface profile at Time = 2880 minutes along the longitudinal section $y = 20$ is given in Figure 9.

(b) Southerly Wind at 70 Miles Per Hour:

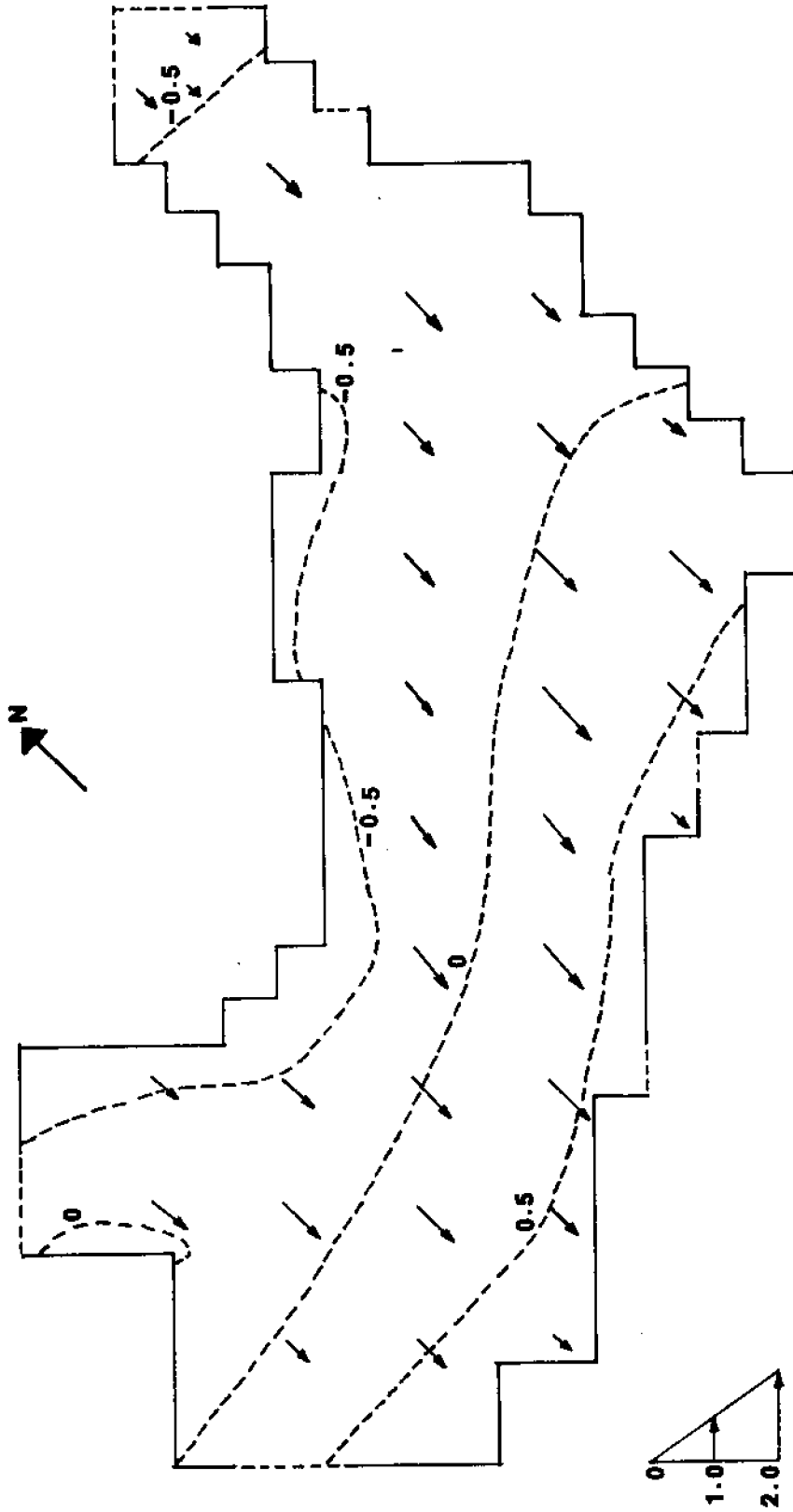
Here the wind is blowing from the South, making an angle of 45° with the positive x-direction.

(c) Westerly Wind at 70 Miles Per Hour:

When the wind is from the west making an angle of 315° with the positive x-axis, then for $\Delta t = 4$ minutes, the circulation pattern for 240 minutes is shown in Figure 10. The water surface profile for this case is given in Figure 9.

Pamlico Sound Subjected to Variable Wind Stress

The wind force acting over Pamlico Sound is rarely uniform and constant in nature. Generally, the wind stress would differ from point to point and would vary with respect to time. The procedure for computing circulation patterns would be fundamentally the same as for uniform winds with requirement that the wind field should be prescribed with time.



Scale For Velocity Vectors, ft/sec.

----- Water Stage From MLW, ft.

FIGURE 8. Variation In Velocity And Depth Of Water At $t = 29$ Minutes, With A Northerly Wind At 70 M. P. H. No Inflow Or Outflow Of Water, $C_d = 2.50 \times 10^{-3}$

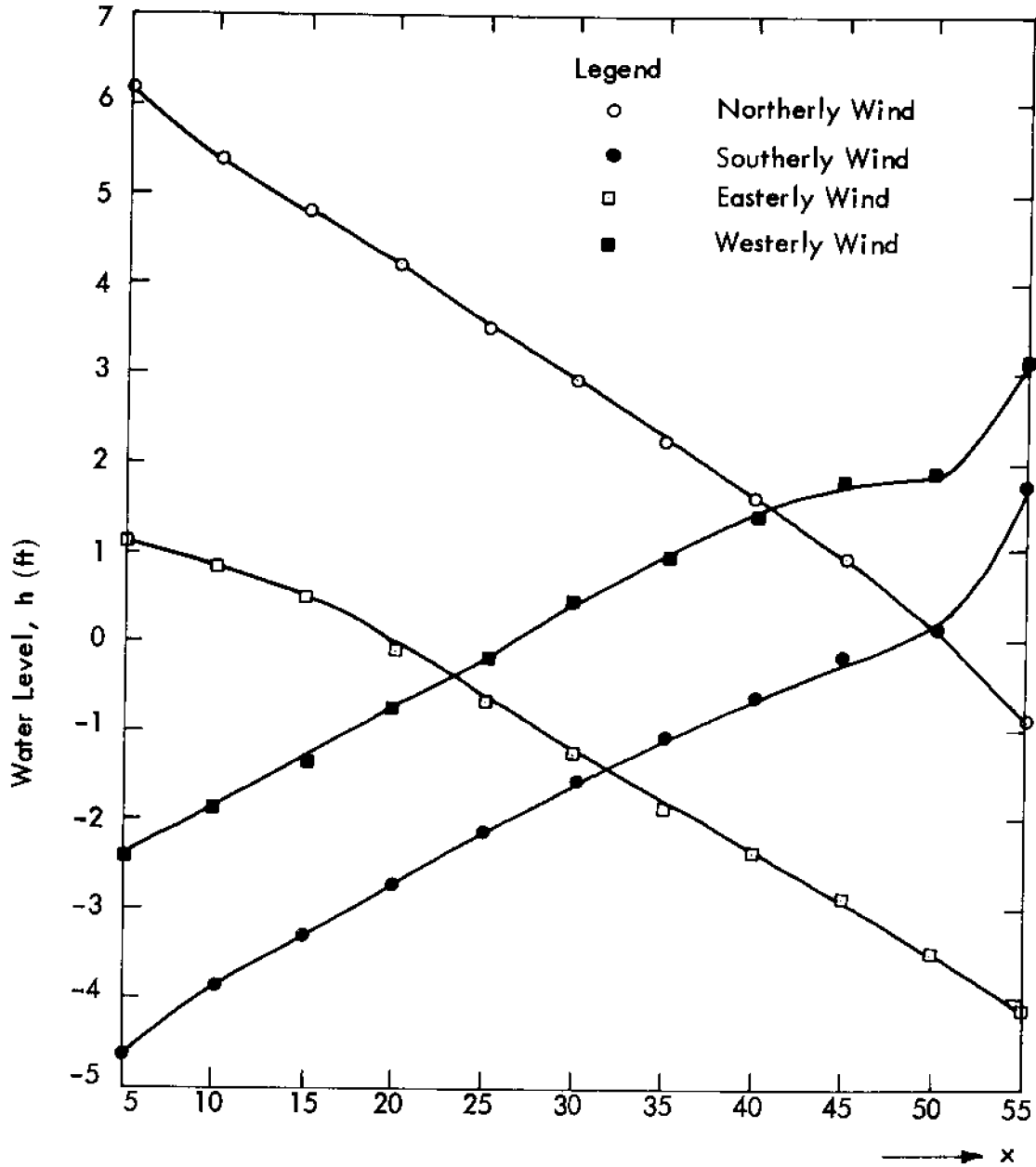


FIGURE 9. Water Surface Profiles Along Longitudinal Section at $y = 20$ at Time = 2880 Minutes for 70 MPH Winds from Different Directions as Indicated.

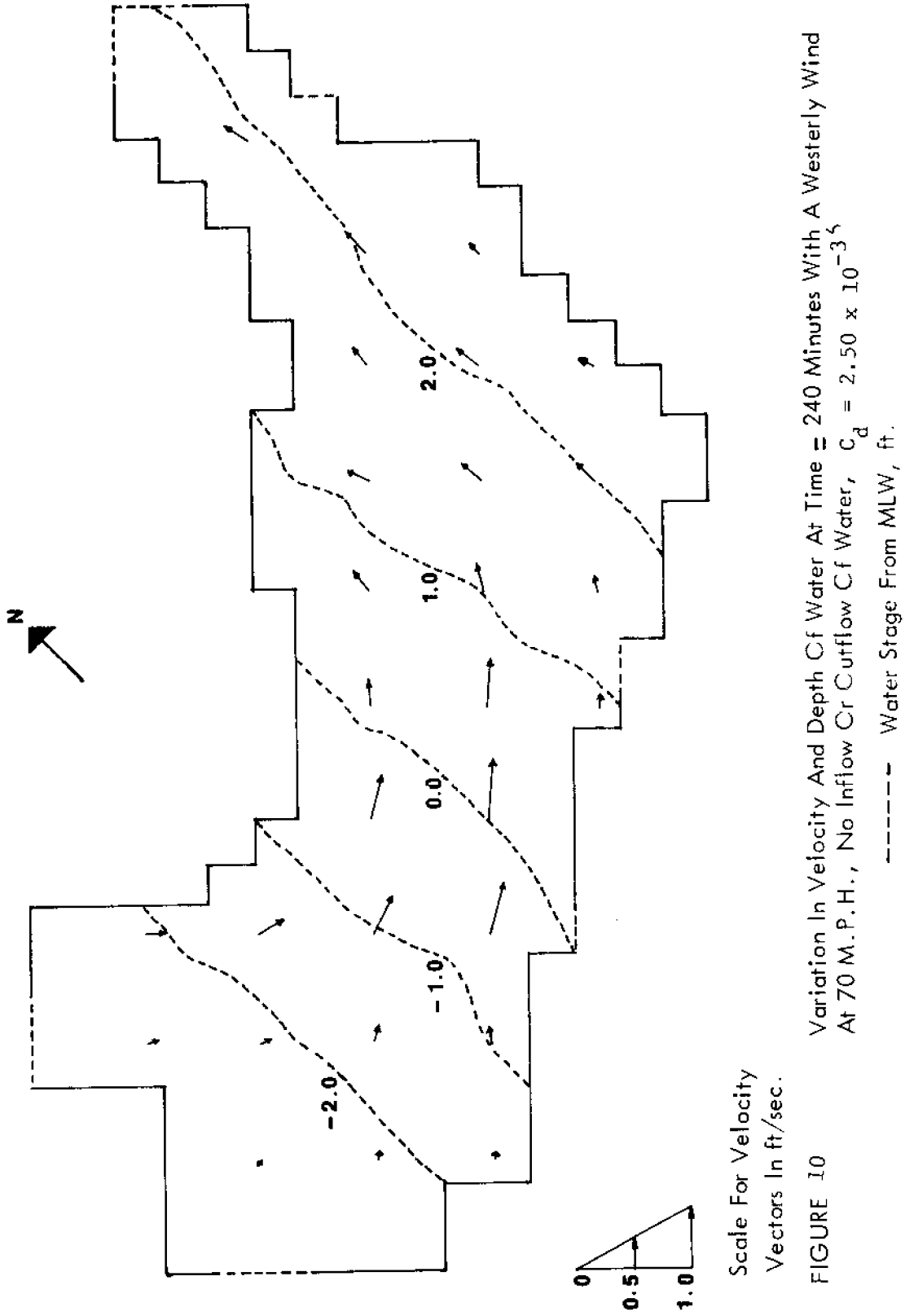


FIGURE 10 Variation In Velocity And Depth Of Water At Time = 240 Minutes With A Westerly Wind At 70 M.P.H., No Inflow Or Outflow Of Water, $C_d = 2.50 \times 10^{-3}$

Effect of Size of Time Step

In order to evaluate the effects of Δt on the stability of the results, the computations were performed using the time-step values varying from 1 to 6 minutes. The results are summarized for each run at selected grid points in Table 6. It is noted that the program becomes unstable beyond $\Delta t = 5$ minutes. However, there is slow impairment in accuracy of the results as the value of Δt is increased. There is, however, significant savings in computing time at higher values of Δt as shown in Table 7. Therefore, the size of time-step should be selected based upon the desired accuracy of results subject to the stability considerations.

VIII. MODELING OF HURRICANE SURGE

Numerical modeling is an effective tool for predicting surges caused by hurricanes. The irregular boundary, the non-uniform bottom topography, the changing wind pattern, the variable barometric pressure and other causes can be included, and the dynamics of surge movement can be calculated. This technique can be useful in the planning and operation of hazard warning systems and also in land use management.

It would be highly desirable that the model should be verified so that its accuracy and reliability be established. It is also important to know what type of information must be provided to generate useful results. Unfortunately, it is costly and hazardous to obtain precise data under hurricane conditions. In this section, application of the numerical model for the purpose of predicting the surge during hurricane Donna will be given. It should be emphasized that the application is primarily for purposes of illustration. Although limited data on the hurricane wind and on shore surge heights are available, the data lack precision and are at best rough estimates of actual conditions.

Hurricane Donna of September 1960 was the first storm with hurricane

TABLE 6.
EFFECT OF TIME STEP ON THE COMPUTED VALUES OF PARAMETERS
AFTER 1440 MINUTES OF FLOW

POINTS	1 MINUTE		2 MINUTES		3 MINUTES		4 MINUTES		5 MINUTES		6 MINUTES	
	V fps	h ft.	V fps	h ft.	V fps	h ft.	V fps	h ft.	V fps	h ft.	V fps	h ft.
(5,25)	0.20	0.0	0.20	0.0	0.20	0.0	0.20	0.0	0.20	0.0	0.20	0.0
(15,15)	0.04	-88.81	0.03	-59.75	0.02	-64.99	0.02	-65.75	0.02	-68.39	0.02	-68.39
(15,25)	0.13	269.92	0.10	-77.66	0.08	-74.18	0.07	-72.59	0.07	-71.53	0.07	-71.53
(15,35)	0.30	270.00	0.31	270.00	0.31	270.00	0.31	270.00	0.31	270.00	0.31	270.00
(25,15)	0.02	-81.70	0.05	-26.06	0.03	-35.30	0.02	-52.52	0.02	-57.49	0.02	-57.49
(25,20)	0.02	-81.34	0.05	-20.98	0.04	-20.28	0.03	-16.15	0.03	-14.34	0.02	-14.34
(35,10)	0.00	-35.86	0.01	266.51	0.02	247.39	0.03	208.97	0.03	206.58	0.03	206.58
(35,20)	0.00	-44.40	0.00	95.66	0.01	172.74	0.02	172.73	0.02	173.89	0.02	173.89
(45,10)	0.00	208.35	0.01	245.72	0.02	232.87	0.02	233.43	0.02	233.16	0.02	233.16
(45,20)	0.02	188.38	0.08	197.09	0.09	196.04	0.10	195.56	0.10	194.90	0.11	194.90
(55,25)	0.10	228.13	0.31	228.73	0.43	228.79	0.49	228.68	0.53	228.60	0.53	228.60
(59,29)	0.54	225.00	0.52	225.00	0.52	225.00	0.52	225.00	0.52	225.00	0.52	225.00

Instability of
results after
360 minutes of
flow

*Angle in degrees measured counterclockwise from positive X-axis.

TABLE 7. EFFECT OF TIME-STEP ON COMPUTATION COST*

Time-Step Minutes	CPU Minutes: Seconds	Core Time, K-sec.	Time Used Minutes; Seconds
1	3:59.4	44563	4:57.1
2	2:25.0	30428	3:22.8
3	1:48.7	24975	2:46.5
4	1:31.6	22416	2:29.4
5	1:18.4	20434	2:16.2
6	Instability of results after 360 minutes of flow		

*In each case, $t_f = 1440$ minutes and the results were printed after every 60 minutes.

force winds in Florida, Middle Atlantic States, and New England in a 75-year record (U.S. Department of Commerce, 1971). The track of hurricane Donna is shown in Figure 11. After traversing the Florida Peninsula, it continued in a northeasterly direction in the Atlantic Ocean until its second landfall in the Cape Fear area in North Carolina. The diameter of the eye of Donna was generally about 60 miles, but varied from 50 to 75 miles. The forward movement of Donna in the vicinity of Pamlico Sound is shown in Figure 12. The wind speed and direction recorded by weather stations at Hatteras, Cherry Point, New Bern and Elizabeth City are given in Table 8.

For the computation of wind effects, the Pamlico Sound was divided into six zones as shown in Figure 13. The velocity and direction of wind for different zones are found by interpolation. The resulting data are given in Table 9. It is noted that the values used for Zone 2 in Table 9 are the actual observations at Hatteras station.

The starting time $t = 0$ was set at 1500 hours on September 11, so that the first set of observations at 1600 hours could be used as data for $t = 1$ hour. In this way, the data for a total of 17 hours (up to 0800 hours on September 12) were used. After that, the last values in different zones were assumed to remain constant with respect to time. The values of wind speed and direction at any intermediate time were found by straight line interpolation between the two sets of hourly values. These values are used in the expressions for w_x and w_y , the wind stress parameters in x and y directions as given by equations (4.12) and (4.13) respectively.

The wind data for hurricane Donna given in Table 6 was used along with freshwater inflow and tidal exchange. The report of U. S. Army Corps of Engineers (1961) showed that on the morning of 11 September 1960, the mean water level in Pamlico Sound was about 1.0 foot above the mean sea level. The sound water elevations were given according to a datumline at 4.0 ft. below mean sea level to avoid any negative numbers.

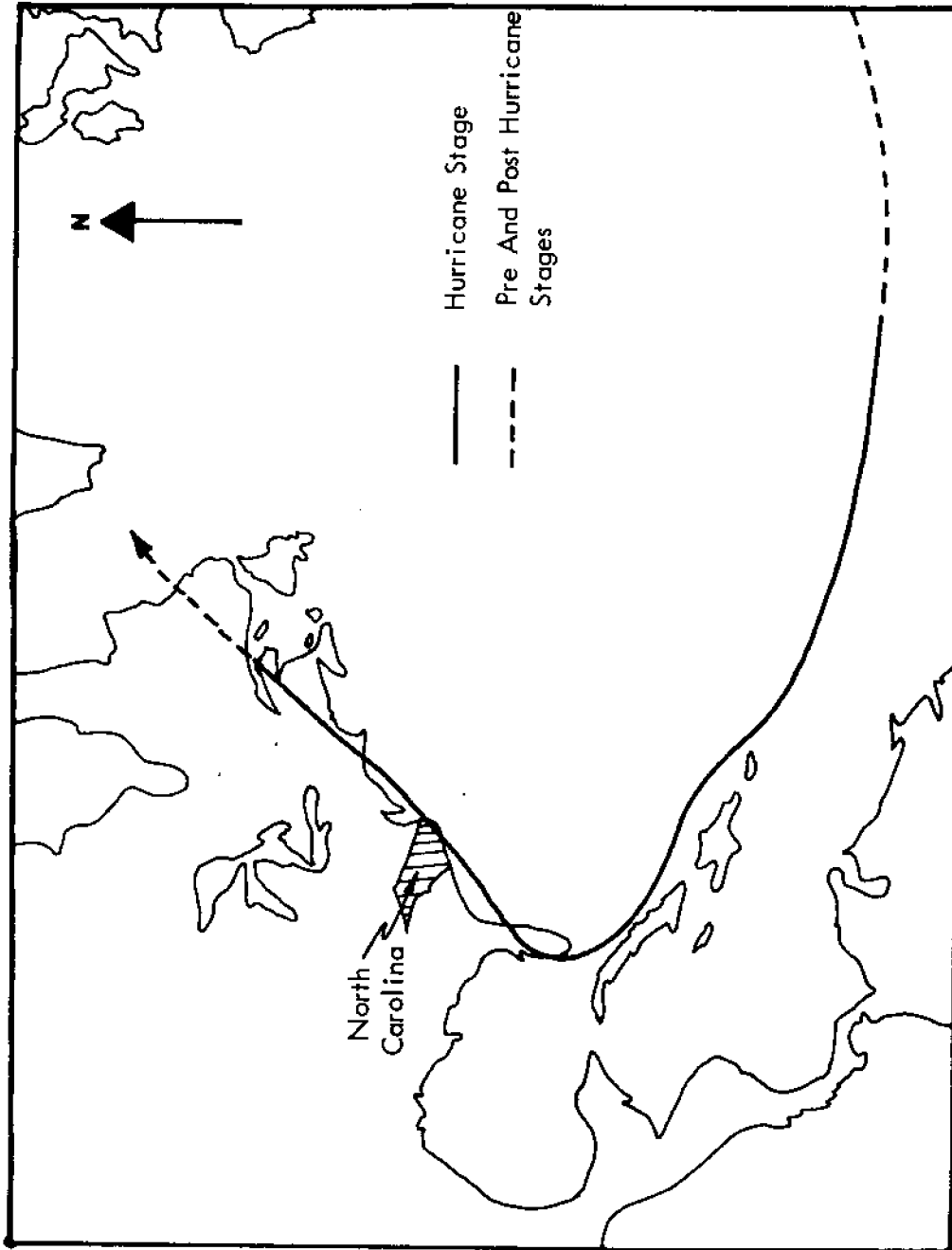


FIGURE 11 The Track Of Hurricane Donna During August 30, 1960 To September 13, 1960

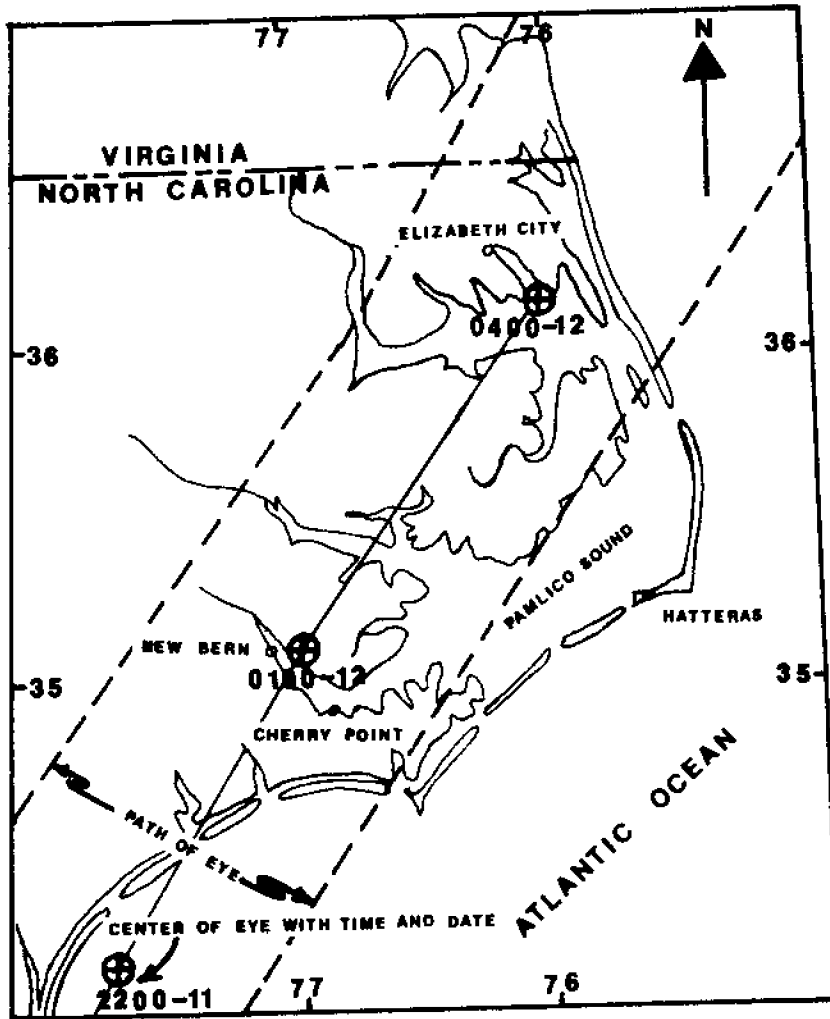


FIGURE 12 The Forward Movement Of Hurricane Donna In The Vicinity Of Pamlico Sound, 11-12 Sept. 1960

Scale : 1" = 40 Miles

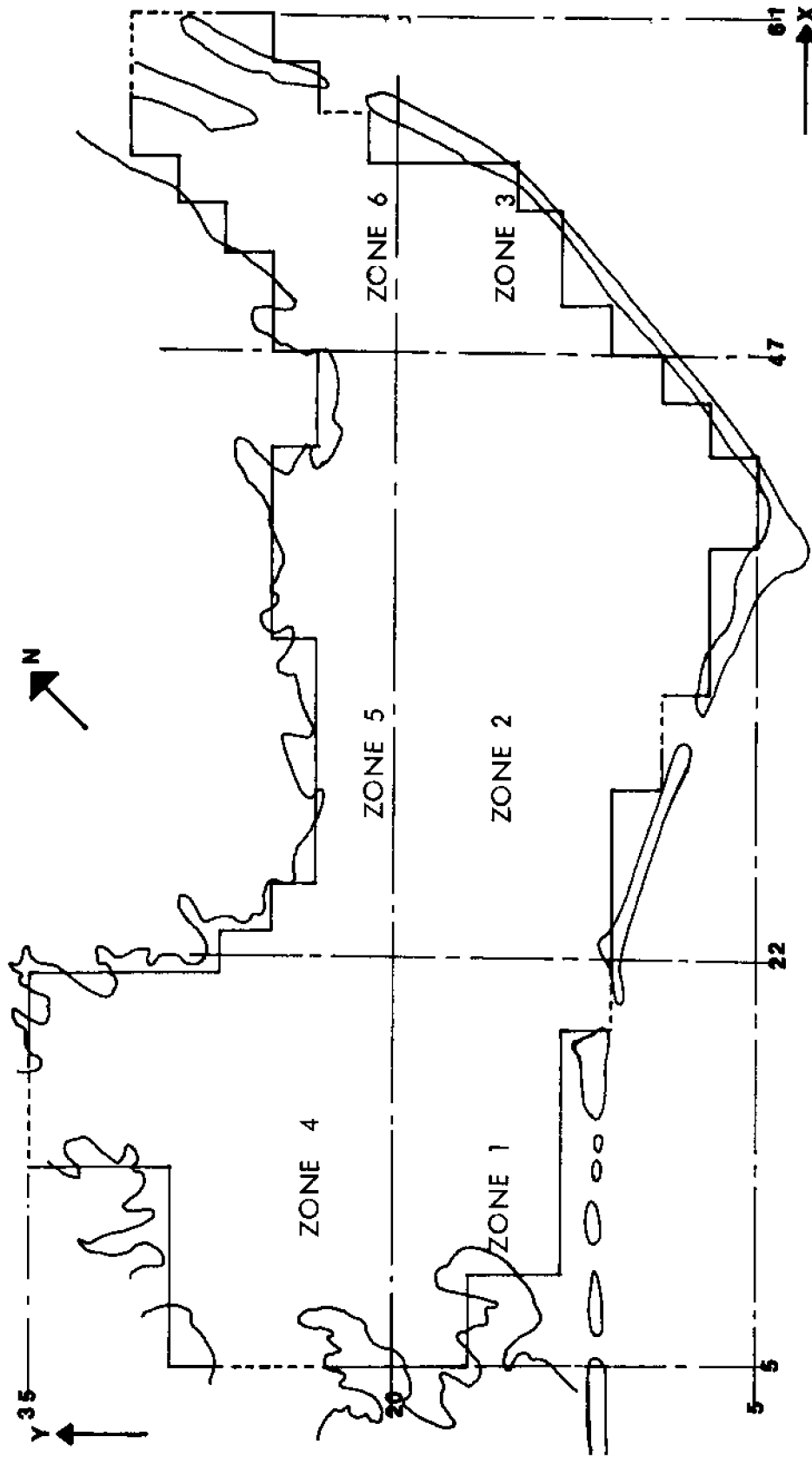


FIGURE 13 Division Of Pamlico Sound In Six Zones For Variable Wind Stress

TABLE 8. VELOCITY (IN MILES PER HOUR) AND DIRECTION OF WIND AT FOUR STATIONS DURING HURRICANE DONNA OF 1960*

Time e.s.t.	Elizabeth City		New Bern		Cherry Point		Hatteras	
	Velocity	Direction	Velocity	Direction	Velocity	Direction	Velocity	Direction
September 11, 1960								
1600	14	SE.	14	SE.	16	ESE.	20	SE.
1700	14	SSE.	7	ESE.	14	E.	21	SE.
1800	15	SSE.	9	SE.	18	E.	22	SE.
1900	14	SSE.	17	ENE.	17	E.	24	ESE.
2000	16	SE.	17	ESE.	23	E.	24	ESE.
2100	16	SE.	23	ENE.	37	E.	29	ESE.
2200	18	SE.	23	SE.	35	ESE.	35	ESE.
2300	25	ESE.	23	E.	44	ESE.	43	ESE.
2400	37	ESE.	23	SE.	42	SE.	46	SE.
September 12, 1960								
0100	35	SE.	C	(EYE)	12	S.	54	SSE.
0200	40	SE.	40	WNW.	35	WSW.	60	S.
0300	40	SE.	57	WNW.	40	W.	63	S.
0400	9	S.	35	WNW.	28	WSW.	55	SW.
0500	23	NW.	--	----	23	WSW.	65	WSW.
0600	29	NW.	17	W.	22	WSW.	38	SW.
0700	17	NW.	--	----	21	WSW.	36	WSW.
0800	14	WNW.	14	W.	14	SW.	30	WSW.
0900	16	WNW.	12	WSW.	14	SW.	32	SW.
1000	20	WNW.	12	WSW.	14	SW.	23	WSW.
1100	14	WNW.	12	WNW.	13	SW.	23	WSW.
1200	17	WNW.	12	WNW.	14	SW.	18	ESE.

*Source: U. S. Army Corps of Engineers (1961)

TABLE 9. VELOCITY AND DIRECTION OF WIND - IN WIND ZONES

Time (hrs.)	ZONE 1		ZONE 2		ZONE 3		ZONE 4		ZONE 5		ZONE 6	
	Vw, MPH	δ*										
1	18.0	101.0	20.0	90.0	17.0	90.0	17.0	90.0	20.0	90.0	17.0	90.0
2	18.0	112.0	21.0	90.0	17.0	78.0	14.0	101.0	21.0	90.0	17.0	78.0
3	20.0	112.0	22.0	90.0	18.0	78.0	15.0	90.0	22.0	90.0	18.0	78.0
4	20.0	123.0	24.0	112.0	19.0	90.0	20.0	135.0	24.0	112.0	19.0	90.0
5	23.0	123.0	24.0	112.0	20.0	101.0	20.0	112.0	24.0	112.0	20.0	101.0
6	33.0	123.0	29.0	112.0	22.0	101.0	26.0	135.0	29.0	112.0	22.0	101.0
7	35.0	112.0	35.0	112.0	30.0	101.0	29.0	112.0	35.0	112.0	30.0	101.0
8	43.0	112.0	43.0	112.0	34.0	112.0	33.0	132.0	43.0	112.0	34.0	112.0
9	44.0	90.0	46.0	90.0	41.0	101.0	34.0	90.0	46.0	90.0	41.0	101.0
10	33.0	56.0	54.0	68.0	44.0	78.0	27.0	67.0	54.0	68.0	44.0	78.0
11	47.0	22.0	60.0	45.0	50.0	67.0	50.0	338.0	60.0	45.0	50.0	67.0
12	51.0	0.0	63.0	45.0	50.0	67.0	60.0	338.0	63.0	45.0	50.0	67.0
13	41.0	349.0	55.0	0.0	55.0	0.0	45.0	328.0	55.0	0.0	55.0	0.0
14	40.0	338.0	65.0	338.0	44.0	292.0	45.0	315.0	65.0	338.0	44.0	292.0
15	30.0	349.0	38.0	0.0	33.0	292.0	27.0	338.0	38.0	0.0	33.0	292.0
16	28.0	338.0	36.0	338.0	26.0	292.0	25.0	328.0	36.0	338.0	26.0	292.0
17	17.0	349.0	30.0	338.0	22.0	292.0	22.0	338.0	30.0	338.0	22.0	292.0

*Measured in degrees counterclockwise from positive x-axis.

During calculations, a minimum depth of 2.0 feet was assumed to avoid any singularity condition. The initial and boundary conditions used provided for adjustment in inflow and outflow according to the changing water elevations at the junctions in the sound. Figures 14, 16, 18 and 20 show the sound water elevations for hurricane Donna as calculated by the model and Figures 15, 17, 19 and 21 show the contours as sketched by the staff of the U. S. Army Corps of Engineers (1961) from observed tide gage records.

After a close examination it can be noted that the contours for water elevations from the computations are similar to the contours from "observed" data. Some discrepancy between "observed" and computed data would be expected. The observations reflect the conditions in the Sound prior to the start of hurricane wind action. In the model, the imposition of instantaneous inflows, winds and other factors provide a different set of initial conditions. Moreover, the data are extrapolated from four distant points and represent only approximations of the actual wind speeds. Therefore, only the overall trend of the observations need to be compared, especially because there were no actual measurements of water surface elevations inside the Sound and the contours were sketched from tide gages, some of which were considerable distances away from the Sound. The model shows great potential for the prediction of circulation and water surface heights under given wind conditions.

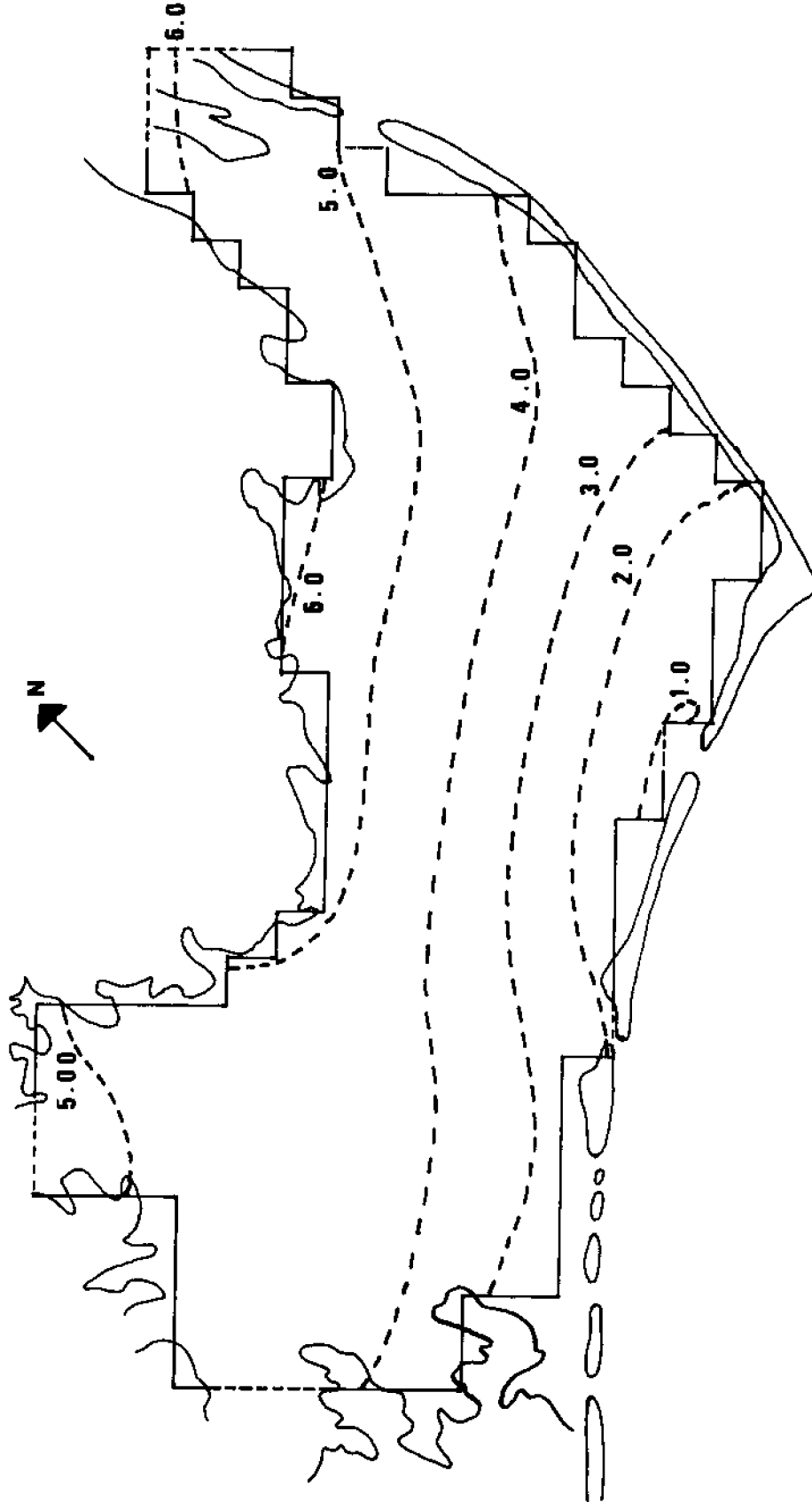


FIGURE 14 Calculated Water Elevations In Pamlico Sound Due To Hurricane Donna At time \approx 10.0 Hours,
Inflow And Outflow Permitted, $C_d = 2.50 \times 10^{-3}$
Datum is -4.0 MLW

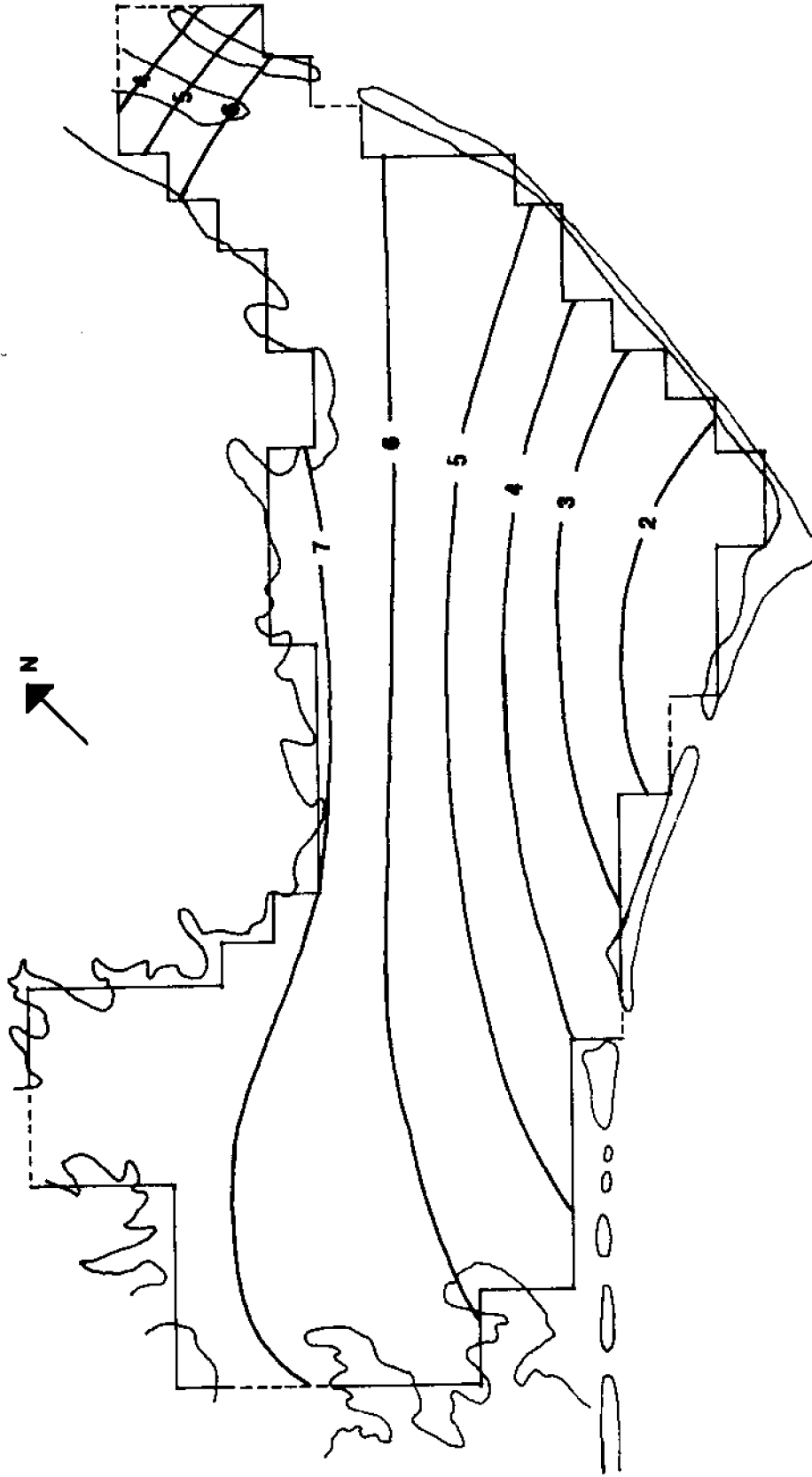


FIGURE 15 Observed Water Elevations In Pamlico Sound Due To Hurricane Donna at
Time = 10.0 Hours
Datum is -4.0 MLW Scale: 1" = 10 Miles

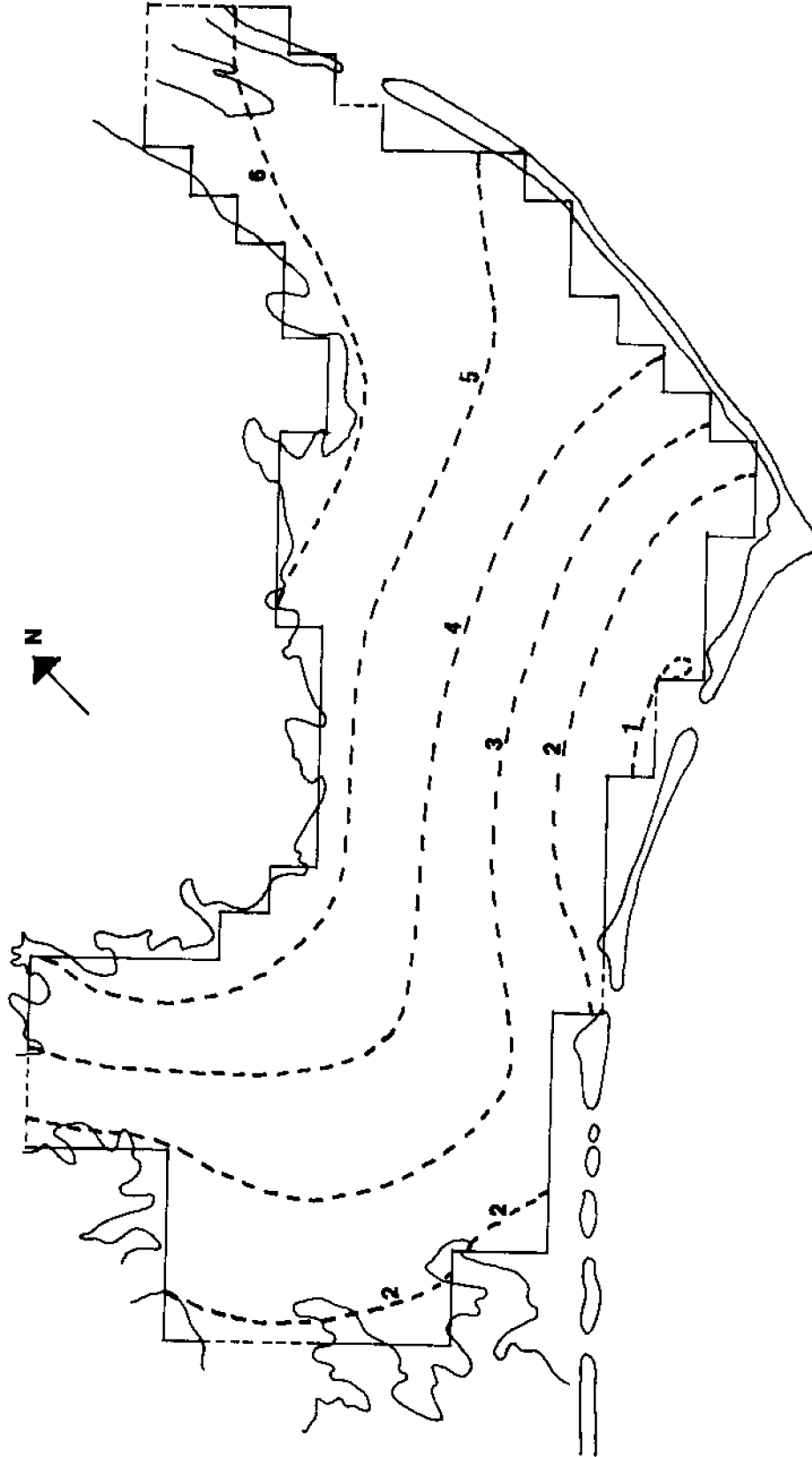


FIGURE 16
Calculated Water Elevations In Pamlico Sound Due To Hurricane Donna
At time = 11 Hours, Inflow And Outflow Permitted, $C_d = 2.50 \times 10^{-3}$
Datum is -4.0 MLW

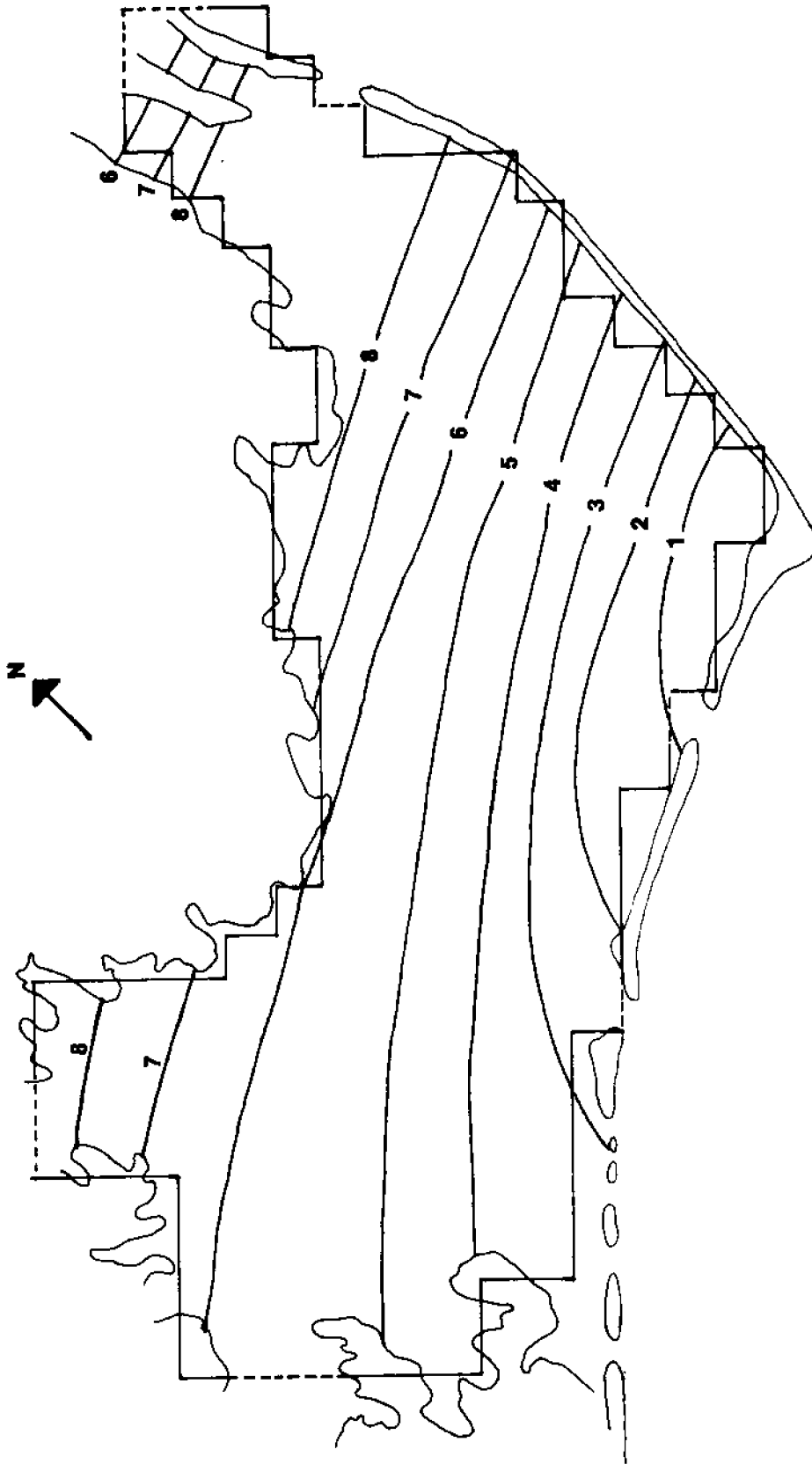


FIGURE 17
Observed Water Elevations In Pamlico Sound Due To
Hurricane Donna At time = 11.0 Hours,
Datum is - 4.0 MLW Scale : 1" = 10 Miles

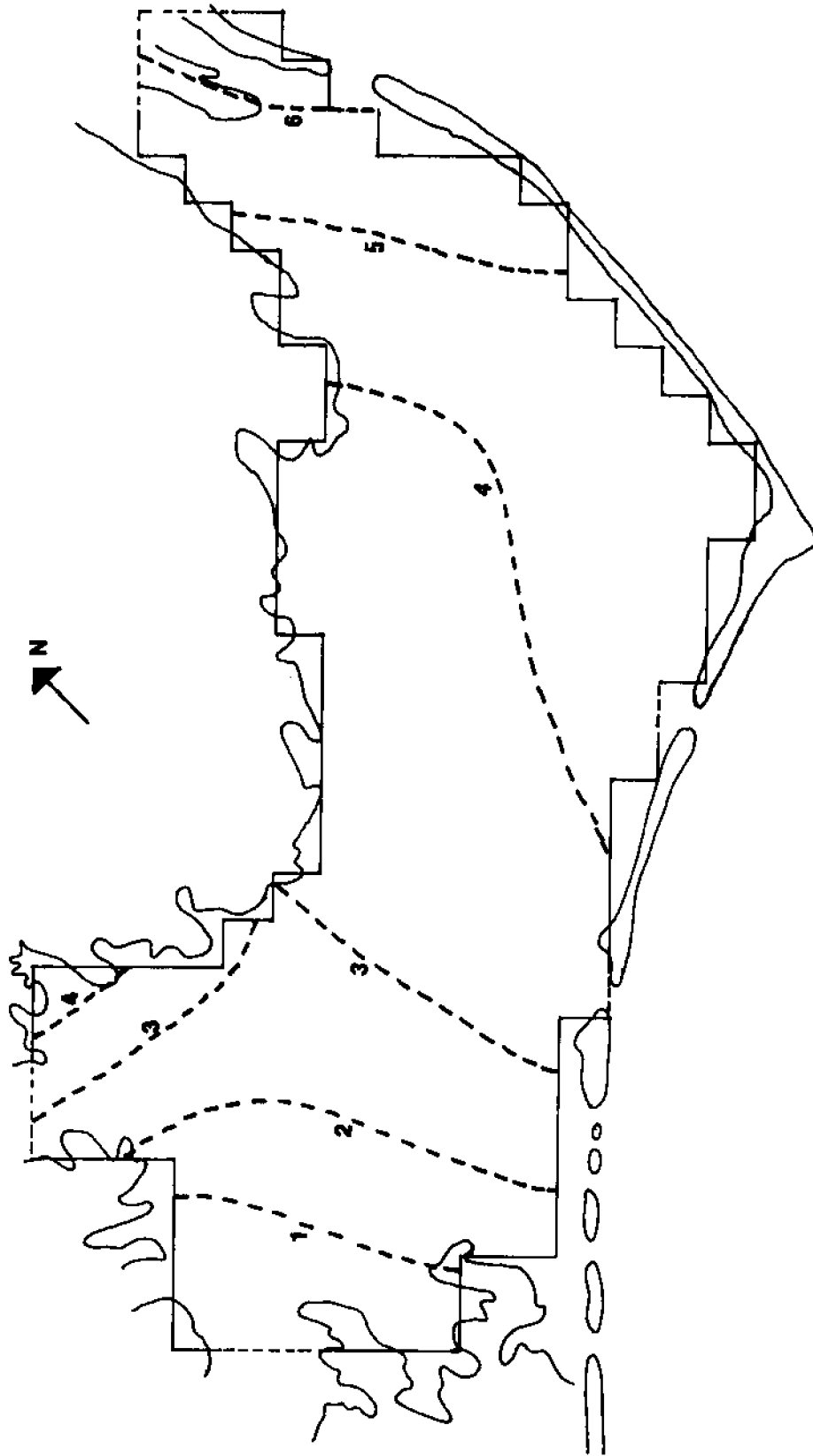


FIGURE 18
Calculated Water Elevations In Pamlico Sound Due To
Hurricane Donna At time = 14 Hours, Inflow And Outflow
Permitted, $C_d = 2.50 \times 10^{-3}$
Datum is - 4.0' MLW

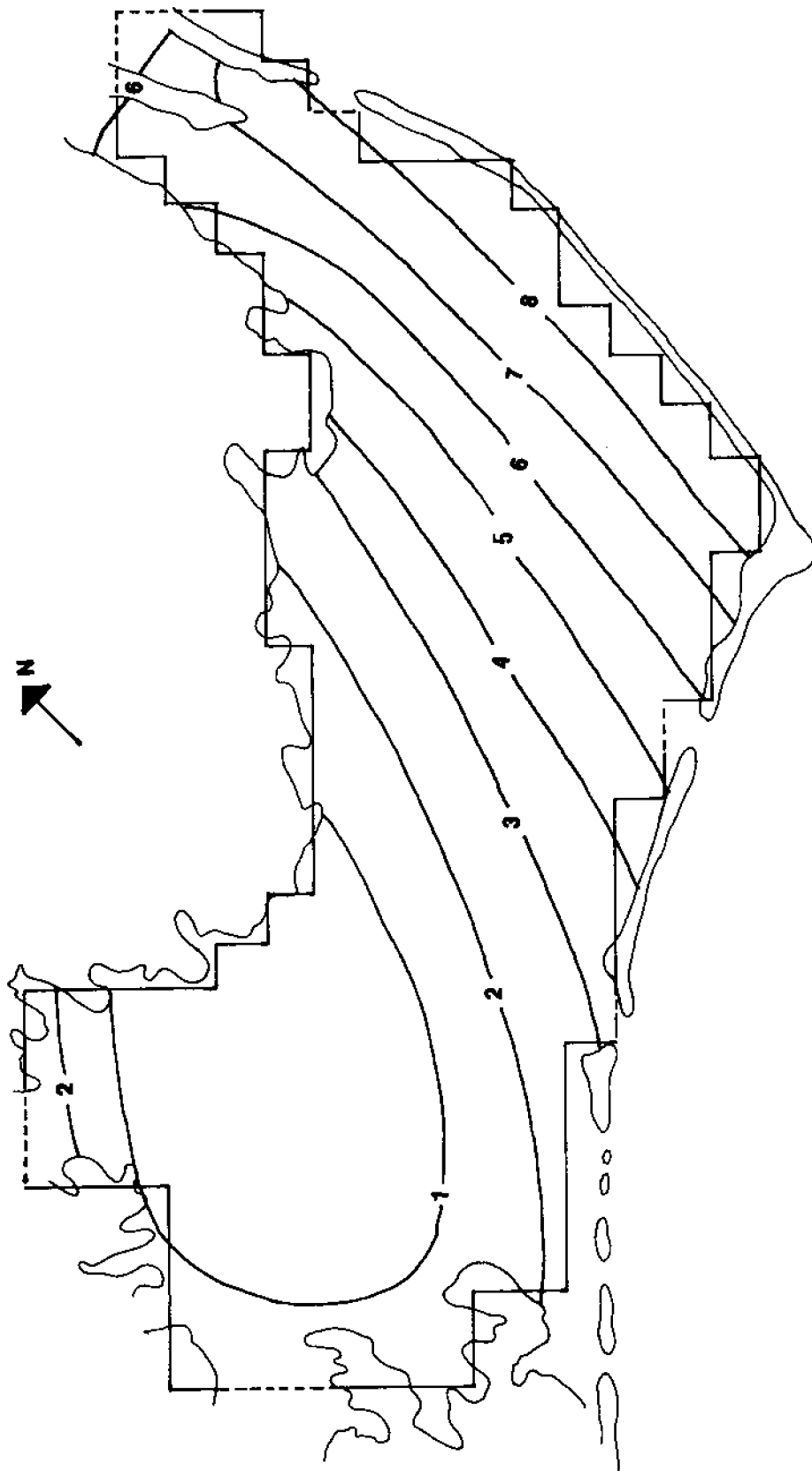


FIGURE 19 Observed Water Elevations In Pamlico Sound Due To
Hurricane Donna At time = 14.0 Hours
Datum: -4.0 MLW Scale: 1" = 10 Miles

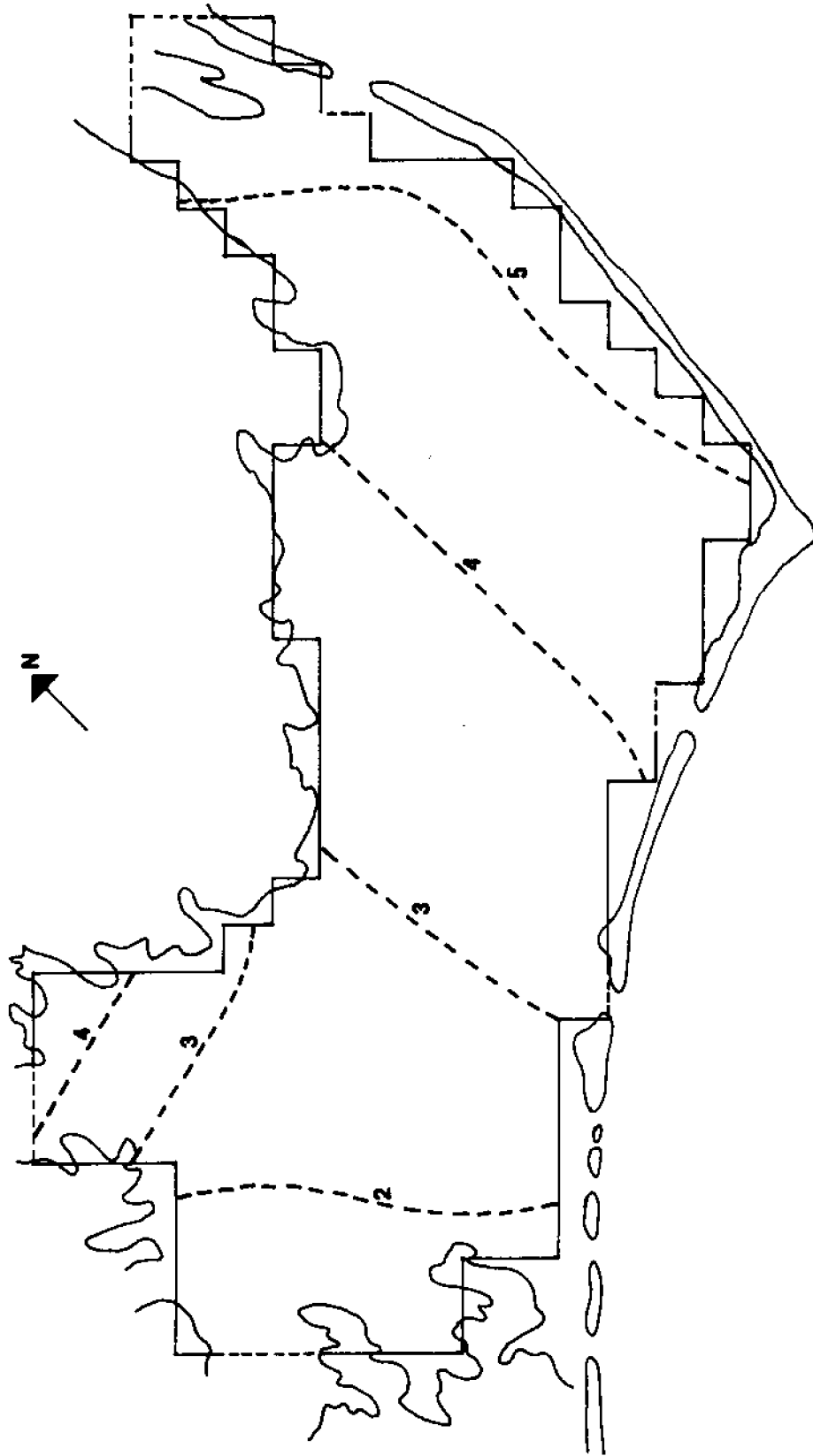


FIGURE 20
Calculated Water Elevations In Pamlico Sound Due To
Hurricane Donna At time ≈ 16.0 Hours, Inflow And
Outflow Permitted, $C_d = 2.50 \times 10^{-3}$
Datum is -4.0 MLW

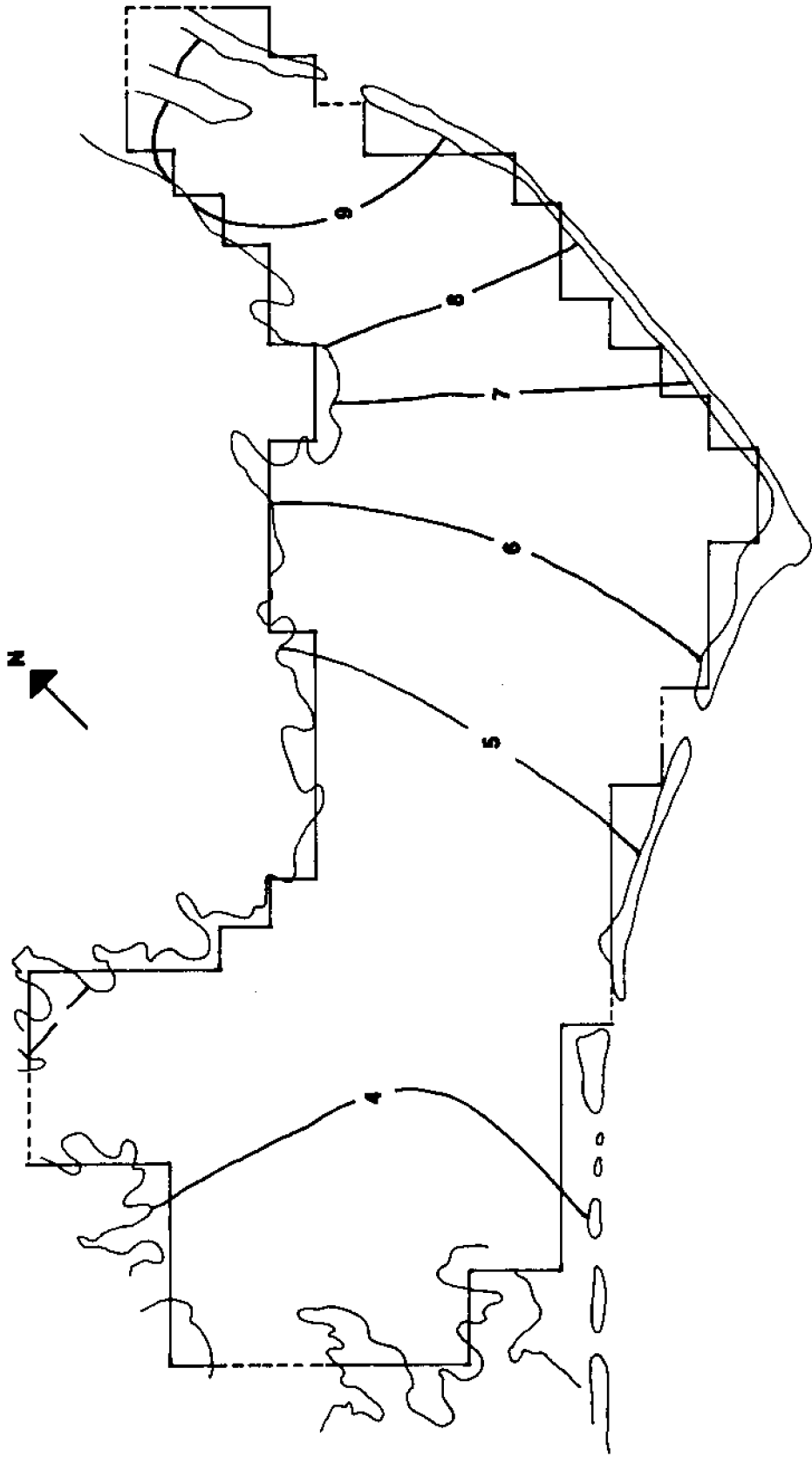


FIGURE 21 Observed Water Elevations In Pamlico Sound Due To
Hurricane Donna At time = 16.0 Hours
Datum: -4.0 MLW Scale : 1" = 10 Miles

IX. SUMMARY AND DISCUSSION

This study presents the development and applications of a two-dimensional model for circulation under unsteady flow conditions. The physical laws governing the water movement are given by partial differential equations of the hyperbolic type. The analytical solution for these equations is not feasible without making simplifying assumptions. In this study, the complete equations have been numerically solved by the explicit method using a fixed network of points. Therefore, the results are expected to be more representative of the actual processes.

The basic equations of motion and continuity are solved subject to the initial and boundary conditions. The size of time-step for computations was determined on the basis of stability considerations for the numerical scheme. The computer program was developed with deliberate emphasis on simplicity so that the model can be actually used by concerned agencies for real management problems. A users' manual has been prepared and included in the appendix with necessary instructions regarding the input and output data. The model was used to simulate the water movement in Pamlico Sound, North Carolina. The input data used were based upon the available information for the sound. First, the factors affecting the fluid transport in the sound were studied. It was found that surface wind stress, freshwater inflow, and tidal exchange are the controlling parameters, in that order of significance. Therefore, the investigations were limited to the effects of changes in these factors on the circulation.

The Pamlico Sound was represented by a 61 x 35 grid with a zig-zag boundary. In the first case, it was assumed that there is no outflow from the sound and no wind forces are acting. Thus, only the freshwater inflows and their effects on the sound, were studied. It was found that the circulation pattern develops very slowly. As no outflow is allowed, the water level continues to rise, even though

the absolute increase is not so high because of the vast size of the sound. The sound was then subjected to uniform wind stresses. It was assumed that the wind blows at a certain speed, and from a certain direction uniformly over the sound and remains constant with respect to time. As expected, it was found that the water surface is pushed below the original level on windward side and was driven above its level on leeward side. Various wind speeds from different directions were studied with the same general result. It was noted that at some points near the boundary, there was a tendency for wave formation. It was found that wind forces did have pronounced influence on the flow of water in the sound. Finally, the model was used to compute hurricane surge. The available data for hurricane Donna were used after necessary extrapolation. It was assumed that the tidal inlets are open and the flow through them is dependent upon the difference in water levels in the sound and the Atlantic Ocean.

It was observed that the circulation pattern changes with the corresponding change in wind speed or direction at any point. The circulation results were compared against actual water elevations in the sound during hurricane Donna, furnished by the U. S. Army Corps of Engineers (1961). Due to the limitations of the field data and uncertainty in the choice of coefficients, strict model verification is not expected. The field data could be used to determine if the model results are reasonable. It was noted that the general trend of contours was similar.

The model developed here can be used as a powerful diagnostic and predictive tool in regional water management for rivers and estuaries and hurricane protection in coastal areas. Given the necessary physical and hydrological data on a water body, its inflows, outflows, and wind forces at a time, the changing circulation patterns can be studied. The model provides tables and/or plots of the computed results at selected times of flow. Thus, it would be useful in simulating a time-history of the change in magnitude and direction of velocity and water stage at any point in the sound. A spatial variation of these parameters can be obtained

by drawing water surface profiles along selected longitudinal or lateral sections. A steady state model can be obtained by simply assigning zero values to all those terms in the basic equations which involve partial differentials with respect to time, t .

The model can be used to determine the exchange of water between the sound and the sea by specifying the appropriate coefficients of discharge, the characteristics of the inlets and the value of mean sea level. Accordingly, the model can be used to find the flushing time for the sound and also for verifying any data obtained by field monitoring of the flow conditions. The model can prove invaluable in studying the expected flooding conditions and designing effective measures for controlling the resulting damage in coastal areas during unusual flow conditions, such as hurricane force winds from the most critical direction.

It should be mentioned that in order to improve the model further, more field data need to be collected on the variation in currents and stage with respect to time at various points in the sound. The incoming flows should also be measured over time. Similarly, the direction and velocity of wind at standard anemometer heights should be observed at different representative locations in the area. With more data available, the model can be calibrated with greater precision. The validity of any assumptions made can also be established.

It would also be advisable to test other numerical methods for solving the equations and for comparing their efficiency in terms of accuracy of results, stability of the numerical scheme and requirements of computation time. The model should also be used with other values of inflows and a more sophisticated relationship for tidal exchange. The effect of changing the grid size and the use of variable grid size should also be investigated. In the present study, the sound was divided into six zones for variable wind analysis. If better data are available, a different value of wind speed and direction can be used at every grid point.

The solution of equations near the boundaries should also be improved. Presently, the depth values at boundary points are obtained by geometrical compatibility. This procedure could be introducing some error in the results. A better method of handling the computations at the boundary points should be investigated.

X. REFERENCES

- Abbott, M. B., and F. Ionescu. 1967. "On the Numerical Computation of Nearly Horizontal Flows", Journal of the Hydraulic Research, Vol. 5, pp. 97-117.
- Airan, D. S., 1974. "Explicit Modeling of Circulation and Water Quality for Two-Dimensional Unsteady Flows", Ph.D. thesis, North Carolina State University, Raleigh, N. C.
- Amein, M. 1966 a. "A Method for Determining the Behavior of Long Waves Climbing a Sloping Beach", Journal of Geophysical Research, Vol. 71, No. 2 pp. 401-410.
- Amein, M. 1966 b. "Streamflow Routing on Computer by Characteristics", Water Resources Research, Vol. 2, No. 1, pp. 123-130.
- Amein, M. 1967. "Some Recent Studies on Numerical Flood Routing", Proceedings of the Third Annual American Water Resources Conference, AWRA, Urbana, Illinois.
- Amein, M. 1968. "An Implicit Method for Numerical Flood Routing", Water Resources Research, Vol. 4, No. 4, pp. 719-726.
- Amein, M., and C. S. Fang, 1969. "Streamflow Routing With Applications to North Carolina Rivers", Report No. 17, Water Resources Institute of the University of North Carolina, Raleigh, North Carolina.
- Amein, M. 1971. "Circulation in Pamlico Sound", Report to the N. C. Board of Science & Technology, Department of Civil Engineering, North Carolina State University of Raleigh, North Carolina.
- Ames, W. F. 1969. "Numerical Methods of Partial Differential Equations", Barnes & Noble, Inc., New York.
- Baines, W. D. 1957. "Tidal Currents in Constricted Inlets", Proc. Conf. Coastal Engineering, pp. 545-561.
- Baines, W. D., and D. J. Knapp 1965. "Wind Driven Water Currents", Journal of the Hydraulics Division, ASCE, Vol. 91, No. HY 2, pp. 205-221.
- Baltzer, R. A., and C. Lai, 1972. "Closure" to Discussions on their paper "Computer Simulation of Unsteady Flows in Waterways", Vol. 98, No. HY 2, pp. 383-386.
- Broome, T. G. 1968. "An Analysis of Flow in Tidal Inlets", Unpublished M. S. Thesis, Department of Civil Engineering, North Carolina State University at Raleigh, North Carolina.
- Brown, E. I. 1928. "Inlets on Sandy Coasts", Proceedings American Society of Civil Engineers, Vol. 54, Part I, pp. 505-553.
- Chu, H. L. 1970. "Numerical Techniques For Non-Linear Wave Refraction and For Propagation of Long Waves in a Two-Dimensional Shallow Water Basin", unpublished PhD dissertation, Department of Civil Engineering, North Carolina State University at Raleigh, North Carolina.

Dronkers, J. J. and J. C. Schonfeld. 1955. "Tidal Computations in Shallow Water", Proceedings American Society of Civil Engineers, 81(714): 29-31.

Dronkers, J. J. 1964. "Tidal Computations in Rivers and Coastal Waters", North Holland Publishing Company, New York.

Ellis, John. 1970. "Unsteady Flow in Channel of Variable Cross Section", Journal of the Hydraulics Division, ASCE, Vol. 96, No. HY10, pp. 1927-1945.

Fletcher, A. S., and W. S. Hamilton. 1967. "Flood Routing in an Irregular Channel" Journal of the Engineering Mechanics Division, ASCE, Vol. 93, No. EM3, pp. 45-62.

Fread, D. L. 1973. "Effects of Time Step Size in Implicit Dynamic Routing", Water Resources Bulletin, AWRA, Vol. 9, No. 2, pp. 338-351.

Garrison, J. M., J. P. Granju, and J. T. Price. 1969. "Unsteady Flow Simulation in Rivers and Reservoirs", Journal of the Hydraulics Division, ASCE, Vol. 95, No. HY5, pp. 1559-1576.

Hammack, J. L. 1969. "A Mathematical Investigation of Freshwater Flow through Pamlico Sound, North Carolina", Unpublished M. S. Thesis, Department of Civil Engineering, North Carolina State University at Raleigh, North Carolina.

Hansen, W., 1956., "Theorie zur Errechnung des Wasserstandes und der Stromungen in Randmeeren nebst Anwendungen," Tellus, Vol. 8, No. 3, pp. 207-216.

Harris, D. Lee and C. P. Jelesnianski, 1964, "Some Problems Involved in the Numerical Solutions of Tidal Hydraulic Equations", Monthly Weather Review, Vol. 92, No. 9, Sept. 1964, pp. 409-422.

Heaps, N. S., 1969, "A Two-Dimensional Numerical Sea Model", Philosophical Transactions of the Royal Society of London, Series A, Vol. 265, No. 1160, pp. 93-137.

Hess, K. W. and F. M. White, 1974. "A Numerical Tidal Model of Narragansett Bay", University of Rhode Island, Marine Technical Report No. 20, Kinston, R. I.

Hildebrand, F. B. 1968. "Finite Difference Equations and Simulations", Prentice-Hall, Inc. New Jersey.

Ippen, A. T. 1966. "Estuary and Coastline Hydrodynamics", McGraw-Hill Book Company, Inc., New York.

Isaacson, E., J.J. Stoker, and B. A. Troesch. 1954. "Numerical Solution of Flood Prediction and River Regulation Problems - Report II", New York University Institute of Mathematical Sciences, Report No. IMM-NYU-205.

Isaacson, E., J.J. Stoker, and B. A. Troesch, 1956. "Numerical Solution of Flood Prediction and River Regulation Problems - Report III", New York University Institute of Mathematical Sciences, Report No. IMM - NYU-235.

Isaacson, E., J.J. Stoker, and B. A. Troesch. 1958. "Numerical Solution of Flow Problems in Rivers", Journal of the Hydraulics Division, ASCE, Vol. 84, No. HY5, Proc. Paper 1810.

- Jarrett, T.J. 1966. "A Study of the Hydrology and Hydraulics of the Pamlico Sound and their Relations to the Concentration of Substances in the Sound", Unpublished M.S. Thesis, Department of Civil Engineering, North Carolina State University at Raleigh, North Carolina.
- Jelesnianski, C.P., 1966, "Numerical Computations of Storm Surges Without Bottom Stress", Monthly Weather Review, Vol. 94, No. 6, pp. 379-394.
- Keulegan, G. H., and J.V. Hall 1950. "A Formula for the Calculation of the Tidal Discharge Through an Inlet.", U.S. Beach Erosion Board Bulletin, Vol. 4, No. 1, pp. 15-29.
- Keulegan, G. H. 1967. "Tidal Flow in Entrances - Water Level Fluctuations of Basins in Communication with Seas", Technical Bulletin No. 14, Committee on Tidal Hydraulics, U. S. Army Corps of Engineers, Vicksburg, Mississippi.
- Lamb, H. 1932. "Hydrodynamics", Dover Publications, New York.
- Leendertse, J.J. 1967. "Aspects of a Computational Model for Long Period Water Wave Propagation", RM-5294-PR, The Rand Corporation, Santa Monica, California.
- Leendertse, J.J. 1970. "A Water Quality Simulation Model for Well Mixed Estuaries and Coastal Seas: Volume 1, Principles of Computation", RMO-6230-RC, The Rand Corporation, Santa Monica, California.
- Leendertse, J.J. and E.C. Gritton. 1971 a. "A Water Quality Simulation Model for Well Mixed Estuaries and Coastal Seas, Vol. 11 - Computation Procedures", The New York City Rand Institute, New York. R-708-NYC.
- Liggett, J.A. and D.A. Woolhiser. 1967. "Difference Solution of the Shallow Water Equations", Journal of the Engineering Mechanics Division, ASCE, Vol. 95, No. EM2, pp. 39-71.
- Masch, F.D., N.J. Shankar, M. Jeffrey, R.J. Brandes, and W.A. White. 1969 "A Numerical Model for the Simulation of Tidal Hydrodynamics in Shallow Irregular Estuaries", Technical Report HYD 12-6901, Department of Civil Engineering, The University of Texas at Austin, Texas.
- Mitchell, A.R. 1969. "Computational Methods in Partial Difference Equations", John Wiley & Sons, New York.
- O'Brien, G.G., M.A. Hyman, and S. Kaplan. 1951. "A Study for the Numerical Solution of Partial Differential Equations", Journal of Mathematics and Physics, Vol. 29, No. 4, pp. 223-251.
- Phillips, O.M. 1969. "The Dynamics of the Upper Ocean", The University Press, Cambridge.
- Posner, G.S. 1959. "Preliminary Oceanographic Studies of the Positive Bar Built Estuaries of North Carolina, U.S.A.", International Oceanographic Congress, American Association for the Advancement of Science, Washington, D.C.
- Reid, R.O., and B.R. Bodine. 1968. "Numerical Model for Storm Surges in Galveston Bay", Journal of the Waterways and Harbors Division, ASCE, Vol. 94, No. WW1, pp. 33-57.

- Richtmyer, R.D., and K.W. Morton. 1967. "Difference Methods for Initial Value Problems", Second Edition, Interscience Publishers, Inc., New York.
- Roelofs, E.W., and D.F. Bumpus. 1953. "The Hydrography of Pamlico Sound", Bulletin of Marine Science of the Gulf and Caribbean, Vol. 3, No. 3, pp. 181-205.
- Schaake, J.C., Jr. 1965. "Synthesis of the Inlet Hydrograph", Technical Report No. 3, Department of Sanitary Engineering and Water Resources, The John Hopkins University, Baltimore, Maryland.
- Smallwood, C., Jr., and M. Amein. 1967. "A Mathematical Model for the Hydrology and Hydraulics of Pamlico Sound", Proceedings Symposium on Hydrology of the Coastal Waters of North Carolina, Report No. 5, Water Resources Research Institute of The University of North Carolina, Raleigh, North Carolina.
- Sobey, R.J., 1970, Finite-Difference Schemes Compared for Wave-Deformation Characteristics in Mathematical Modeling of Two-Dimensional Long-Wave Propagation", Tech. Mem No. 32, Coastal Engineering Research Center, 29 pp.
- Stark, P.A. 1970. "Introduction to Numerical Methods", The Macmillan Company, New York.
- Stoker, J.J. 1953. "Numerical Solution of Flood Prediction and River Regulation Problems - Report 1", New York University Institute of Mathematical Sciences, Report No. IMM - NYU - 200.
- Stoker, J.J. 1957. "Water Waves, The Mathematical Theory with Applications", Interscience Publishers, Inc., New York.
- Strelkoff, T. 1979. "Numerical Solution of Saint-Venant Equations", Journal of the Hydraulics Division, ASCE, Vol. 96, No. HY1, pp. 223-252.
- U.S. Army Corps of Engineers. 1961. "Report on the Tropical Hurricane of September 1960(Donna)", Wilmington, North Carolina.
- U.S. Department of Commerce. 1971. "Some Devastating North Atlantic Hurricanes of the 20th Century", U.S. Government Printing Office, Washington, D.C.
- U.S. Geological Survey. 1963. "Water Supply Characteristics of North Carolina Streams", Water Supply Paper 1761, U.S. Government Printing Office, Washington, D.C.
- Wagner, P. 1973. "Report on Neuse River", Environmental Protection Agency, Region IV, Atlanta, Georgia.
- Water Resources Engineers, Inc. 1966. "A Hydraulic - Water Quality Model of Suisun and San Pablo Bays", Report of an Investigation for the Federal Water Pollution Control Administration, Lafayette, California.
- Welander, P. 1961. "Numerical Prediction of Storm Surges", Advances in Geophysics, Vol. 8, pp. 315-379.
- Wilson, B.W. 1970. "Note on Surface Wind Stress Over Water at Low and High Wind Speeds", Journal of Geophysical Research, Vol. 65, pp. 3377-3382.

Woods, W.J. 1967. "Hydrographic Studies in Pamlico Sound", Proceedings Symposium on Hydrology of the Coastal Waters of North Carolina, Report No. 5, Water Resources Research Institute of the University of North Carolina, Raleigh, North Carolina.

Wylie, E.B. 1970. "Unsteady Free-Surface Flow Computations", Journal of the Hydraulics Division, ASCE, Vol. 96, No. HY11, pp. 2241-2251.

XI. COMPUTER PROGRAMS

Introduction

The purpose of this manual is to acquaint the users with the computer programs and give pertinent information about their input and output data. The program listings are also provided. The computer programs are written in Fortran IV language and were run on an IBM 370/165 model.

The program is written for Pamlico Sound, North Carolina with a zig-zag boundary. The program uses the explicit finite difference method for numerical solution of a set of hydrodynamic equations with appropriate boundary and initial conditions. The operation of this program produces a time history and spatial distribution of water depths, magnitude and direction of water velocity.

The general programs can be run for a number of different flow conditions, as will be described later, by making minor changes in the input data. The deck of cards for each program has five parts, that is, JCL cards, main program, subroutines, data deck, and plotting program. The JCL cards provide vital information about the job to the machine operator. The programmer specifies the time for computations, maximum number of pages for print out, etc. The main program and other parts are described in the following section. The plotting program is not given because some of the subroutines are not available at other installations, and the type of plot desired is subject to the individual's choice.

Description of Programs

Main Program

The main program writes the title and assumptions used, specifies real and integer variables, assigns storage spaces, defines all the variables, initializes all parameters, reads and echo prints the input data, specifies initial boundary conditions at all points of inflow and outflow, and coordinates all the desired computations. It sets the basin conditions to be considered and calls

the necessary subroutines for performing the numerical calculations at interior and boundary points in each time step. The results of computations are printed according to specified formats. The main program also transfers information to the plotting program through two discs. When the program is satisfactorily completed, a statement to this effect is printed and the computations are terminated.

Subroutine WIND

This subroutine computes the shear stress term due to wind at all grid points at any time. The body of water is divided into six zones and a set of values for each zone are given as input data. From the data the wind stress term with longitudinal and lateral directions are determined for any time step at all interior points.

Subroutine COMPU

This subroutine computes the longitudinal velocity (u), lateral velocity (v), and depth of water (h), at selected grid points in any time step.

Subroutine HCBDRY

This subroutine computes h , u , and v at the boundary points in any time step. The values of h at all boundary points are calculated by the conditions of geometrical compatibility. Mid-side points are used in writing the equations for straight boundaries and corner points for those at the corners. For points next to corners, the average of values computed for boundary points on either side are used. The values of u and v are zero at all boundary points except at inflow and outflow junctions where they are calculated from the corresponding values at the nearest interior points or from computed values of discharge and depth.

Subroutine UVCI C2

This subroutine prints the values of u , and v at all grid points in a given time step. The values of time step and time increment are also printed.

Data Deck

This part contains all the input data for the operation of circulation. The data are punched on cards, using all 80 columns according to specified formats and are in the order required by READ statements in the main program. Each new READ statement taps information starting from a new data card.

Plotting Program

The plotting program plots the boundary of appropriate waterbody, velocity vectors (showing magnitude and direction of velocity) at selected grid points, contours for depth and necessary titles. The data used in this program are transferred from the main program through two discs. The program includes five subroutines named CONTUR, PLOTT, INTERP, CONEX, and CONFOL used in computation and location of appropriate points for plotting the contours.

Description of Input Data

All of the input data required by the programs are in card form. Table 10.2 shows the various characteristics of input data used. The formats used for each type of data are also given along with pertinent explanations. Input data are given following the program listing.

The variable wind force data are based upon the actual observations for Hurricane Donna. The velocity and direction of wind for the different zones are found by following interpolation. The 16-hour duration used for the hurricane corresponds to the time period from 16:00 hours on September 11, 1960 to 8:00 hours on September 12, 1960. The input data are rearranged and printed after necessary computations according to the specified formats.

Description of Output Data

The outputs generated by the programs at any time step are of five categories: Wind speed, wind direction and other information at the current time step. Values of u and v , all grid points in separate tables. Values of absolute velocity and direction of water movement and water depth h at

selected grid points.

Values of absolute velocity and direction of water movement and water depth, h at all grid points in one table.

Plots of velocity vectors at selected points and contours for h .

Sample listings of the printer output are shown in the following pages.

Use of Basic Programs for Various Flow Conditions

The programs described in this report can be adapted to another two dimensional body of water by using the appropriate data on its geometry and other related information. Corresponding changes in the computational steps will also be needed. However, for Pamlico Sound, North Carolina, the given programs can be used for various flow conditions with only minor changes in the input data or initial and boundary conditions. Some important cases are as follows:

HYDROPS

If the value of wind stress coefficient on data card No. 8 and the discharge coefficients on data card No. 9 are equated to zero, it would imply that there is no wind stress and no outflow. The hydrodynamic (circulation) behavior of the waterbody can then be studied under various inflow conditions.

UNIWIND

If the V_w and δ values are kept constant in all six zones and at all times, the model gives the circulation patterns under the influence of uniform wind stresses. Depending upon the inflow/outflow values on data card No. 3, and the information on data card No. 9, the circulation for no inflow and no outflow or inflow but no outflow conditions can be obtained.

VARWIND

If the V_w and δ values vary in the six zones and with respect to time, then the circulation patterns can be studied for the variable wind field and any combination of inflow and outflow.

TIDALEX

By using appropriate values for discharge coefficients for the tidal inlets, the effect of tidal exchange on the circulation can be studied.

DEFINITIONS

- CD = coefficient of drag for wind stress, dimensionless.
- CM = Manning's coefficient of bottom stress
- CORIO = Coriolis coefficient
- D(I,J) = depth of water at mean sea level, in ft., at grid point (I,J).
- DS = distance step in the x and y-directions, in ft.
- DT = time step for computations, in seconds.
- G = gravitational constant, in ft./sec.²
- H(I,J) = water surface elevation above mean sea level at point (I,J) at latest time, in ft.
- HHS = water depth above mean sea level at Hatteras Inlet, in ft.
- HO(I,J) = water surface elevation above mean sea level at point (I,J) at previous time, in ft.
- HMS = elevation of the sea above mean sea level, in ft.
- HOC = water depth above mean sea level at Ocracoke Inlet, in ft.
- HOR = depth of water above mean sea level at Oregon Inlet, in ft.
- I = an index identifying the x-position of a grid point.
- IB(N) = an index identifying the x-position of boundary point numbered N.
- J = an index identifying the y-position of a grid point.
- JB(N) = an index identifying the y-position of the boundary point numbered N.
- JL(I) = index identifying the y-position of the boundary point on the Column I, having the lowest J value.
- JU(I) = index identifying the y-position of the boundary point on the column I, having the highest J value.
- KHS = coefficient of discharge for Hatteras Inlet.
- KOC = coefficient of discharge for Ocracoke Inlet.
- KOR = coefficient of discharge for Oregon Inlet.
- KT = a number identifying time, in hours at which wind data are given.
- N = a number identifying all boundary points.
- NBI(K) = values of N identifying boundary points of type 1.

NB2(K) = values of N, identifying boundary points of type 2.
NB3(K) = values of N, identifying boundary points of type 3.
NB4(K) = values of N, identifying boundary points of type 4.
NB5(K) = values of N, identifying boundary points of type 5.
NB6(K) = values of N, identifying boundary points of type 6.
NB7(K) = values of N, identifying boundary points of type 7.
NB8(K) = values of N, identifying boundary points of type 8.
NDUM = a dummy variable for counting the rounds of computations.
NI = no. of grid points on the x-axis.
NJ = no. of grid points on the y-axis.
NKT = the final time for which data are given, in hours.
NM = total number of boundary points.
NN = maximum no. of time intervals as input.
NZ = a number identifying the wind zone, see figure.
Q1 = Neuse River flow, in cfs.
Q2 = Pamlico River flow, in cfs.
Q3 = initial inflow from Croatan Sound, in cfs.
Q4 = initial inflow through Oregon Inlet, in cfs. (positive for flow to the sea).
Q5 = initial inflow through Hatteras Inlet in cfs. (positive for flow to the sea).
Q6 = initial flow through Ocracoke Inlet (positive for flow to the sea), in cfs.
QHS = flow through Hatteras Inlet, in cfs.
QOC = flow through Ocracoke Inlet, in cfs.
QOR = flow through Oregon Inlet, in cfs.
T = Time, in Minutes
TFIN = time for which computations will be terminated in hours.
THETA(I,J) = angle which the velocity vector makes with the x-axis, measured counterclockwise, in degrees.

- TPRINT = time at which printed output is desired, in hours.
- U(I,J) = velocity in the x-direction at current time step, at point (I,J), in ft./sec.
- VO(I,J) = velocity in the x-direction at previous time step, at point (I,J), in ft./sec.
- V(I,J) = velocity in the y-direction at current time step, at point (I,J), in ft./sec.
- VO(I,J) = velocity in the y-direction at previous time step at point (I,J), in ft./sec.
- VL(I,J) = absolute value of average velocity, at point (I,J), in ft./sec.
- VWD(NZ,KT) = wind direction in zone NZ at time KT, measured counterclockwise from the x-axis, in degrees.
- VWS(NZ,KT) = wind speed in zone NZ at time KT, in miles per hour.
- WSC = a coefficient equal to $C_d (\rho_a / \rho_w) (5280/3600)^2$ used in the computation of wind stress, when wind speed is given in miles per hour.
- WX(I,J) = wind shear stress in the x-direction divided by the water density, in ft^2/sec^2 .
- WY(I,J) = wind shear stress in the y-direction divided by the water density, in ft^2/sec^2 .

```

C
C *****
C *
C *           C I R C U L A T I O N           *
C *
C *           A N D                           *
C *
C *           H U R R I C A N E   S U R G E   *
C *
C *
C *
C * TIME-DEPENDENT MATHEMATICAL MODELS FOR PREDICTION OF *
C * CIRCULATION AND HURRICANE SURGE                 *
C * IN                                               *
C *
C *           P A M L I C O   S O U N D ,   N O R T H   C A R O L I N A *
C *
C *****

```

```

C *****
C          DEFINITION OF VARIABLES USED
C *****

```

```

C U=VELOCITY IN THE X-DIRECTION, FEET PER SECOND
C V=VELOCITY IN THE Y-DIRECTION, FEET PER SECOND
C D=DEPTH UP TO THE MEAN SEA LEVEL (MSL), FEET
C H=VARIATION IN DEPTH W.R.T. THE MSL, FEET

```

```

C THE SUBSCRIPT ZERO DENOTES PREVIOUS TIME STEP

```

```

C CM=MANNING COEFFICIENT
C CORIC=CORIOLIS COEFFICIENT
C G=GRAVITATIONAL CONSTANT, FT/SEC SQUARED
C Q1 =DISCHARGE TO THE SOUND FROM NEUSE RIVER ENTRANCE IN CFS
C Q2 =DISCHARGE TO THE SOUND FROM PAMLICO RIVER IN CFS
C Q3 =DISCHARGE TO THE SOUND FROM ROANOKE AND CRATON SOUNDS IN CFS
C Q4=INITIAL OUTFLOW THROUGH OREGON INLET.
C Q5=INITIAL OUTFLOW THROUGH HATTERAS INLET.
C Q6=INITIAL OUTFLOW THROUGH CRACKER INLET.
C VL=ABSOLUTE MAGNITUDE OF VELOCITY IN FEET PER SECOND
C THETA=THE DIRECTION OF VELOCITY IN DEGREES (COUNTERCLOCKWISE FROM
C THE X-AXIS

```

```

C DT=TIME INTERVAL FOR CALCULATIONS IN SECONDS
C TFIN=FINAL TIME OF FLOW FOR COMPUTATIONS, IN MINUTES
C NDOM=A DUMMY VARIABLE FOR COUNTING THE ROUNDS OF COMPUTATIONS
C DS=SIZE OF THE RECTANGULAR GRID IN FEET
C IB(N) AND JB(N) ARE THE COORDINATES OF THE POINTS ON BOUNDARY
C JMIN AND JMAX ARE MINIMUM AND MAXIMUM VALUES OF J, ON THE BOUNDARY
C FOR EACH I
C IG(K) AND JG(K) ARE COORDINATES OF POINTS MARKED BY CIRCLES
C ONE GRID INSIDE THE BOUNDARIES

```

```

C NB1(K)= BOUNDARY POINTS OF TYPE 1
C NB2(K)= BOUNDARY POINTS OF TYPE 2

```

```

C NB3(K)= BOUNDARY POINTS OF TYPE 3
C NB4(K)= BOUNDARY POINTS OF TYPE 4
C NB5(K)= BOUNDARY POINTS OF TYPE 5
C NB6(K)= BOUNDARY POINTS OF TYPE 6
C NB7(K)= BOUNDARY POINTS OF TYPE 7
C NB8(K)= BOUNDARY POINTS OF TYPE 8
C
C QOR= OUTFLOW THROUGH OREGON INLET AT ANY TIME, CFS
C QHS=OUTFLOW THROUGH HATTERAS INLET AT ANY TIME, CFS
C QCC=OUTFLOW THROUGH OCRACCKE INLET AT ANY TIME, CFS
C KOR=COEFF. OF DISCHARGE AT OREGON INLET
C KHS=COEFF. OF DISCHARGE AT HATTERAS INLET
C KCC=COEFF. OF DISCHARGE AT OCRACCKE INLET
C HOR=AVERAGE VALUE OF H AT OREGON INLET AT ANY TIME
C HHS=AVERAGE VALUE OF H AT HATTERAS INLET AT ANY TIME
C HOC=AVERAGE VALUE OF H AT OCRACCKE INLET AT ANY TIME
C HMSL=VARIATION IN THE WATER LEVEL OF ATLANTIC OCEAN W.R.T. ITS MSL
C VWS=VARIABLE WIND SPEED IN A ZONE AT A TIME, MILES PER HOUR
C VWD=VARIABLE WIND DIRECTION IN A ZONE AT A TIME, DEGREES
C COUNTERCLOCKWISE FROM THE X-AXIS
C CD=COEFFICIENT OF DRAG FOR WIND STRESS, DIMENSIONLESS
C WSC=A COEFFICIENT USED TO COMPUTE WIND STRESS WHEN THE WIND SPEED
C IS GIVEN IN MILES PER HOUR
C WX=VALUE OF WIND STRESS IN X-DIRECTION
C WY=VALUE OF WIND STRESS IN Y-DIRECTION
C NZ=NUMBERED ZONE OF PAMLICC SOUND FOR VARIABLE WIND STRESS.
C KT=TIME ELAPSED FROM THE START OF HURRICANE, HOURS
C NKT=FINAL VALUE OF KT = TCTAL DURATION OF HURRICANE, HOURS

```

```

REAL KOR,KHS,KCC
DIMENSION VL(65,36),THETA(65,36)
COMMON U(65,36),V(65,36),F(65,36),UO(65,36),VO(65,36),HO(65,36),
1D(65,36),IB(195),JB(195),JU(65),JL(65),IG(100),JG(100),
2 G,DTDS,DT60,WX,WY,WXDT,WYDT,CMSQ,GDT,GTS,CORDT,TPRINT,
3I,J,M,N,Q1,QN,Q2,QP,Q3,QC,DS,DTSSQ,TIME,DT,PI,WSC,Q4,Q5,Q6,NZ,
4VWD(6,17),KT,KKT,NKT,NI,NJ,NM,NN,SWX(65,36),SWY(65,36),T,
5HS(65,36),KOR,KHS,KCC,HMSL,HCR,HHS,HCC,
6VWS(6,17),QOR,QHS,QCC,VWX(6,17),VWY(6,17),
7NB1(40),NB2(40),NB3(40),NB4(40),NB5(40),NB6(40),NB7(40),NB8(40),
8NB9(40),NB10(40)
DIMENSION AA(20),AB(20),AC(20),AD(20)

```

```

C *****
C INITIALIZATION OF ALL PARAMETERS
C *****

```

```

C
C KT=1
C T=0.
C TIME=0.
C NDUM=0
C DO 1 I=1,65
C DO 1 J=1,36
C D(I,J)=0.
C U(I,J)=0.
C V(I,J)=0.
C H(I,J)=1.
C UO(I,J)=0.

```

```

VO(I,J)=0.
HO(I,J)=1.
SWX(I,J)=0.
SWY(I,J)=0.

```

```
1 CONTINUE
```

```

*****
C          INPUT DATA
C          *****

```

```
*** PERMANENT DATA ***
```

```

READ(1,10) DS,CORIO,CM
READ(1,10) Q1,Q2,Q3,Q4,Q5,Q6
READ(1,11) CD
WSC=CD*0.0026833
READ(1,10) KOR,KHS,KCC,HMSL

```

```

2 FORMAT(/10X,'WIND STRESS COEFFICIENT,      CD=',F10.7/
*      10X,'DURATION OF HURRICANE, HRS.  NKT=',I7/
*10X,'COEFF. OF DISCHARGE AT OCRACOKE INLET KOC=',F11.2/
*10X,'COEFF. OF DISCHARGE AT HATTERAS INLET KHS=',F11.2/
*10X,'COEFF. OF DISCHARGE AT OREGON INLET KOR=',F11.2/
*10X,'VARIATION IN THE WATER LEVEL W.R.T. ITS MSL,HMSL=',F11.2)

```

```
10 FORMAT(8F10.2)
```

```
11 FORMAT(F10.7)
```

```
12 FORMAT(5F10.2,F10.6)
```

```
15 FORMAT(6I10)
```

```

READ(1,30) (IB(N),N=1,192)
READ(1,30) (JB(N),N=1,192)
READ(1,30) (JL(I),I=5,61)
READ(1,30) (JU(I),I=5,61)

```

```

C *
DATA  NNB1,NNB2,NNB3,NNB4,NNB5/13,39,20,31,7/
DATA  NNB6,NNB7,NNB8,NNB9,NNB10/8,9,7,31,27/

```

```

READ(1,31) (NB1(K),K=1,NNB1)
READ(1,31) (NB2(K),K=1,NNB2)
READ(1,31) (NB3(K),K=1,NNB3)
READ(1,31) (NB4(K),K=1,NNB4)
READ(1,31) (NB5(K),K=1,NNB5)
READ(1,31) (NB6(K),K=1,NNB6)
READ(1,31) (NB7(K),K=1,NNB7)
READ(1,31) (NB8(K),K=1,NNB8)
READ(1,31) (NB9(K),K=1,NNB9)
READ(1,31) (NB10(K),K=1,NNB10)
READ(1,31) (IG(K),K=1,92)
READ(1,31) (JG(K),K=1,92)

```

```

C
C DEPTH VALUES AT POINTS MARKED BY CIRCLES ON ODD I COLUMN
READ (1,120)((D(I,J),J=2,36,2),I=1,65,2)

```

```
*** CASE DATA ***
```

```

C
C READ(1,18) (AA(I),I=1,20)
C READ(1,18) (AB(I),I=1,20)
C READ(1,18) (AC(I),I=1,20)
C READ(1,18) (AD(I),I=1,20)

```

```

C      AA(I),AB(I),AC(I),AD(I) ARE IDENTIFICATION TITLES
C
C      READ(1,10) DT,TFIN,DATUM
C      DATUM IS THE DIFFERENCE IN ELEVATION BETWEEN THE CONTOUR OF
C      ZERO DEPTH AND THE MEAN SEA LEVEL. IT IS USED ONLY FOR
C      PLOTTING PURPOSES.
C
C      READ(1,15) NKT
C      DO 17 NZ=1,6
C      READ(1,20) (VWS(NZ,KKT),KKT=1,NKT)
17 READ(1,21) (VWD(NZ,KKT),KKT=1,NKT)
18 FORMAT(20A4)
C
C
20 FORMAT(17F4.1)
21 FORMAT(17F4.0)
30 FORMAT(40I2)
31 FORMAT(25I3)
32 FORMAT(1X,12I5)
WRITE (3,35)
35 FORMAT (//18X,'-: INPUT DATA :-')
WRITE(3,18) (AA(I),I=1,20)
WRITE(3,18) (AB(I),I=1,20)
WRITE(3,18) (AC(I),I=1,20)
WRITE(3,18) (AD(I),I=1,20)
40 FORMAT(//10X,'FINAL TIME IN MINUTES          TFIN=',F10.2/
1      10X,'TIME INCREMENT IN SECONDS          DT=',F10.2/
2      10X,'SQUARE GRID IN FEET                DS=',F10.2/
5      10X,'CORIOLIS COEFFICIENT              CORIO=',F10.2/
6      10X,'MANNING COEFFICIENT                CM=',F10.2/
7      10X,'NEUSE RIVER DISCHARGE             Q1=',F10.2/
8      10X,'PAMLICJ RIVER DISCHARGE           Q2=',F10.2/
9      10X,'ROANOKE AND CROATAN DISCHARGE     Q3=',F10.2/
*      10X,'OUTFLCW FROM CREGON INLET         Q4=',F10.2/
*      10X,'OUTFLCW FROM HATTERAS INLET      Q5=',F10.2/
*      10X,'OUTFLCW FROM OCCRACCKE INLET     Q6=',F10.2)
WRITE(3,40)TFIN,DT,DS,CORIO,CM,Q1,Q2,Q3,Q4,Q5,Q6
WRITE(3,2)CD,NKT,KOC,KHS,KOR,HMSL
WRITE(3,41)
41 FORMAT(/5X,'VARIABLE WIND SPEED AT DIFFERENT VALUES OF NZ,6KT'/)
WRITE(3,42) (KKT,KKT=1,17)
42 FORMAT(/7X,17(3X,'( ',I2,' )'/))
DO 43 NZ=1,6
43 WRITE(3,46) NZ,(VWS(NZ,KKT),KKT=1,NKT)
WRITE(3,44)
44 FORMAT(/5X,'VARIABLE WIND DIREC. AT DIFFERENT VALUES OF NZ,6KT'/)
WRITE(3,42) (KKT,KKT=1,17)
DO 45 NZ=1,6
45 WRITE(3,46) NZ,(VWD(NZ,KKT),KKT=1,NKT)
46 FORMAT(3X,'( ',I2,' )',17(2X,F5.1))
47 FORMAT(//30X,'LOWER AND UPPER BOUND OF J FOR EACH I')
WRITE(3,47)
48 FORMAT(//13X,'-I-',5X,'JL(I)',6X,'JU(I)',7X,'-I-',6X,'JL(I)'
1,5X,'JU(I)',6X,'-I-',5X,'JL(I)',5X,'JU(I)'/)
WRITE(3,48)
DO 49 I=5,23

```

```

I1=19+I
I2=38+I
49 WRITE(3,70) I,JL(I),JU(I),I1,JL(I1),JU(I1),I2,JL(I2),JU(I2)
70 FORMAT(5X,2(5X,I5))
78 FORMAT(//50X,'COORDINATES OF THE PCINTS ON THE BOUNDARY')
80 FORMAT(///10X,'-N-',5X,'(IB(N),JB(N))',10X,'-N-',5X,'(IB(N),JB(N))
1',10X,'-N-',5X,'(IB(N),JB(N))',10X,'-N-',5X,'(IB(N),JB(N))'//)
WRITE(3,81)
81 FORMAT(//35X,'COORDINATES OF PCINTS MARKED BY CIRCLES ONE POINT GR
1ID INSIDE THE BOUNDARY')
WRITE(3,82)
82 FORMAT(///10X,'-K-',5X,'(IG(K),JG(K))',10X,'-K-',5X,'(IG(K),JG(K))
1',10X,'-K-',5X,'(IG(K),JG(K))',10X,'-K-',5X,'(IG(K),JG(K))'//)
DO 83 K=1,23
I1=23+K
I2=46+K
I3=69+K
83 WRITE(3,100) K,IG(K),JG(K),I1,IG(I1),JG(I1),I2,IG(I2),JG(I2),
I13,IG(I3),JG(I3)

```

C

```

WRITE(3,78)
WRITE(3,80)
DO 90 N=1,48
N1=48+N
N2=96+N
N3=144+N
90 WRITE(3,100) N, IB(N),JB(N),N1, IB(N1),JB(N1),N2,
1 IB(N2),JB(N2),N3, IB(N3),JB(N3)
100 FORMAT(4(8X,I5,5X,'( ',I5,', ',I5,', ')'))
101 FORMAT(//20X,'BOUNDARY PCINTS OF TYPE 1 I.E.,NB1(K)'//)
102 FORMAT(//20X,'BOUNDARY PCINTS OF TYPE 2 I.E.,NB2(K)'//)
103 FORMAT(//20X,'BOUNDARY PCINTS OF TYPE 3 I.E.,NB3(K)'//)
104 FORMAT(//20X,'BOUNDARY PCINTS OF TYPE 4 I.E.,NB4(K)'//)
105 FORMAT(//20X,'BOUNDARY PCINTS OF TYPE 5 I.E.,NB5(K)'//)
106 FORMAT(//20X,'BOUNDARY PCINTS OF TYPE 6 I.E.,NB6(K)'//)
107 FORMAT(//20X,'BOUNDARY PCINTS OF TYPE 7 I.E.,NB7(K)'//)
108 FORMAT(//20X,'BOUNDARY PCINTS OF TYPE 8 I.E.,NB8(K)'//)
109 FORMAT(//20X,'BOUNDARY PCINTS OF TYPE 9 I.E.,NB9(K)'//)
110 FORMAT(//20X,'BOUNDARY PCINTS OF TYPE 10 I.E.,NB10(K)'//)
112 FORMAT(10(1X,I3,'( ',I2,', ',I2,', ')'))
120 FORMAT(18(F4.0))

```

C

```

WRITE(3,101)
WRITE(3,112) ((NB1(K),IB(NB1(K)),JB(NB1(K))),K=1,NNB1)
WRITE(3,102)
WRITE(3,112) ((NB2(K),IB(NB2(K)),JB(NB2(K))),K=1,NNB2)
WRITE(3,103)
WRITE(3,112) ((NB3(K),IB(NB3(K)),JB(NB3(K))),K=1,NNB3)
WRITE(3,104)
WRITE(3,112) ((NB4(K),IB(NB4(K)),JB(NB4(K))),K=1,NNB4)
WRITE(3,105)
WRITE(3,112) ((NB5(K),IB(NB5(K)),JB(NB5(K))),K=1,NNB5)
WRITE(3,106)
WRITE(3,112) ((NB6(K),IB(NB6(K)),JB(NB6(K))),K=1,NNB6)
WRITE(3,107)
WRITE(3,112) ((NB7(K),IB(NB7(K)),JB(NB7(K))),K=1,NNB7)

```

```

WRITE(3,108)
WRITE(3,112) ((NB8(K),IB(NB8(K)),JB(NB8(K))),K=1,NNB8)
WRITE(3,109)
WRITE(3,112) ((NB9(K),IB(NB9(K)),JB(NB9(K))),K=1,NNB9)
WRITE(3,110)
WRITE(3,112) ((NB10(K),IB(NB10(K)),JB(NB10(K))),K=1,NNB10)

```

C

LOCAL DEPTHS AT ALL GRID POINTS

C

C DEPTH VALUES AT POINTS MARKED BY CIRCLES ON EVEN I COLUMNS

```
DO 130 I=2,64,2
```

```
DO 130 J=3,35,2
```

```
130 D(I,J)=(D(I-1,J+1)+D(I-1,J-1)+D(I+1,J-1)+D(I+1,J+1))/4.
```

C

C DEPTH VALUES AT ALL POINTS(I,1), I=1,65

```
DO 132 I=1,65,2
```

```
132 D(I,1) = D(I,2)
```

```
DO 134 I=2,64,2
```

```
134 D(I,1) = D(I,3)
```

C

C DEPTH VALUES AT POINTS MARKED BY SQUARES ON EVEN I COLUMNS

```
DO 140 I=2,64,2
```

```
DO 140 J=2,34,2
```

```
140 D(I,J)=(D(I,J-1)+D(I,J+1)+D(I-1,J)+D(I+1,J))/4.
```

C

C DEPTH VALUES AT POINTS MARKED BY SQUARES ON ODD I COLUMNS

```
DO 150 I=3,63,2
```

```
DO 150 J=3,35,2
```

```
150 D(I,J)=(D(I,J-1)+D(I,J+1)+D(I-1,J)+D(I+1,J))/4.
```

```
WRITE (3,155)
```

```
155 FORMAT('1'./10X,'LOCAL DEPTH AT MEAN SEA LEVEL. D AT ALL POINTS')
```

```
WRITE (3,160) (J,J=5,19)
```

```
160 FORMAT (/7X,15(3X,'(,I2,')')/)
```

```
165 FORMAT(//7X,16(3X,'(,I2,')')/)
```

```
DO 170 I=5,61
```

```
170 WRITE(3,180) I,(D(I,J),J=5,19)
```

```
180 FORMAT (3X,'(,I2,')',15(1X,F6.2))
```

```
185 FORMAT (3X,'(,I2,')',16(1X,F6.2))
```

```
WRITE (3,165) (J,J=20,35)
```

```
DO 190 I=5,61
```

```
190 WRITE(3,185) I,(D(I,J),J=20,35)
```

C

C

C

INITIAL BOUNDARY CONDITIONS

C

VALUES OF U,V ,GH AT TIME=0.0 MINUTES

C

C

C

NEUSE RIVER JUNCTION WITH SCUND

C

```
QN=Q1/(4.0*DS)
```

```
N=192
```

```
I=IB(N)
```

```
J=JB(N)
```

```
U(I,J)=QN/(D(I,J)+H(I,J))
```

```
V(I,J)=0.
```

```
U(I+1,J)=U(I,J)
```

```
U(I+2,J)=U(I,J)
```

```
U(I+3,J)=U(I,J)
```

C

C

```

DO 192 N=1,4
I=IB(N)
J=JB(N)
U(I,J)=QN/(D(I,J)+H(I,J))
V(I,J)=0.
U(I+1,J)=U(I,J)
U(I+2,J)=U(I,J)
192 U(I+3,J)=U(I,J)

```

```

C
C           PAMLIC RIVER JUNCTION WITH SOUND
C

```

```

QP=-Q2/(4.*DS)
DO 193 N=20,24
I=IB(N)
J=JB(N)
U(I,J)=0.
V(I,J)=QP/(D(I,J)+H(I,J))
V(I,J-1)=V(I,J)
V(I,J-2)=V(I,J)
193 V(I,J-3)=V(I,J)

```

```

C
C           CROATAN AND ROANCKE SOUNDS
C

```

```

QC=-Q3
DO 194 N=88,91
I=IB(N)
J=JB(N)
U(I,J)=QC/(3.*DS*(D(I,J)+H(I,J)))
V(I,J)=0.
U(I-1,J-1)=U(I,J)
194 V(I-1,J-1)=V(I,J)

```

```

C
C           OREGON INLET BETWEEN PAMLIC SOUND AND ATLANTIC OCEAN.
C

```

```

DO 195 N=104,106
I=IB(N)
J=JB(N)
U(I,J)=Q4/(2.0*DS*(D(I,J)))
195 V(I,J)=0.

```

```

C
C           HATTERAS INLET BETWEEN PAMLIC SOUND AND ATLANTIC OCEAN
C

```

```

DO 196 N=150,152
I=IB(N)
J=JB(N)
U(I,J)=0.
196 V(I,J)=-Q5/(2.0*DS*(D(I,J)))

```

```

C
C           CCRACCKE INLET BETWEEN PAMLIC SOUND AND ATLANTIC OCEAN
C

```

```

DO 197 N=164,166
I=IB(N)
J=JB(N)
U(I,J)=0.
197 V(I,J)=-Q6/(2.0*DS*(D(I,J)))

```

```

C

```

```

C
C   WRITING THE VALUE OF U,V&H           AT TIME=0.0 MINUTES
C
C   *****REMCVE THE FOLLOING CARD IF YOU WANT PRINTOUT
C   OF VALUES AT ALL PCINTS *****
C   GO TO 202
200 CALL UVC1C2
202 WRITE(3,310) TIME,DT
    WRITE(3,203)
203 FORMAT (10X,'VARIATION IN DEPTH ,H, AT SELECTED POINTS'/)
    WRITE(3,160)(J,J=5,35,5)
    DO 204 I=5,61,5
204 WRITE(3,180) I,(H(I,J),J=5,35,5)
C
C
C   *       *       *       *       *       *
C   THE FOLLOWING INFORMATION IN THIS SECTION IS TO BE USED LATER IN
C   PLECTING PROGRAM
    WRITE(10,12) TFIN,DT,Q1,Q2,Q3,*SC
    WRITE(10,30) (IB(N),N=1,192)
    WRITE(10,30) (JB(N),N=1,192)
    IMIN=5
    IMAX=61
    WRITE(10,30) IMIN,IMAX,(JL(I),JU(I),I=IMIN,IMAX)
C   *****
C   COMPUTATION OF SOME CONSTANTS TO BE USED LATER
C   *****
C
    DT60=DT/60.
    DTDS=DT/(2.*DS)
    DTSSQ=DT/(DS*DS)
    CORDT=COR10*DT
    G=32.2
    GDT=G*DT
    GTS=G*DTDS
    CMSQ=CM*CM
    PI=3.1416
    *WRITE(3,205)
205 FORMAT (/40X,'PRINT CUT OF THE DIFFERENT COMPUTED CONSTANTS')
    WRITE(3,206) (DT60,DTDS,DTSSQ,CORDT,G,GDT,GTS,CMSQ,PI)
206 FORMAT(' DT60=',F10.5,1X,'DTDS=',F10.5,1X,'DTSSQ=',F10.8,1X,
1'CORDT=',F10.5,1X,'G=',F5.2,1X,'GDT=',F15.5,1X,'GTS=',F10.5,1X,
*'CMSQ=',F10.5,/' PI=',F10.4)
C
    DO 207 NZ=1,6
    DO 207 KT=1,NKT
        VWX(NZ,KT)=VWS(NZ,KT)*VWS(NZ,KT)*CCS(VWD(NZ,KT)*PI/180.0)
207 VWY(NZ,KT)=VWS(NZ,KT)*VWS(NZ,KT)*SIN(VWD(NZ,KT)*PI/180.0)
        KT=1
208 READ(1,209) TPRINT
209 FORMAT(F10.1)
C
C   *****
C   COMPUTATIONS FOR U,V AND H AT ALL GRID POINTS.
C   *****
C

```

```

210 IF (TIME.GE.(60.*KT)) KT=KT+1
C   THE ABOVE STEP IMPLIES THAT AT TIME=0.0 MINUTES KT=1 HOUR AND IT
C   WILL HAVE THE SAME VALUE UNTILL TIME=59.0 MINUTES . SIMILARLY
C   WHEN TIME=60.0 MINUTES, KT=2 HOURS.
   TIME=TIME+DT60
   NDUM=NDUM+1
212 T=TIME-60.*(KT-1)
C
C   COMPUTATION FOR U,V AND H      AT INTERIOR GRID POINTS MARKED BY SQUARES.
C   HYDRODYNAMIC EQUATIONS ARE USED FOR ALL THESE POINTS
C
214 CALL WIND
   DO 215 I=6,60,2
     J1=JL(I)+1
     J2=JU(I)-1
     DO 215 J=J1,J2,2
       WX=WSC*SWX(I,J)
       WY=WSC*SWY(I,J)
       WXDT=WX*DT
       WYDT=WY*DT
215 CALL COMPU
   DO 220 I=7,59,2
     J1=JL(I)+2
     J2=JU(I)-2
     DO 220 J=J1,J2,2
       WX=WSC*SWX(I,J)
       WY=WSC*SWY(I,J)
       WXDT=WX*DT
       WYDT=WY*DT
220 CALL COMPU
   DO 225 I=7,59,2
     J=JL(I)+1
     WX=WSC*SWX(I,J)
     WY=WSC*SWY(I,J)
     WXDT=WX*DT
     WYDT=WY*DT
225 CALL COMPU
   DO 230 I=7,59,2
     J=JU(I)-1
     WX=WSC*SWX(I,J)
     WY=WSC*SWY(I,J)
     WXDT=WX*DT
     WYDT=WY*DT
230 CALL COMPU
C   COMPUTATION OF U,V AND H AT POINTS MARKED BY CIRCLES ONE GRID
C   INSIDE THE BOUNDARY. HYDRODYNAMIC EQUATIONS ARE USED AT
C   THESE POINTS
   DO 227 K=1,92
     I=IG(K)
     J=JG(K)
     WX=WSC*SWX(I,J)
     WY=WSC*SWY(I,J)
     WXDT=WX*DT
     WYDT=WY*DT
227 CALL COMPU
C

```

```

C
C   COMPUTATION OF U,V AND H AT ALL OTHER INTERIOR POINTS MARKED BY
C   CIRCLES. AVERAGING THE VALUES AT NEIGHBORING POINTS IS
C   USED AT THESE POINTS
DO 240 I=7,59,2
  J1=JL(I)+3
  J2=JU(I)-3
  DO 240 J=J1,J2,2
    U(I,J)=(U(I,J-1)+U(I,J+1)+U(I-1,J)+U(I+1,J))/4.
    V(I,J)=(V(I,J-1)+V(I,J+1)+V(I-1,J)+V(I+1,J))/4.
    H(I,J)=(H(I,J-1)+H(I,J+1)+H(I-1,J)+H(I+1,J))/4.
240 CONTINUE
DO 250 I=8,58,2
  J1=JL(I)+2
  J2=JU(I)-2
  DO 250 J=J1,J2,2
    U(I,J)=(U(I,J-1)+U(I,J+1)+U(I-1,J)+U(I+1,J))/4.
    V(I,J)=(V(I,J-1)+V(I,J+1)+V(I-1,J)+V(I+1,J))/4.
    H(I,J)=(H(I,J-1)+H(I,J+1)+H(I-1,J)+H(I+1,J))/4.
250 CONTINUE
C
C   COMPUTATIONS FOR U,V AND H           AT GRID POINTS ON THE BOUNDRY.
C
C   CALL HCBDRY
C
C
C   CONVERTING THE CURRENT VALUES INTO THE PREVIOUS TIME STEP VALUES
C   FOR THE NEXT TIME STEP.
C
258 DO 260 I=5,61
  DO 260 J=5,35
    U0(I,J)=U(I,J)
    V0(I,J)=V(I,J)
    H0=H(I,J)+D(I,J)
    IF (H0.GE.1.0) GO TO 259
    H(I,J)=1.0-D(I,J)
259 H0(I,J)=H(I,J)
260 CONTINUE
    IF(TIME.EQ.TPRINT) GO TO 270
    GO TO 210
C
C   *****
C   CALCULATION OF ABSOLUTE MAGNITUDE OF VELOCITY AND ITS DIRECTION
C   *****
C
C   ?????? USE II=1, IF YOU WANT VALUES AT ALL POINTS.
C   USE II=5 FOR VALUES AT SELECTED POINTS
270 II=5
  DO 300 I=5,60,II
  DO 300 J=5,35,II
    U1=U(I,J)
    V1=V(I,J)
    VL(I,J)=SQRT(U1*U1+V1*V1)
    IF(U1.GT.0.0.AND.V1.EQ.0.) THETA(I,J)=0.
    IF(U1.EQ.0.0.AND.V1.GT.0.) THETA(I,J)=90.

```

```

IF(U1.LT.0.0.AND.V1.EQ.0.) THETA(I,J)=180.
IF(U1.EQ.0.0.AND.V1.LT.0.) THETA(I,J)=270.
IF(U1.EQ.0.0.AND.V1.EQ.0.) THETA(I,J)=360.
IF(U1.GT.0.0.AND.V1.GT.0.) THETA(I,J)=180.*ATAN(V1/U1)/PI
IF(U1.GT.0.0.AND.V1.LT.0.) THETA(I,J)=360.+180.*ATAN(V1/U1)/PI
300 IF(U1.LT.0.0.AND.V1.NE.0.) THETA(I,J)=180.+180.*ATAN(V1/U1)/PI

```

```

C
C *****
C PRINT CUT OF THE RESULTS
C *****
C
WRITE(3,310) TIME,DT
WRITE(3,303)
303 FORMAT(/5X,'WRITING THE VALUES OF H(I,J), D(I,J), AND THEIR SUM,HD
11 AT ALL POINTS WHERE IT WENT BELOW 1.0 FEET'/)
DO 305 I=5,61
DO 305 J=7,31
HD1=H(I,J)+D(I,J)
IF (HD1.GE.1.0) GO TO 305
WRITE (3,304) I,J,H(I,J),D(I,J),HD1
HD1=1.0
H(I,J)=1.0-D(I,J)
304 FORMAT(' AT POINT (',I2,',',I2,'): H(I,J)=',F6.2,5X,'D(I,J)=',
1F6.2,5X,'HD1=',F6.2)
305 CONTINUE
310 FORMAT('*1',/' * TIME=',F8.2,2X,'MINUTES. THE TIME INCREMENT USED I
1S, DT=',F8.2,2X,'SECONDS')
WRITE(3,311)
311 FORMAT(///1X,'OUTFLC# DATA AT OREGON, HATTERAS, AND OCRACOE INLETS
1 RESPECTIVELY'/)
WRITE(3,312) QCR,KCR,HCR,QHS,KHS,HHS,QCC,KCC,HCC
312 FORMAT(1X,'QCR=',F10.2,1X,'KCR=',F10.2,1X,'HCR=',F5.1,1X,
1 'QHS=',F10.2,1X,'KHS=',F10.2,1X,'HHS=',F5.1,1X,
2 'QCC=',F10.2,1X,'KCC=',F10.2,1X,'HCC=',F5.1/)
C *****REMOVE THE FOLLOWING CARD IF YOU WANT PRINTOUT
C OF VALUES AT ALL POINTS *****
GO TO 313
314 CALL UVC1C2
313 WRITE(3,310) TIME,DT
WRITE (3,315) NDUM
315 FORMAT('/ NUMBER OF TIME STEPS COMPLETED=',I5/)
WRITE (3,320)
320 FORMAT(//45X,'COMPUTED VALUES OF VL,THETA&H AT SELECTED GRID
1 POINTS'/)
WRITE (3,330)
330 FORMAT(//8X,'GRID POINT',7X,'VL',7X,'THETA',8X,'H',17X,
1 'GRID POINT',7X,'VL',7X,'THETA',8X,'H',2X/)
DO 340 I=5,30,5
IA=I+30
DO 340 J=5,35,5
340 WRITE (3,350) I,J,VL(I,J),THETA(I,J),H(I,J),IA,J,VL(IA,J),
1 THETA(IA,J),H(IA,J)
350 FORMAT(9X,'(',I3,',',I3,')',6X,F4.1,2(6X,F5.1),16X,
1 '(',I3,',',I3,')',6X,F4.1,2(6X,F5.1))
C *****REMOVE THE FOLLOWING CARD IF YOU WANT PRINTOUT
C OF VALUES AT ALL POINTS *****

```

```

GO TO 492
351 WRITE (3,310) TIME,DT
    WRITE (3,410)
410 FORMAT(//45X,'COMPUTED VALUES OF VL,THETA AND H AT EACH GRID POINT
1')
    WRITE (3,420) (J,J=6,10)
420 FORMAT(/4X,5(9X,'(,I2,)',,6X)/)
    WRITE (3,430)
430 FORMAT (/5X,5(6X,'VL',1X,'THETA',3X,'H',1X)//)
    DO 440 I=5,61
440 WRITE (3,450) (I,(VL(I,J),THETA(I,J),H(I,J),J=6,10))
450 FORMAT (' ', '(,I2,)',,5(4X,F4.1,1X,2F5.1))
    WRITE (3,420) (J,J=11,15)
    WRITE (3,430)
    DO 460 I=5,61
460 WRITE (3,450) (I,(VL(I,J),THETA(I,J),H(I,J),J=11,15))
    WRITE (3,420) (J,J=16,20)
    WRITE (3,430)
    DO 470 I=5,61
470 WRITE (3,450) (I,(VL(I,J),THETA(I,J),H(I,J),J=16,20))
    WRITE (3,420) (J,J=21,25)
    WRITE (3,430)
    DO 480 I=5,61
480 WRITE (3,450) (I,(VL(I,J),THETA(I,J),H(I,J),J=21,25))
    WRITE (3,420) (J,J=26,30)
    WRITE (3,430)
    DO 490 I=5,61
490 WRITE (3,450) (I,(VL(I,J),THETA(I,J),H(I,J),J=26,30))
    WRITE (3,420) (J,J=31,35)
    WRITE (3,430)
    DO 491 I=5,61
491 WRITE (3,450)(I,(VL(I,J),THETA(I,J),H(I,J),J=31,35))
C     THE FOLLOWING INFORMATION IS FOR DRAWING VELOCITY VECTORS IN THE
C     PLOTTING PROGRAM
492 WRITE(10,493) TIME
493 FORMAT(F9.3)
    DO 494 I=5,30,5
    IA=I+30
    DO 494 J=5,35,5
494 WRITE (10,496) I,J,U(I,J),V(I,J),VL(I,J),THETA(I,J),IA,J,U(IA,J),
1V(IA,J),VL(IA,J),THETA(IA,J)
496 FORMAT(2(2I4,3F7.2,F8.2))
C     THE FOLLOWING INFORMATION IS TO DRAW THE CONTOURS FOR DEPTH.
    NPCINT=0
    WRITE(4) NPCINT
    GINT=1.
    WRITE(4) GINT
    IMIN=5
    IMAX=61
    DO 510 I=IMIN,IMAX
    JSTRT=JL(I)
    JSTOP=JU(I)
    WRITE(4) I,JSTRT,JSTOP
    DO 500 J=JSTRT,JSTOP
500 HS(I,J)=100.*(H(I,J)+DATUM)
510 WRITE (4) (HS(I,J),J=JSTRT,JSTOP)

```

```
C      HS(I,J)=100.*H(I,J) IS USED BECAUSE THE CONTOUR INTERVAL HAS TO BE
C      SPECIFIED AS AN INTEGER. HOWEVER, DURING THE ANNOTATION OF CONTOUR
C      S, THE VALUES OF HS ARE DIVIDED BY 100. TO SHOW THE CORRECT VALUE
C      OF DEPTH,H
      NPOINT=10000
      WRITE(4) NPOINT,NPCINT,NPCINT
      IF (TIME.LT.TFIN) GO TO 208
      WRITE (3,550)
550  FORMAT(/ /10X,'THE PROGRAM HAS BEEN SATISFACTORILY COMPLETED'/)
551  STOP
      END
```

```

C *****
  SUBROUTINE WIND
C *****
  COMMON U(65,36),V(65,36),H(65,36),U0(65,36),V0(65,36),H0(65,36),
  1D(65,36),IB(195),JB(195),JU(65),JL(65),IG(100),JG(100),
  2      G,DTDS,DT60,WX,WY,WXDT,WYDT,CMSQ,GDT,GTS,CORDT,TPRINT,
  3I,J,M,N,Q1,QN,Q2,QP,Q3,QC,DS,DTSSQ,TIME,DT,PI,WSC,Q4,Q5,Q6,NZ,
  4VWD(6,17),KT,KKT,NKT,NI,NJ,NM,NN,SWX(65,36),SWY(65,36),T,
  5HS(65,36),KOR,KHS,KCC,HMSL,HOR,HMS,HOC,
  6VWS(6,17),QOR,QHS,QOC,VWX(6,17),VWY(6,17),
  7NB1(40),NB2(40),NB3(40),NB4(40),NB5(40),NB6(40),NB7(40),NB8(40),
  8NB9(40),NB10(40)

C
C   SUBROUTINE WIND COMPUTES THE COMPONENTS ALONG THE X- AND Y- AXIS
C   OF THE SQUARE OF THE WIND VELOCITY IN SQ. FT/ SEC. SQ. AT ALL
C   GRID POINTS AT A GIVEN TIME
C
  IF(KT.GE.NKT) GO TO 250
230 DO 240 I=1,22
    DO 240 J=1,20
      NZ=1
      SWY(I,J)=VWY(NZ,KT)+(VWY(NZ,KT+1)-VWY(NZ,KT))*T/60.
240 SWX(I,J)=VWX(NZ,KT)+(VWX(NZ,KT+1)-VWX(NZ,KT))*T/60.
      DO 241 I=23,47
        DO 241 J=1,20
          NZ=2
          SWY(I,J)=VWY(NZ,KT)+(VWY(NZ,KT+1)-VWY(NZ,KT))*T/60.
241 SWX(I,J)=VWX(NZ,KT)+(VWX(NZ,KT+1)-VWX(NZ,KT))*T/60.
          DO 242 I=48,60
            DO 242 J=1,20
              NZ=3
              SWY(I,J)=VWY(NZ,KT)+(VWY(NZ,KT+1)-VWY(NZ,KT))*T/60.
242 SWX(I,J)=VWX(NZ,KT)+(VWX(NZ,KT+1)-VWX(NZ,KT))*T/60.
              DO 243 I=1,22
                DO 243 J=21,35
                  NZ=4
                  SWY(I,J)=VWY(NZ,KT)+(VWY(NZ,KT+1)-VWY(NZ,KT))*T/60.
243 SWX(I,J)=VWX(NZ,KT)+(VWX(NZ,KT+1)-VWX(NZ,KT))*T/60.
                  DO 244 I=23,47
                    DO 244 J=21,35
                      NZ=5
                      SWY(I,J)=VWY(NZ,KT)+(VWY(NZ,KT+1)-VWY(NZ,KT))*T/60.
244 SWX(I,J)=VWX(NZ,KT)+(VWX(NZ,KT+1)-VWX(NZ,KT))*T/60.
                      DO 245 I=48,60
                        DO 245 J=21,35
                          NZ=6
                          SWY(I,J)=VWY(NZ,KT)+(VWY(NZ,KT+1)-VWY(NZ,KT))*T/60.
245 SWX(I,J)=VWX(NZ,KT)+(VWX(NZ,KT+1)-VWX(NZ,KT))*T/60.
                          GO TO 270
250 KT=NKT
      DO 256 I=1,22
        DO 256 J=1,20
          NZ=1
          SWY(I,J)=VWY(NZ,KT)
256 SWX(I,J)=VWX(NZ,KT)
      DO 257 I=23,47

```

```
DO 257 J=1,20
  NZ=2
  SWY(I,J)=VWY(NZ,KT)
257 SWX(I,J)=VWX(NZ,KT)
  DO 258 I=48,60
  DO 258 J=1,20
  NZ=3
  SWY(I,J)=VWY(NZ,KT)
258 SWX(I,J)=VWX(NZ,KT)
  DO 259 I=1,22
  DO 259 J=21,35
  NZ=4
  SWY(I,J)=VWY(NZ,KT)
259 SWX(I,J)=VWX(NZ,KT)
  DO 261 I=23,47
  DO 261 J=21,35
  NZ=5
  SWY(I,J)=VWY(NZ,KT)
261 SWX(I,J)=VWX(NZ,KT)
  DO 263 I=48,60
  DO 263 J=21,35
  NZ=6
  SWY(I,J)=VWY(NZ,KT)
263 SWX(I,J)=VWX(NZ,KT)
270 RETURN
  END
```

```

C *****
C SUBROUTINE CCMPU
C *****
  REAL KQR,KHS,KCC
  COMMON U(65,36),V(65,36),H(65,36),UO(65,36),VO(65,36),HO(65,36),
  1D(65,36),IB(195),JB(195),JU(65),JL(65),IG(100),JG(100),
  2 G,DTDS,DT60,WX,WY,WXDT,WYDT,CMSQ,GDT,GTS,CORDT,TPRINT,
  3I,J,M,N,Q1,QN,Q2,QP,Q3,QC,DS,DTSSQ,TIME,DT,PI,WSC,Q4,Q5,Q6,NZ,
  4VWD(6,17),KT,KKT,NKT,NI,NJ,NM,NN,SWX(65,36),SWY(65,36),T,
  5HS(65,36),KQR,KHS,KCC,HMSL,HOR,HHS,HCC,
  6VWS(6,17),QQR,QHS,QQC,VWX(6,17),VWY(6,17),
  7NB1(40),NB2(40),NB3(40),NB4(40),NB5(40),NB6(40),NB7(40),NB8(40),
  8NB9(40),NB10(40)

C
C SUBROUTINE CCMPU CCMPUTES U,V&H AT SELECTED GRID POINTS
C
  UBAR=(UO(I+1,J)+UO(I-1,J)+UO(I,J+1)+UO(I,J-1))/4.
  VBAR=(VO(I+1,J)+VO(I-1,J)+VO(I,J+1)+VO(I,J-1))/4.
  HBAR=(HO(I+1,J)+HO(I-1,J)+HO(I,J+1)+HO(I,J-1))/4.
C THE STEP BELOW IMPLIES THAT WHENEVER THE TOTAL DEPTH AT A POINT
C FALLS BELOW 1.0 FOOT, IT IS CORRECTED FOR FURTHER COMPUTATIONS
C FOR U,V,AND H.
  HD=HBAR+D(I,J)
  IF (HD.GT.1.0) GO TO 640
  HBAR=1.-D(I,J)
  HD=1.0
640 RAD=SQRT(UBAR*UBAR + VBAR*VBAR)
  IF (ABS(RAD)-0.1) 651,651,650
651 SF=0.0
  GO TO 660
650 SF=CMSQ*SQRT(UBAR*UBAR+VBAR*VBAR)/(2.22*HD**(4./3.))
660 U(I,J)=-UBAR*(UO(I+1,J)-UO(I-1,J))*DTDS
  1 -VBAR*(UO(I,J+1)-UO(I,J-1))*DTDS
  2+CORDT*VBAR-GTS*(HO(I+1,J)-HO(I-1,J))
  3+WXDT/(D(I,J)+HO(I,J))-SF*UBAR*GDT+UBAR
  V(I,J)=-UBAR*(VO(I+1,J)-VO(I-1,J))*DTDS
  1 -VBAR*(VO(I,J+1)-VO(I,J-1))*DTDS
  2-CORDT*UBAR-GTS*(HO(I,J+1)-HO(I,J-1))
  3+WYDT/(D(I,J)+HO(I,J))-SF*VBAR*GDT+VBAR
  H(I,J)=-UO(I+1,J)*(HO(I+1,J)+D(I+1,J))-UO(I-1,J)*(HO(I-1,J)
  1 +D(I-1,J))*DTDS-(VO(I,J+1)*(HO(I,J+1)+D(I,J+1))
  2 -VO(I,J-1)*(HO(I,J-1)+D(I,J-1)))*DTDS+HBAR
680 RETURN
  END

```

```

C *****
  SUBROUTINE HCBDRY
C *****
  REAL KOR,KHS,KOC
  COMMON U(65,36),V(65,36),H(65,36),UO(65,36),VO(65,36),HO(65,36),
  1D(65,36),IB(195),JB(195),JU(65),JL(65),IG(100),JG(100),
  2      G,DTDS,DT60,WX,WY,WXDT,WYDT,CMSQ,GDT,GTS,CORDT,TPRINT,
  3I,J,M,N,Q1,QN,Q2,QP,Q3,QC,DS,DTSSQ,TIME,DT,PI,WSC,Q4,Q5,Q6,NZ,
  4VWD(6,17),KT,KKT,NKT,NI,NJ,NM,NN,SWX(65,36),SWY(65,36),T,
  5HS(65,36),KOR,KHS,KCC,HMSL,HOR,HHS,HOC,
  6VWS(6,17),QDR,QHS,QDC,VWX(6,17),VWY(6,17),
  7NB1(40),NB2(40),NB3(40),NB4(40),NB5(40),NB6(40),NB7(40),NB8(40),
  8NB9(40),NB10(40)
C
C SUBROUTINE HCBDRY CCMPTES      H,U, AND V AT THE GRID POINTS ON
C BOUNDARY.
  DATA  NN81,NN82,NN83,NN84,NN85/13,39,20,31,7/
  DATA  NN86,NN87,NN88,NN89,NNB10/8,9,7,31,27/
  DO 31 K=1,NN81
    N=NB1(K)
    I=IB(N)
    J=JB(N)
  31 H(I,J)=H(I+1,J+1) + H(I+1,J-1) - H(I+2,J)
    DO 33 K=1,NN82
      N=NB2(K)
      I=IB(N)
      J=JB(N)
  33 H(I,J)=H(I+1,J-1) + H(I-1,J-1) - H(I,J-2)
    DO 35 K=1,NN83
      N=NB3(K)
      I=IB(N)
      J=JB(N)
  35 H(I,J)=H(I-1,J+1) + H(I-1,J-1) - H(I-2,J)
    DO 37 K=1,NN84
      N=NB4(K)
      I=IB(N)
      J=JB(N)
  37 H(I,J) = H(I+1,J+1) + H(I-1,J+1) - H(I,J+2)
    DO 39 K=1,NN85
      N=NB5(K)
      I=IB(N)
      J=JB(N)
  39 H(I,J)=H(I+1,J-1)*2.0 - H(I+2,J-2)
    DO 41 K=1,NN86
      N=NB6(K)
      I=IB(N)
      J=JB(N)
  41 H(I,J)=H(I-1,J-1)*2.0 -H(I-2,J-2)
    DO 43 K=1,NN87
      N=NB7(K)
      I=IB(N)
      J=JB(N)
  43 H(I,J)=H(I-1,J+1)*2.0 - H(I-2,J+2)
    DO 45 K=1,NN88
      N=NB8(K)
      I=IB(N)

```


C
C
C
C

OREGON INLET BETWEEN PAMLICO SOUND AND ATLANTIC OCEAN.

```

HOR=(H(57,21)+H(57,22)+H(57,23))/3.
IF (ABS(HOR) - 0.1) 192,192,119
119 IF (HOR - 0.0) 190,191,191
190 QOR=-KOR*SQRT(HMSL-HOR)
    GO TO 194
191 QOR=KOR*SQRT(HCR-HMSL)
    GO TO 194
192 QOR = 0.0
194 DO 195 N=104,106
    I=IB(N)
    J=JB(N)
    U(I,J)=(QOR)/(2.0*DS*(D(I,J)))
195 V(I,J)=0.
    
```

C
C
C

HATTERAS INLET BETWEEN PAMLICO SOUND AND ATLANTIC OCEAN

```

HHS=(H(31,9)+H(32,9)+H(33,9))/3.
IF (ABS(HHS) - 0.1) 202,202,198
198 IF (HHS-0.0) 200,201,201
200 QHS=-KHS*SQRT(HMSL-HHS)
    GO TO 203
201 QHS=KHS*SQRT(HMS-HMSL)
    GO TO 203
202 QHS=0.0
203 DO 205 N=150,152
    I=IB(N)
    J=JB(N)
    V(I,J)=-QHS/(2.0*DS*(D(I,J)))
205 U(I,J)=0.
    
```

C
C
C

CCRACKE INLET BETWEEN PAMLICO SOUND AND ATLANTIC OCEAN

```

HOC=(H(19,11)+H(20,11)+H(21,11))/3.
IF (ABS(HOC) - 0.1) 214,214,206
206 IF (HOC - 0.0) 211,212,212
211 QOC=-KOC*SQRT(HMSL-HOC)
    GO TO 215
212 QOC=KOC*SQRT(HOC-HMSL)
    GO TO 215
214 QOC=0.0
215 DO 216 N=164,166
    I=IB(N)
    J=JB(N)
    V(I,J)=-QOC/(2.0*DS*(D(I,J)))
216 U(I,J)=0.
    RETURN
    END
    
```

```

C *****
  SUBROUTINE UVC1C2
C *****
  COMMON U(65,36),V(65,36),H(65,36),U0(65,36),V0(65,36),H0(65,36),
  1D(65,36),IB(195),JB(195),JU(65),JL(65),IG(100),JG(100),
  2      G,DTDS,DT60,WX,WY,WXDT,WYDT,CMSQ,GDT,GTS,CORDT,TPRINT,
  3I,J,M,N,Q1,QN,Q2,OP,Q3,QC,DS,DTSSQ,TIME,DT,PI,WSC,Q4,Q5,Q6,NZ,
  4VWD(6,17),KT,KKT,NKT,NI,NJ,NM,NN,SWX(65,36),SWY(65,36),T,
  5HS(65,36),KOR,KHS,KOC,HMSL,HOR,HHS,HOC,
  6VWS(6,17),QOR,QHS,QOC,VWX(6,17),VWY(6,17),
  7NB1(40),NB2(40),NB3(40),NB4(40),NB5(40),NB6(40),NB7(40),NB8(40),
  8NB9(40),NB10(40)

C
C   SUBROUTINE UVC1C2 PRINTS THE VALUES OF U AND V AT ALL POINTS
C   IN A GIVEN TIME STEP.
C
  WRITE (3,310) TIME,DT
  WRITE(3,100)
100 FORMAT(/10X,'VALUES OF THE X-COMPONENT OF VELOCITY,U AT ALL POINTS
  1'/)
  WRITE (3,160) (J,J=5,19)
  DO 110 I=5,61
110 WRITE(3,180) I,(U(I,J),J=5,19)
  WRITE (3,165) (J,J=20,35)
  DO 120 I=5,61
120 WRITE (3,185) I,(U(I,J),J=20,35)
  WRITE (3,310) TIME,DT
  WRITE(3,130)
130 FORMAT(/10X,'VALUES OF THE Y-COMPONENT OF VELOCITY,V AT ALL POINTS
  1'/)
  WRITE (3,160) (J,J=5,19)
  DO 140 I=5,61
140 WRITE(3,180) I,(V(I,J),J=5,19)
  WRITE (3,165) (J,J=20,35)
  DO 150 I=5,61
150 WRITE (3,185) I,(V(I,J),J=20,35)
160 FORMAT (/7X,15(3X,'(',I2,')')/)
165 FORMAT(/7X,16(3X,'(',I2,')')/)
180 FORMAT (3X,'(',I2,')',15(1X,F6.2))
185 FORMAT (3X,'(',I2,')',16(1X,F6.2))
310 FORMAT('1',/' * TIME=',F8.2,2X,'MINUTES. THE TIME INCREMENT USED I
  1S, DT=',F8.2,2X,'SECONDS')
  RETURN
  END

```

--: INPUT DATA :-
 H U R R I C A N E S U R G E
 HURRICANE DONNA OF SEPTEMBER 11 - 12 1960
 INITIAL TIME = 0 15 16.00 EST SEPTEMBER 11, 1960
 ZONES 2 AND 5 USE DATA AT HATTERAS

FINAL TIME IN MINUTES IFIN= 960.00
 TIME INCREMENT IN SECONDS DT= 180.00
 SQUARE GRID IN FEET DS= 7422.00
 CORIOLIS COEFFICIENT CCORIC= 0.0
 MANNING COEFFICIENT CM= 0.02
 NEUSE RIVER DISCHARGE Q1= 70000.00
 PAMLICO RIVER DISCHARGE Q2= 80000.00
 RANOCHE AND CROATAN DISCHARGE Q3= 211400.00
 OUTFLOW FROM OREGON INLET Q4= 0.0
 OUTFLOW FROM HATTERAS INLET Q5= 0.0
 OUTFLOW FROM CCRACOCK INLET Q6= 0.0

WIND STRESS COEFFICIENT, CD= 0.0010200
 DURATION OF HURRICANE, HRS, MKT= 17
 COEFF. OF DISCHARGE AT CCRACOCK INLET KCC= 165400.00
 COEFF. OF DISCHARGE AT HATTERAS INLET KHS= 108500.00
 COEFF. OF DISCHARGE AT OREGON INLET KCR= 98000.00
 VARIATION IN THE WATER LEVEL W.R.T. ITS MSL, HMSL= 0.0

VARIABLE WIND SPEED AT DIFFERENT VALUES OF NZ, EKT

	(1)	(2)	(3)	(4)	(5)	(6)	(7)	(8)	(9)	(10)	(11)	(12)	(13)	(14)	(15)	(16)	(17)
(1)	17.0	17.0	18.0	19.0	20.0	22.0	30.0	34.0	41.0	44.0	50.0	50.0	55.0	44.0	33.0	26.0	22.0
(2)	17.0	17.0	18.0	19.0	20.0	22.0	30.0	34.0	41.0	44.0	50.0	50.0	55.0	44.0	33.0	26.0	22.0
(3)	17.0	14.0	15.0	20.0	20.0	26.0	33.0	34.0	27.0	27.0	50.0	60.0	45.0	45.0	27.0	25.0	22.0
(4)	20.0	21.0	22.0	24.0	24.0	25.0	35.0	43.0	46.0	54.0	60.0	63.0	53.0	65.0	38.0	36.0	30.0
(5)	17.0	17.0	18.0	19.0	20.0	22.0	30.0	34.0	41.0	44.0	50.0	50.0	55.0	44.0	33.0	26.0	22.0
(6)	18.0	18.0	20.0	20.0	23.0	33.0	35.0	43.0	44.0	33.0	47.0	51.0	41.0	44.0	30.0	28.0	17.0

VARIABLE WIND DIRECTION, AT DIFFERENT VALUES OF NZ, EKT

	(1)	(2)	(3)	(4)	(5)	(6)	(7)	(8)	(9)	(10)	(11)	(12)	(13)	(14)	(15)	(16)	(17)
(1)	90.0	78.0	78.0	90.0	101.0	101.0	101.0	112.0	101.0	78.0	67.0	67.0	0.0	292.0	292.0	292.0	292.0
(2)	90.0	78.0	78.0	90.0	101.0	101.0	101.0	112.0	101.0	78.0	67.0	67.0	0.0	292.0	292.0	292.0	292.0
(3)	90.0	101.0	90.0	135.0	112.0	135.0	112.0	132.0	90.0	67.0	338.0	338.0	323.0	315.0	338.0	328.0	328.0
(4)	90.0	90.0	90.0	112.0	112.0	112.0	112.0	112.0	90.0	68.0	45.0	45.0	3.0	338.0	0.0	338.0	338.0
(5)	90.0	78.0	78.0	90.0	101.0	101.0	101.0	112.0	101.0	75.0	67.0	67.0	0.0	292.0	292.0	292.0	292.0
(6)	101.0	112.0	112.0	123.0	123.0	112.0	112.0	112.0	90.0	56.0	22.0	0.0	343.0	338.0	349.0	338.0	349.0

LOWER AND UPPER BOUND OF J FOR EACH I

	-I-	JL(I)	JU(I)	-I-	JL(I)	JU(I)	-I-	JL(I)	JU(I)
5	17	29	29	24	11	25	43	7	23
6	17	29	29	25	11	23	44	7	23
7	17	29	29	26	11	23	45	9	23
8	17	29	29	27	11	23	46	9	23
9	17	29	29	28	11	23	47	11	23
10	13	29	29	29	11	23	48	11	25

11	13	29	30	9	23	49	13	25
12	13	29	31	9	23	50	13	25
13	13	29	32	9	23	51	13	25
14	13	35	33	9	23	52	13	27
15	13	35	34	7	23	53	15	27
16	13	35	35	7	23	54	15	29
17	13	35	36	7	25	55	21	29
18	13	35	37	7	25	56	21	31
19	13	35	38	7	25	57	23	31
20	11	35	39	7	25	58	23	31
21	11	27	40	5	25	59	25	31
22	11	27	41	5	25	60	25	31
23	11	25	42	5	25	61	25	31

COORDINATES OF POINTS MARKED BY CIRCLES ONE POINT GRID INSIDE THE BOUNDARY

-K-	{IG(K),JG(K)}	-K-	{IG(K),JG(K)}	-K-	{IG(K),JG(K)}	-K-	{IG(K),JG(K)}
1	(6, 25)	24	(31, 22)	47	(59, 26)	70	(35, 8)
2	(6, 27)	25	(33, 22)	48	(58, 25)	71	(34, 9)
3	(7, 28)	26	(35, 22)	49	(57, 24)	72	(33, 10)
4	(9, 28)	27	(36, 23)	50	(56, 23)	73	(31, 10)
5	(11, 28)	28	(37, 24)	51	(55, 22)	74	(30, 11)
6	(13, 28)	29	(39, 24)	52	(54, 21)	75	(29, 12)
7	(14, 29)	30	(41, 24)	53	(54, 19)	76	(27, 12)
8	(14, 31)	31	(42, 23)	54	(54, 17)	77	(25, 12)
9	(14, 33)	32	(43, 22)	55	(53, 16)	78	(23, 12)
10	(15, 34)	33	(45, 22)	56	(52, 15)	79	(21, 12)
11	(17, 34)	34	(47, 22)	57	(51, 14)	80	(20, 13)
12	(14, 34)	35	(48, 23)	58	(49, 14)	81	(19, 14)
13	(20, 34)	36	(49, 24)	59	(48, 13)	82	(17, 14)
14	(20, 31)	37	(51, 24)	60	(47, 12)	83	(15, 14)
15	(20, 29)	38	(52, 23)	61	(46, 11)	84	(13, 14)
16	(20, 27)	39	(53, 26)	62	(45, 10)	85	(11, 14)
17	(21, 26)	40	(54, 27)	63	(44, 9)	86	(10, 15)
18	(22, 25)	41	(55, 28)	64	(43, 8)	87	(10, 17)
19	(23, 24)	42	(56, 29)	65	(42, 7)	88	(9, 18)
20	(24, 23)	43	(57, 30)	66	(41, 6)	89	(7, 18)
21	(25, 22)	44	(59, 30)	67	(40, 7)	90	(6, 19)
22	(27, 22)	45	(60, 29)	68	(39, 8)	91	(6, 21)
23	(29, 22)	46	(60, 27)	69	(37, 8)	92	(6, 23)

COORDINATES OF THE POINTS ON THE BOUNDARY

-N-	{IB(N),JB(N)}	-N-	{IB(N),JB(N)}	-N-	{IB(N),JB(N)}
1	(5, 24)	49	(30, 23)	97	(61, 26)
2	(5, 25)	50	(31, 23)	98	(61, 25)
3	(5, 26)	51	(32, 23)	99	(60, 25)
4	(5, 27)	52	(33, 23)	100	(59, 25)
5	(5, 28)	53	(34, 23)	101	(59, 24)
6	(5, 29)	54	(35, 23)	102	(59, 23)
7	(6, 29)	55	(35, 24)	103	(58, 23)
8	(7, 29)	56	(35, 25)	104	(57, 23)
9	(8, 29)	57	(36, 25)	105	(57, 22)
10	(9, 29)	58	(37, 25)	106	(57, 21)
11	(10, 29)	59	(38, 25)	107	(56, 21)
12	(11, 29)	60	(39, 25)	108	(55, 21)
13	(12, 29)	61	(40, 25)	109	(55, 20)
14	(13, 29)	62	(41, 25)	110	(55, 19)

15 (13. 30) 63 (42. 25) 111 (55. 18) 159 (26. 11)
 16 (13. 31) 64 (43. 25) 112 (55. 17) 160 (25. 11)
 17 (13. 32) 65 (43. 24) 113 (55. 16) 161 (24. 11)
 18 (13. 33) 66 (43. 23) 114 (55. 15) 162 (23. 11)
 19 (13. 34) 67 (44. 23) 115 (54. 15) 163 (22. 11)
 20 (13. 35) 68 (45. 23) 116 (53. 15) 164 (21. 11)
 21 (14. 35) 69 (46. 23) 117 (53. 14) 165 (20. 11)
 22 (15. 35) 70 (47. 23) 118 (53. 13) 166 (19. 11)
 23 (16. 35) 71 (47. 24) 119 (52. 13) 167 (19. 12)
 24 (17. 35) 72 (47. 25) 120 (51. 13) 168 (19. 13)
 25 (18. 35) 73 (48. 25) 121 (50. 13) 169 (18. 13)
 26 (19. 35) 74 (49. 25) 122 (49. 13) 170 (17. 13)
 27 (20. 35) 75 (50. 25) 123 (49. 12) 171 (16. 13)
 28 (21. 35) 76 (51. 25) 124 (49. 11) 172 (15. 13)
 29 (21. 34) 77 (51. 26) 125 (48. 11) 173 (14. 13)
 30 (21. 33) 78 (51. 27) 126 (47. 11) 174 (13. 13)
 31 (21. 32) 79 (52. 27) 127 (47. 10) 175 (12. 13)
 32 (21. 31) 80 (53. 27) 128 (47. 9) 176 (11. 13)
 33 (21. 30) 81 (53. 28) 129 (46. 9) 177 (10. 13)
 34 (21. 29) 82 (53. 29) 130 (45. 9) 178 (9. 13)
 35 (21. 28) 83 (54. 29) 131 (45. 8) 179 (9. 14)
 36 (21. 27) 84 (55. 29) 132 (45. 7) 180 (9. 15)
 37 (22. 27) 85 (55. 30) 133 (44. 7) 181 (9. 16)
 38 (23. 27) 86 (55. 31) 134 (43. 7) 182 (9. 17)
 39 (23. 26) 87 (56. 31) 135 (43. 6) 183 (8. 17)
 40 (23. 25) 88 (57. 31) 136 (43. 5) 184 (7. 17)
 41 (24. 25) 89 (58. 31) 137 (42. 5) 185 (6. 17)
 42 (25. 25) 90 (59. 31) 138 (41. 5) 186 (5. 17)
 43 (25. 24) 91 (60. 31) 139 (40. 5) 187 (5. 18)
 44 (25. 23) 92 (61. 31) 140 (39. 5) 188 (5. 19)
 45 (26. 23) 93 (61. 30) 141 (39. 6) 189 (5. 20)
 46 (27. 23) 94 (61. 29) 142 (39. 7) 190 (5. 21)
 47 (28. 23) 95 (61. 28) 143 (38. 7) 191 (5. 22)
 48 (29. 23) 96 (61. 27) 144 (37. 7) 192 (5. 23)

BOUNDARY POINTS OF TYPE 1 I.E.NB1(K)

1 (5.24) 2 (5.25) 3 (5.26) 4 (5.27) 16(13.31) 17(13.32) 18(13.33) 180(9.15) 188(5.19) 189(5.20)
 190(5.21) 191(5.22) 192(5.23)

BOUNDARY POINTS OF TYPE 2 I.E.NB2(K)

5 (7.29) 9 (9.29) 10 (9.29) 11(10.29) 12(11.29) 13(12.29) 14(13.29) 22(15.35) 23(16.35) 24(17.35)
 25(19.35) 26(19.35) 45(26.23) 46(27.23) 47(28.23) 48(29.23) 49(30.23) 50(31.23) 51(32.23) 52(33.23)
 53(34.23) 54(35.23) 58(37.25) 59(38.25) 60(39.25) 61(40.25) 62(41.25) 67(44.23) 68(45.23) 69(46.23)
 70(47.23) 74(49.25) 75(50.25) 76(51.25) 80(53.27) 84(55.29) 86(57.31) 89(58.31) 90(59.31)

BOUNDARY POINTS OF TYPE 3 I.E.NB3(K)

30(21.33) 31(21.32) 32(21.31) 33(21.30) 34(21.29) 36(21.27) 94(61.29) 95(61.28) 96(61.27) 100(59.25)
 104(57.23) 108(55.21) 110(55.19) 111(55.18) 112(55.17) 116(53.15) 122(49.13) 126(47.11) 130(45. 9) 134(43. 7)

BOUNDARY POINTS OF TYPE 4 I.E.NB4(K)

120(51.13) 121(50.13) 138(41. 5) 142(39. 7) 143(38. 7) 144(37. 7) 145(36. 7) 146(35. 7) 150(33. 9) 151(32. 9)
 152(31. 9) 156(29.11) 157(28.11) 158(27.11) 159(26.11) 160(25.11) 161(24.11) 162(23.11) 163(22.11) 164(21.11)
 168(19.13) 169(18.13) 170(17.13) 171(16.13) 172(15.13) 173(14.13) 174(13.13) 175(12.13) 176(11.13) 183(8.17)
 184(7.17)

BOUNDARY POINTS OF TYPE 5 I.E.NB5(K)

6(9,24) 20(13,35) 50(35,29) 72(47,29) 78(51,27) 82(53,29) 86(55,31)

BOUNDARY POINTS OF TYPE 6 I.E.NB6(K)

28(21,35) 39(23,27) 40(23,25) 42(25,25) 44(25,23) 54(43,25) 66(43,23) 92(61,31)

BOUNDARY POINTS OF TYPE 7 I.E.NB7(K)

92(61,25) 102(59,23) 106(57,21) 114(55,15) 118(53,13) 124(49,11) 128(47, 9) 132(45, 7) 136(43, 5)

BOUNDARY POINTS OF TYPE 8 I.E.NB8(K)

140(39, 5) 148(23, 7) 154(29, 9) 166(19,11) 178(9,13) 182(9,17) 186(5,17)

BOUNDARY POINTS OF TYPE 9 I.E.NB9(K)

5(5,28) 15(13,30) 19(13,34) 29(21,34) 35(21,28) 39(23,26) 43(25,24) 56(35,24) 65(43,24) 71(47,24)
77(51,26) 81(53,28) 85(55,30) 93(61,39) 97(61,26) 101(59,24) 105(57,22) 109(55,20) 113(53,16) 117(53,14)
123(49,12) 127(47,10) 131(45, 8) 135(43, 6) 141(39, 6) 149(33, 8) 155(29,10) 167(19,12) 173(9,14) 181(9,14)
187(5,18)

BOUNDARY POINTS OF TYPE 10 I.E.NB10(K)

7(6,29) 21(14,35) 27(20,35) 37(22,27) 41(24,25) 57(36,25) 63(42,25) 73(48,25) 79(52,27) 83(54,29)
87(56,31) 91(60,31) 99(60,25) 103(58,23) 107(56,21) 115(54,15) 119(52,13) 125(48,11) 129(46, 9) 137(44, 7)
137(42, 5) 139(40, 5) 147(34, 7) 153(30, 5) 165(20,11) 177(10,13) 185(6,17)

(5)	9.00	8.00	8.00	11.06	12.00	12.56	13.00	12.50	12.00	11.75	12.00	10.19	9.00	8.89
(6)	8.81	9.50	10.13	11.00	12.06	13.25	14.25	14.75	14.81	13.88	11.86	10.50	9.38	9.30
(7)	10.00	11.25	12.00	13.25	14.00	15.50	17.00	16.50	17.00	16.00	13.63	12.00	10.44	9.00
(8)	11.88	13.50	14.88	16.00	16.94	17.75	18.19	18.00	17.38	16.50	15.25	13.50	11.69	9.31
(9)	14.00	15.63	16.00	18.19	20.00	19.13	20.00	18.31	18.00	16.00	15.00	11.00	9.94	9.00
(10)	15.44	17.00	18.19	18.75	18.25	15.94	15.94	14.50	13.00	11.50	10.25	9.50	9.13	8.00
(11)	17.00	17.75	19.00	18.50	17.81	17.81	15.94	14.00	13.00	11.00	10.36	9.00	8.56	8.50
(12)	17.31	18.00	18.31	18.25	17.94	17.50	16.75	15.00	14.00	11.13	10.00	9.19	8.56	8.50
(13)	18.00	18.00	18.00	18.06	18.00	17.44	17.00	15.38	14.00	12.31	11.00	9.00	8.00	8.13
(14)	17.81	18.00	18.00	17.81	17.25	16.31	15.00	14.44	13.44	11.75	10.25	8.53	8.00	8.00
(15)	18.00	17.88	18.00	17.88	18.00	16.81	16.00	14.44	13.00	11.06	9.00	8.56	8.00	7.94
(16)	16.88	17.50	17.75	17.50	16.88	16.00	14.94	13.75	12.31	10.50	8.88	7.63	7.50	7.50
(17)	16.00	17.00	18.00	16.94	16.00	15.00	14.00	13.00	12.00	10.06	8.00	7.00	6.94	7.00
(18)	15.31	16.50	16.94	16.25	15.06	14.00	13.06	12.25	11.25	9.75	8.25	7.25	6.63	6.00
(19)	15.00	16.19	17.00	15.69	14.00	13.19	12.00	11.44	11.00	9.25	8.00	6.53	5.00	5.25
(20)	15.25	16.25	16.44	15.50	14.06	12.75	11.56	10.50	9.44	8.25	7.13	6.25	5.06	5.00
(21)	16.00	16.38	17.00	15.38	14.00	12.44	11.00	9.75	8.00	7.50	6.00	5.25	5.00	5.06
(22)	15.81	16.25	16.06	15.00	13.50	12.00	10.63	9.50	8.56	7.75	7.06	6.50	5.50	5.75
(23)	16.00	15.88	16.00	14.25	13.00	11.38	10.00	9.38	9.00	8.19	8.00	7.30	6.00	5.44
(24)	15.75	15.25	14.31	13.00	10.63	9.63	9.00	8.50	8.50	8.00	7.50	6.56	5.94	5.50
(25)	16.00	14.50	13.00	11.56	10.00	9.38	9.00	8.31	8.00	7.38	7.00	6.44	6.00	5.44
(26)	15.31	13.75	12.00	10.25	8.81	8.00	7.56	7.25	6.94	6.06	5.75	5.56	5.50	5.25
(27)	15.00	13.19	11.00	9.38	7.00	7.00	6.00	6.38	6.00	5.75	5.00	5.13	5.00	5.06
(28)	15.00	13.00	11.06	9.25	7.81	7.00	6.56	6.25	5.94	5.00	5.13	5.00	5.00	5.00
(29)	15.00	13.13	11.00	9.50	7.38	7.00	6.44	6.00	5.50	5.00	5.00	5.00	5.00	5.00
(30)	15.50	13.50	11.56	9.75	8.31	7.50	7.00	6.50	6.00	5.50	5.00	5.00	5.00	5.00
(31)	16.00	14.00	12.00	10.19	8.00	7.00	7.00	6.50	6.00	5.50	5.00	5.00	5.00	5.00
(32)	16.13	14.50	12.88	11.00	9.25	8.00	7.13	6.50	6.00	5.50	5.00	5.00	5.00	5.00
(33)	16.00	15.25	14.00	12.19	10.00	8.81	7.00	6.75	6.00	5.63	5.00	5.00	5.00	5.00
(34)	17.56	16.50	15.31	13.75	12.00	10.25	8.69	7.50	6.63	6.00	5.25	5.06	5.00	5.00
(35)	19.00	17.69	17.00	15.13	14.00	11.56	10.00	8.25	7.00	6.38	6.00	5.00	5.00	5.00
(36)	19.94	18.25	17.25	15.75	13.94	12.00	10.13	8.50	7.25	6.00	5.50	5.13	5.00	5.00
(37)	19.00	18.31	18.00	15.69	14.00	11.81	10.00	8.38	7.00	6.38	6.00	5.44	5.00	5.00
(38)	18.88	18.00	16.75	15.00	13.06	11.25	9.56	8.00	6.75	6.00	5.56	5.06	5.00	5.00
(39)	19.00	17.63	16.00	14.38	12.00	10.75	9.00	7.63	6.00	5.63	5.00	5.00	5.00	5.00
(40)	18.38	17.50	16.25	14.50	12.56	10.75	9.06	7.50	6.25	5.50	5.13	5.00	5.00	5.00
(41)	18.00	17.50	17.00	14.50	13.00	10.69	9.00	7.31	6.00	5.44	5.00	5.00	5.00	5.00
(42)	18.31	17.50	16.19	14.25	12.06	10.00	8.19	6.75	5.75	5.25	5.06	5.00	5.00	5.00
(43)	19.00	17.25	16.00	13.50	11.00	9.13	7.00	6.13	5.00	5.06	5.00	5.00	5.00	5.00
(44)	17.69	16.50	14.81	12.75	10.56	8.50	6.81	5.75	5.19	5.00	5.00	5.00	5.00	5.00
(45)	17.00	15.19	14.00	11.75	10.00	7.88	6.00	5.50	5.00	5.00	5.00	5.00	5.00	5.00
(46)	14.44	13.25	11.88	10.25	8.56	7.00	5.81	5.25	5.06	5.00	5.00	5.00	5.00	5.00
(47)	12.00	11.75	10.00	9.00	7.00	6.25	5.00	5.06	5.00	5.00	5.00	5.00	5.00	5.00
(48)	12.68	11.75	10.38	6.75	7.19	6.00	5.25	5.00	5.00	5.00	5.00	5.00	5.00	5.00
(49)	14.00	12.38	11.00	9.19	7.00	6.38	5.19	5.00	5.00	5.00	5.00	5.00	5.00	5.00
(50)	13.69	12.75	11.44	10.00	8.63	7.00	6.56	5.75	5.19	5.00	5.00	5.00	5.00	5.00
(51)	14.00	12.94	12.00	10.94	10.00	8.75	6.31	5.00	5.00	5.00	5.00	5.00	5.00	5.00
(52)	13.38	13.00	12.44	11.75	10.81	9.50	6.00	6.50	5.38	5.00	5.00	5.00	5.00	5.00
(53)	13.00	12.44	13.00	12.06	12.00	10.06	8.00	6.88	5.00	5.19	5.00	5.00	5.00	5.00
(54)	10.56	10.75	11.06	11.56	10.75	9.44	8.00	6.69	5.00	5.19	5.00	5.00	5.00	5.00
(55)	8.00	8.69	9.00	10.19	12.00	10.75	11.00	9.00	8.00	6.56	5.00	5.06	5.00	5.00
(56)	6.63	7.00	7.56	8.25	8.88	9.25	9.31	9.00	8.38	7.50	6.63	5.56	5.06	5.00
(57)	5.00	5.88	6.00	6.56	6.00	7.56	8.00	8.63	9.00	8.25	8.00	6.75	5.44	5.00
(58)	5.13	5.50	5.88	6.00	6.25	7.00	7.88	8.50	8.75	8.50	7.88	7.00	6.13	5.50
(59)	5.00	5.50	6.00	6.00	6.00	7.00	8.00	8.50	9.00	8.50	8.00	6.00	5.50	5.00
(60)	5.13	5.50	5.88	6.00	6.25	7.00	7.88	8.50	9.75	8.50	7.88	7.00	6.13	5.00
(61)	5.00	5.50	6.00	6.00	6.00	7.00	8.00	8.50	9.00	8.50	8.00	6.00	5.50	5.00

* TIME= 60.00 MINUTES. THE TIME INCREMENT USED IS .01= 180.00 SECONDS
 NUMBER OF TIME STEPS COMPLETED= 20

COMPUTED VALUES OF VL, THETA, H AT SELECTED GRID POINTS

GRID POINT	VL	THETA	H	GRID POINT	VL	THETA	H
(5, 5)	0.0	360.0	1.0	(35, 5)	0.0	360.0	1.0
(5, 10)	0.0	360.0	1.0	(35, 10)	0.1	138.6	0.7
(5, 15)	0.0	360.0	1.0	(35, 15)	0.1	123.1	0.7
(5, 20)	0.0	360.0	0.8	(35, 20)	0.1	48.1	1.2
(5, 25)	0.1	180.0	1.1	(35, 25)	0.0	360.0	1.1
(5, 30)	0.0	360.0	1.0	(35, 30)	0.0	360.0	1.0
(5, 35)	0.0	360.0	1.0	(35, 35)	0.0	360.0	1.0
(10, 5)	0.0	360.0	1.0	(40, 5)	0.0	360.0	1.0
(10, 10)	0.0	360.0	1.0	(40, 10)	0.3	83.0	0.7
(10, 15)	0.1	71.2	0.7	(40, 15)	0.2	86.9	0.9
(10, 20)	0.2	93.2	0.8	(40, 20)	0.1	75.7	1.2
(10, 25)	0.1	88.4	1.2	(40, 25)	0.0	360.0	1.4
(10, 30)	0.0	360.0	1.0	(40, 30)	0.0	360.0	1.0
(10, 35)	0.0	360.0	1.0	(40, 35)	0.0	360.0	1.0
(15, 5)	0.0	360.0	1.0	(45, 5)	0.0	360.0	1.0
(15, 10)	0.0	360.0	1.0	(45, 10)	0.1	75.7	1.0
(15, 15)	0.2	71.6	0.6	(45, 15)	0.2	52.0	0.9
(15, 20)	0.3	89.9	0.9	(45, 20)	0.1	42.4	1.2
(15, 25)	0.4	93.1	1.1	(45, 25)	0.0	360.0	1.0
(15, 30)	0.5	93.6	1.2	(45, 30)	0.0	360.0	1.0
(15, 35)	0.5	90.0	1.1	(45, 35)	0.0	360.0	1.0
(20, 5)	0.0	360.0	1.0	(50, 5)	0.0	360.0	1.0
(20, 10)	0.0	360.0	1.0	(50, 10)	0.0	360.0	1.0
(20, 15)	0.1	84.7	0.7	(50, 15)	0.1	45.3	0.9
(20, 20)	0.3	111.6	0.9	(50, 20)	0.2	41.4	1.0
(20, 25)	0.4	106.6	1.2	(50, 25)	0.0	360.0	1.2
(20, 30)	0.3	88.9	1.2	(50, 30)	0.0	360.0	1.0
(20, 35)	0.0	360.0	1.3	(50, 35)	0.0	360.0	1.0
(25, 5)	0.0	360.0	1.0	(55, 5)	0.0	360.0	1.0
(25, 10)	0.0	360.0	1.0	(55, 10)	0.0	360.0	1.0
(25, 15)	0.1	131.7	0.8	(55, 15)	0.0	360.0	1.0
(25, 20)	0.1	148.7	1.1	(55, 20)	0.0	360.0	0.9
(25, 25)	0.0	360.0	1.3	(55, 25)	0.2	8.7	0.3
(25, 30)	0.0	360.0	1.0	(55, 30)	0.0	360.0	1.0
(25, 35)	0.0	360.0	1.0	(55, 35)	0.0	360.0	1.0
(30, 5)	0.0	360.0	1.0	(60, 5)	0.0	360.0	1.0
(30, 10)	0.1	299.6	0.8	(60, 10)	0.0	360.0	1.0
(30, 15)	0.0	139.0	0.8	(60, 15)	0.0	360.0	1.0
(30, 20)	0.0	0.0	1.1	(60, 20)	0.0	360.0	1.0
(30, 25)	0.0	360.0	1.0	(60, 25)	0.0	360.0	0.9
(30, 30)	0.0	360.0	1.0	(60, 30)	0.0	26.8	1.2
(30, 35)	0.0	360.0	1.0	(60, 35)	0.0	360.0	1.0